PHASES AND PHASE TRANSITIONS IN QUANTUM FERROMAGNETS

by

YAN SANG

A DISSERTATION

Presented to the Department of Physics
and the Graduate School of the University of Oregon
in partial fulfillment of the requirements
for the degree of
Doctor of Philosophy

December 2014

DISSERTATION APPROVAL PAGE

Student: Yan Sang

Title: Phases and Phase Transitions in Quantum Ferromagnets

This dissertation has been accepted and approved in partial fulfillment of the requirements for the Doctor of Philosophy degree in the Department of Physics by:

Dr. Miriam Deutsch	Chair
Dr. Dietrich Belitz	Advisor
Dr. Richard Taylor	Core Member
Dr. James A. Isenberg	Institutional Representative

and

J. Andrew Berglund	Dean of the Graduate School

Original approval signatures are on file with the University of Oregon Graduate School.

Degree awarded December 2014

DISSERTATION ABSTRACT

Yan Sang

Doctor of Philosophy

Department of Physics

December 2014

Title: Phases and Phase Transitions in Quantum Ferromagnets

In this dissertation we study the phases and phase transition properties of quantum ferromagnets and related magnetic materials. We first investigate the effects of an external magnetic field on the Goldstone mode of a helical magnet, such as MnSi. The field introduces a qualitatively new term into the dispersion relation of the Goldstone mode, which in turn changes the temperature dependences of the contributions of the Goldstone mode to thermodynamic and transport properties. We then study how the phase transition properties of quantum ferromagnets evolve with increasing quenched disorder. We find that there are three distinct regimes for different amounts of disorder. When the disorder is small enough, the quantum ferromagnetic phase transitions is generically of first order. If the disorder is in an intermediate region, the ferromagnetic phase transition is of second order and effectively characterized by mean-field critical exponents. If the disorder is strong

enough the ferromagnetic phase transitions are continuous and are characterized by non-mean-field critical exponents.

CURRICULUM VITAE

NAME OF AUTHOR: Yan Sang

GRADUATE AND UNDERGRADUATE SCHOOLS ATTENDED:

University of Oregon, Eugene, Oregon
University of Science and Technology of China, Hefei, China

DEGREES AWARDED:

Doctor of Philosophy in Physics, 2014, University of Oregon
Master of Science in Physics, 2009, University of Oregon
Bachelor of Science in Physics, 2007, University of Science and Techology of China

AREAS OF SPECIAL INTEREST:

Science
Philosophy
Psychology

PROFESSIONAL EXPERIENCE:

Graduate Research Assistant,
University of Oregon, 2009 – 2014
Graduate Teaching Fellow,
University of Oregon, 2007 – 2014

GRANTS, AWARDS AND HONORS:

Qualification Exam First Place Award, University of Oregon, 2008

PUBLICATIONS:

Yan Sang, D. Belitz, and T.R. Kirkpatrick, "Disorder dependence of the ferromagnetic quantum phase transition", Phys. Rev. Lett., **113**, 207201, (2014).

Kwan-yuet Ho, T.R. Kirkpatrick, Yan Sang, and D. Belitz, "Ordered Phases of Itinerant Dzyaloshinsky-Moriya and Their Electronic Properties", Phys. Rev. B, **82**, 134427, (2010).

ACKNOWLEDGEMENTS

First I want to thank my family for their unconditional support at all times. I also want to express my gratitude to my advisor Dr. Dietrich Belitz, who not only taught me technical skills and general physical principles, but also taught me the spirit of science, that is, to accept the physical reality as it is, and try our best to understand it and be open minded all the time. I also want to thank all my committee members, Dr. Miriam Deutsch, Dr. James A. Isenberg and Dr Richard Taylor. My gratitude also goes to Dr. John Toner, from whom I learned how to understand and explain physics in many different ways. My thanks also go to all my fiends who used to be or still are in Eugene: Xiaolu Cheng, Chu Chen, Eryn Cook, and many others. Without them my life would be much harder during these years.

To this world which has made me who I am today.

TABLE OF CONTENTS

LIST OF FIGURES

CHAPTER I

INTRODUCTION

Magnets have been known and used by human beings for thousands of years, but we only started to understand the physical mechanism of magnetism in the nineteenth century. Since then, magnets and magnetism have attracted substantial interest and been the subject of intensive research. The twentieth century saw remarkable progress in understanding magnetism after the development of quantum mechanics. However, there are still many aspects of magnetism that warrant continued research efforts, especially in metallic systems at low temperatures, where abundant quantum effects manifest themselves. In this dissertation we will consider issues related to phases and phase transitions in ferromagnets and related systems at low temperatures.

Ferromagnetic and Related Phases

Ferromagnetic Phase

The term "ferromagnetic order" refers to a spontaneous homogeneous magnetization $\boldsymbol{M}$ due to a spontaneous alignment of the magnetic moments carried by the spin of the electrons. Classically, these magnetic moments interact only via the dipole-dipole interaction, which is too weak to explain the high temperature at which

ferromagnetic order is observed in, e.g., iron or nickel [1]. Quantum mechanics successfully explained ferromagnetism in terms of the exchange interaction mechanism, which describes spin-spin interactions that are governed by the Coulomb interaction under the constraint of the Pauli principle. The Pauli principle keeps electrons with parallel spins apart and therefore reduces the Coulomb energy. At zero temperature, the system is in its lowest energy state. If the exchange interaction is weak enough, the net magnetization of the system is zero. For a sufficiently strong exchange interaction all spins are on average parallel to each other, so there is a nonzero magnetization. When the temperature T is increased from zero, thermal noise randomizes the spins. If the temperature is not too high, a magnetization still persists, but it will decrease with increasing temperature. When the temperature T reaches a critical value T_c, the magnetization vanishes and the material becomes paramagnetic. The critical temperature T_c at which the spontaneous alignment of spins disappears is known as the Curie temperature.

The spin-spin interaction that results from a naive application of the exchange mechanism is actually stronger than the observed ferromagnetic energy scale, i.e., the Curie temperature [1]. This discrepancy was resolved by the realization that many-body and band-structure effects renormalize the exchange interaction and bring it down to the observed ferromagnetic scale of roughly 1,000K or lower [2]. In most ferromagnets, the resulting energy scale is still much larger than the dipole-dipole interaction, or the spin-orbit interaction which is roughly on the same order

as the dipole-dipole interaction. Therefore, the dipole-dipole interaction and spin-orbit interaction are often neglected when describing a ferromagnet.

Helical Magnetic Phases

If the Curie temperature is very low, the ferromagnet is called a weak ferromagnet. In weak ferromagnets, energy scales smaller than the renormalized exchange interaction will start to play a role and may result in interesting superstructure on top of the ferromagnetic order. One well-studied example is a type of helical magnetic order which originates from the spin-orbit interaction in the weak ferromagnets MnSi and FeGe [3, 4]. (These materials are ferromagnets if one neglects the weak spin-orbit interaction, and we will sometimes refer to them as such, although their actual ordered state is a helically modulated one.) One common property of MnSi and FeGe is that both their lattices lack inversion symmetry and it turns out this property is a prerequisite for a helical magnetic superstructure. It has been shown by Dzyaloshinskii and Moriya [5–7] that helical order results from a term in the action that is invariant under simultaneous rotations of real space and the magnetic order parameter $\boldsymbol{M}$, but breaks the spatial inversion symmetry. It has the form $\boldsymbol{M} \cdot (\boldsymbol{\nabla} \times \boldsymbol{M})$, which favors a nonzero curl of the magnetization and thus leads to the observed helical order in the ground state. Such a term arises from the spin-orbit interaction. The helical order is characterized by a specific direction given by the pitch vector $\boldsymbol{q}$ of the helix. In

Figure 1.1. Schematic depiction of a global magnetic helix, where there is ferromagnetic order in planes perpendicular to the pitch vector direction. After Ref. [8].

any given plane perpendicular to $\boldsymbol{q}$ there is ferromagnetic order, but the direction of the magnetization rotates as one goes along the direction of $\boldsymbol{q}$, forming a global helix, as shown in Fig.1.1..

The energy scale of the spin-orbit interaction is small compared to the atomic scale, so the helical order has a much larger length scale than the lattice spacing. If an external magnetic field is applied, a homogeneous magnetization induced by the field will be superimposed on the helical order. The pitch vector of the helix is pinned to the direction of the magnetic field, and the resulting order is called conical, which is shown schematically in Fig. 1.2..

If we consider the effects of the underlying ionic lattice on an even smaller energy scale, the crystal field which originates from the spin-orbit interaction as well will pin the helix in some specific directions. If we denote the coupling constant of the spin-orbit interaction by g_{so}, the crystal-field pinning effects of the helical magnetic

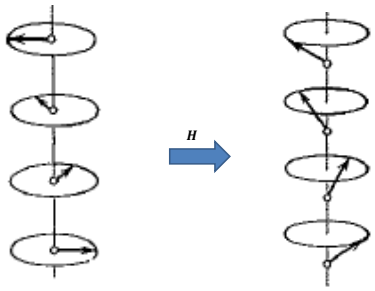

Figure 1.2. Schematic depiction of how the helical magnetic structure changes to a conical one when an external magnetic field **H** is applied. After Ref. [9]

structure are of order g_{so}^2, and hence weaker than the energy scale of the helix by another g_{so}. We will often neglect the crystal-field pinning effects in our discussion.

Goldstone Modes

When the ordered phase spontaneously breaks a continuous symmetry of the system, there will be Goldstone modes according to the Goldstone theorem [10]. Physically, Goldstone modes manifest themselves as diverging susceptibilities, i.e. long-range correlation functions. They are one example of what is called "soft modes", i.e., correlations that diverge in the limit of long wavelengths and small frequencies. Magnetic Goldstone modes can be observed directly by neutron scattering, or indirectly by their contributions to various electronic properties, such as the heat capacity and the electric resistivity. Well known examples of a Goldstone mode are the so-called ferromagnons in the ordered phase of a rotationally invariant ferromagnet, where the ordered phase spontaneously breaks

the spin rotational symmetry of the system, and the transverse fluctuations of the magnetization are the Goldstone modes. In MnSi, there is also a Goldstone mode in the helically ordered phase due to the spontaneously broken translational symmetry. The dispersion relation of the Goldstone mode in the helical phase is anisotropic due to the anisotropy of the helical order itself [11]. An external magnetic field, which breaks the rotational symmetry of the pitch vector of the helix will further change the dispersion relation of the Goldstone mode. This modification will change the temperature dependence of the Goldstone-mode contribution to the electronic properties and thus can be observed in experiments.

Quantum Ferromagnetic Phase Transitions

The ferromagnetic phase transition from a paramagnetic phase to a ferromagnetic one at the Curie temperature in materials such as iron, nickel, or cobalt, is a well-known example of a second order phase transition, where the magnetization changes from zero to nonzero continuously. This kind of ferromagnetic phase transition usually happens at a finite Curie temperature, and is referred to as a thermal phase transition. However, a ferromagnetic phase transition can also happen at zero temperature as a function of some nonthermal control parameter such as pressure, magnetic field, or chemical composition, in which case it is referred to as a quantum phase transition. Theoretically, one can consider a quantum ferromagnetic phase transition as a function of the exchange interaction

amplitude. While the finite-temperature phase transitions are driven by thermal fluctuations, zero-temperature quantum phase transitions are driven by quantum fluctuations which are a consequence of Heisenberg's uncertainty principle. Thermal ferromagnetic phase transitions have been well understood for some time [12, 13]; however, there are still properties of the quantum ferromagnetic phase transition that are mysterious.

Quantum phase transitions in general are interesting not only for fundamental theoretical reasons, they are also important for understanding the behavior of real materials at low temperatures. There are many experimental observations of ferromagnetic phase transitions at very low temperatures. An example is MnSi which, at ambient pressure, has a Curie temperature of about 28K. And this critical temperature can be further suppressed by applying hydrostatic pressure [14]. This motivates efforts to obtain a better understanding of the quantum ferromagnetic phase transition.

A very simple model for a quantum ferromagnetic phase transition is the transverse-field Ising model [15]. The Hamiltonian of an Ising model in a transverse field is

$$\mathcal{H} = -H \sum_i S_i^x - \frac{1}{2} \sum_{ij} J_{ij} S_i^z S_j^z \tag{I.1}$$

where S^α with $\alpha = x, y$ or z are components of spin, i, j indicates lattice sites, and only interactions between nearest neighbors are considered here. We take $1/2$ as the magnitude of the spin in each site. J_{ij}, with a Fourier transform $J(\boldsymbol{k})$, is the

exchange interaction and H is the amplitude of the transverse field. In a mean-field approximation, one of the S_i^z in Eq. (I.1) is replaced by its average. The model then describes a spin vector subject to an effective magnetic field

$$\mathbf{h} = H\hat{\mathbf{x}} + J(0)\,\langle S^z\rangle\,\hat{\mathbf{z}} \tag{I.2}$$

and $\langle S^z\rangle$ needs to be determined self-consistently. From the effective magnetic field, we get the ensemble average amplitude of the spin vector as

$$S = \frac{1}{2}\tanh\frac{1}{2}\beta h \tag{I.3}$$

where we have used the fact that the spin amplitude at each site is $1/2$, and $\beta = 1/T$. The z component of the spin is

$$\begin{aligned}\langle S^z\rangle &= \frac{1}{2}\cos\theta\tanh\frac{1}{2}\beta h \\ &= h\cos\theta/J(0)\end{aligned} \tag{I.4}$$

with θ the angle between the spin and the $\hat{z}$ axis, and we have $\sin\theta = H/h$. From Eq. (I.4) we can see that when $H/J(0)$ is less than $1/2$, $\langle S^z\rangle$ will become nonzero at temperatures less than a critical temperature $T_c(H)$. In the ordered phase, $\cos\theta$ is nonzero and the equation of state is $h/J(0) = \frac{1}{2}\tanh\frac{1}{2}\beta h = S$, with $\sin\theta = H/h$. So the critical temperature T_c at which $\cos\theta$ becomes zero is given by

$$H/J(0) = \frac{1}{2}\tanh\frac{1}{2}\beta_c H \tag{I.5}$$

The critical temperature is sketched as a function of H in Fig. 1.3.. As we can see from Fig. 1.3., at zero temperature there is a continuous quantum ferromagnetic phase transition as a function of the transverse field.

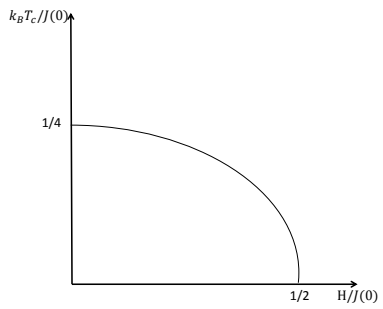

Figure 1.3. Phase diagram of Ising model in a transverse field shown in the temperature-exchange interaction plane. There is a second order transition at zero temperature. After Ref. [15].

The quantum ferromagnetic phase transition in a metallic magnet is much more complicated; it was first described by the Stoner theory of itinerant ferromagnetism [16]. At zero temperature, the systems undergoes a phase transition from a paramagnetic metal to a ferromagnetic one as a function of the exchange coupling J. With increasing J, the conduction band splits into two separate bands for up- and down- spin electrons, with the separation between the two bands known as the Stoner gap. The two separated bands have a common chemical potential, which leads to different densities of the up- and down-spin electron populations, and thus a nonzero magnetization appears. Stoner theory provides a mean-field description of this phase transition.

In 1976, Hertz gave a general scheme for the theoretical treatment of quantum phase transitions [17]. The general idea is to first identify the order parameter of interest, in our case the magnetization, and then perform a Hubbard-Stratonovich

decoupling of the interaction term responsible for the ordering, with the order parameter as the Hubbard-Stratonovich field, and finally to integrate out the fermions to obtain a field theory entirely in terms of the order parameter. The result is a Landau-Ginzburg-Wilson (LGW) theory whose coefficients are given in terms of electronic correlation functions. In quantum statistical mechanics, the statics and the dynamics are automatically coupled, which leads to a description in an effective $(d + z)-$dimensional space, with d the spatial dimension and z the dynamical critical exponent. From a renormalization-group analysis of this LGW theory Hertz concluded that the quantum ferromagnetic phase transition in metals is mean-field like in all systems with spatial dimension $d > 1$. That is, the Stoner theory is exact as far as the static critical behavior is concerned. The dynamics are characterized by the dynamical critical exponent z, which decreases the upper critical dimension d_c^+, above which mean-field theory is exact, by z. In the classical case, $d_c^+ = 4$, and in a clean ferromagnetic system, Hertz found a dynamical critical exponent $z = 3$, so he concluded that the mean-field theory is exact for all $d > 1$ in the quantum case. In the presence of quenched disorder, $z = 4$ as a result of the diffusive electron dynamics, and Hertz theory predicts mean-field critical behavior for all quantum systems with $d > 0$. Millis studied the effects of a nonzero temperature on the quantum ferromagnetic critical behavior [18], which together with Hertz's theory, became the standard description of the ferromagnetic quantum phase transition in metals.

It later became clear that there are problems with Hertz's scheme, in particular for the zero-temperature transition in itinerant ferromagnets. Specifically, it was shown that Hertz's method, if implemented systematically, does not lead to a local quantum field theory for this problem [19]. This nonlocality is due to a coupling of the order-parameter fluctuations to soft modes; i.e., correlation functions that diverge in the limit of zero frequency and wave number. In metallic ferromagnetic systems, soft fermionic particle-hole excitations in the spin-triplet channel couple to the magnetization, and this coupling leads to long-range interactions between the order-parameter fluctuations. In Hertz's scheme, these soft fermionic degrees of freedom are integrated out, and as a result the field theory has vertices that are not finite in the limit of vanishing wave numbers and frequencies. That is, the field theory is non-local. Hertz treated these soft modes in a tree approximation, and as a result crucial qualitative effects were missed. If all of the soft modes, including the order parameter fluctuations and the soft fermionic particle-hole excitations, are kept explicitly on an equal footing, one can derive a local soft-mode field theory by integrating out all massive degrees of freedom. This was done by Belitz et al. [20] for quantum ferromagnets in the presence of quenched disorder. These authors concluded that the fermionic particle-hole excitations which couple to the magnetic fluctuations lead to a continuous ferromagnetic phase transition with non-mean-field critical exponents.

A different result was obtained for clean quantum ferromagnetic systems.

Intuitively one might expect clean systems to be easier to deal with; however, this is not the case because there are more soft modes in clean systems at zero temperature. The nature of the quantum phase transitions in clean itinerant Heisenberg ferromagnet was studied in Ref. [19]. It was found that the fermionic particle-hole excitations in clean systems lead to a fluctuation-induced first-order transition. Thus, the quantum ferromagnetic phase transition in *clean* itinerant ferromagnets is generically of first order. The soft modes responsible for this phenomenon acquire a mass at nonzero temperature, and if the critical temperature is sufficiently high the transition is continuous. There thus is a tricritical point in the phase diagram that separates a line of second-order transitions at relatively high temperatures from a line of first-order transitions at low temperatures. In an external magnetic field, tricritical wings emerge from the tricritical point. The phase diagram of a clean itinerant quantum ferromagnet is shown schematically in Fig. 1.4..

As an example, we also show the observed phase diagram of UGe_2, with a tricritical point and the associated wing structure, in Fig.1.5.. We see that the observed features are the same as in the schematic phase diagram predicted by the theory.

In both the schematic and measured phase diagram, the ferromagnetic transition is of second order at high temperatures, while if the transition temperature is tuned down by the pressure, the transition becomes first order past the tricritical point

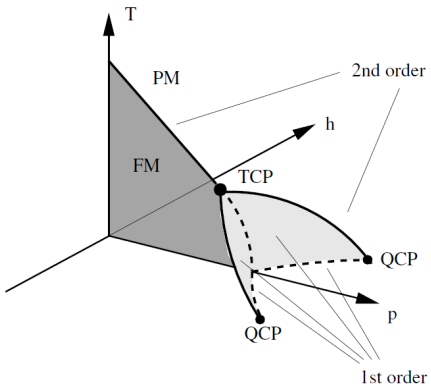

Figure 1.4. Schematic phase diagram of clean itinerant quantum ferromagnets in temprature-pressure-magnetic field space. PM stands for paramagnetic state, FM stands for ferromagnetic state. TCP is a tricritical point, and QCP is the quantum critical point. From [21].

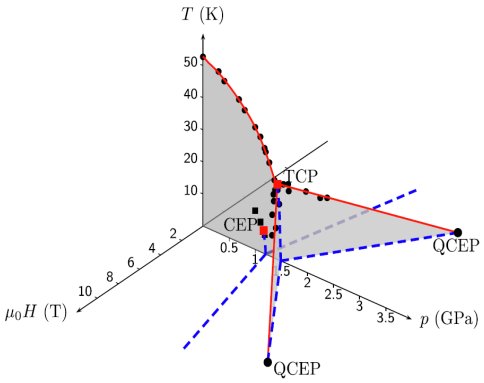

Figure 1.5. Observed wing structure in the temperature-pressure-magnetic-field phase diagram of UGe_2 drawn from resistivity measurement. Gray planes are planes of first order transition. Solid lines are second order lines. From [22].

(TCP). In the presence of an external magnetic field h, tricritical wings connect the tricritical point with two quantum critical points (QCP) in the zero-temperature plane.

This general property of the quantum ferromagnetic phase transition in clean systems, which is very different from Hertz's conclusion, agrees with the experimental observations in all clean systems where the Curie temperature can be tuned to very low temperature. Two well-known examples are $ZrZn_2$ [23] and UGe_2 [24].

Structure of the Dissertation

The purpose of this dissertation is to study some aspects of the phases and phase transitions observed in weak ferromagnets. We will initially focus on the ordered phases of MnSi, and determine the effects of the Goldstone modes on the transport and thermodynamic properties. We then consider how the quantum phase transition evolves from a first-order one in clean systems to a continuous one in disordered systems if one systematically increases the disorder.

This dissertation is organized as follows. In Chapter II, we will discuss the ordered phases of the helical magnet MnSi, focusing on the helical order and the conical order which is formed in an external magnetic field. We will review previous work on the Goldstone mode in the helical phase, and then proceed to derive the

corresponding Goldstone mode in the conical phase. We will then discuss the effects of these Goldstone modes on observable properties.

In Chapter III we study the properties of the quantum ferromagnetic phase transition. As discussed above, the transition at zero temperature in clean systems is generically of first order. Sufficient amounts of quenched disorder will destroy the first order transition and result in a continuous transition with unusual critical exponents. We will develop a comprehensive generalized mean field theory (GMFT) that is suitable for both clean and disordered systems, and study the evolution of the phase diagram with increasing amounts of quenched disorder. We then generalize this GMFT to the case of an anisotropic magnet in an external field, and apply it to the weak ferromagnet URhGe. This system is particularly interesting since the Curie temperature can be tuned to zero by applying a magnetic field transverse to the preferred magnetic axis. We first show that our theory correctly describes the observed phase diagram in clean samples. We then show that quenched disorder decreases the tricritical temperature, and we predict the amount of disorder necessary to drive the transition second order even at zero temperature. These predictions can be directly checked experimentally.

CHAPTER II

HELICAL MAGNETS

Introduction

Introduction to Helical Magnets

Helical magnets are systems in which the long range magnetic order takes the form of a helix. That is, in any given plane perpendicular to a specific direction there is ferromagnetic order, and the direction of the magnetization rotates as one goes along the specific direction, *i.e.*, the direction of the pitch vector $\mathbf{q}$ of the helix. The mechanism for helimagnetism was first proposed by Dzyaloshinskii and Moriya [5–7], who showed that long-period helical superstructures can be caused by an instability of a ferromagnet with respect to the spin-orbit interaction. A necessary condition for the mechanism to work is that the lattice has no inversion symmetry. The lack of inversion symmetry results in a term of the form $\boldsymbol{M}\cdot(\boldsymbol{\nabla}\times\boldsymbol{M})$ in the Hamiltonian or action, with $\boldsymbol{M}$ the magnetic order parameter. This term results from the spin-orbit interaction, and it breaks the spatial inversion symmetry but is invariant under simultaneous rotations of real space and $\boldsymbol{M}$. The presence of such a chiral term favors a nonzero curl of the magnetization and thus leads to a helical ground state.

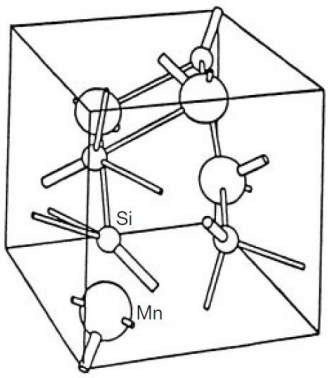

Figure 2.1. Crystal structure of MnSi. There are 4 Mn ions and 4 Si ions in a unit cell. Large and small spheres show Mn and Si, respectively. The positions of Mn and Si ions in a unit cell are given by (u, u, u), (1/2+u, 1/2-u, -u), (-u, 1/2+u, 1/2-u) and (1/2-u, -u, 1/2+u) where u_{Mn} and u_{Si} are 0.138 and 0.845, respectively. From Ref. [25] .

Experimentally, the helical spin arrangement was first observed in FeGe [3], and then in MnSi [4]. Both of these metallic compounds have B20 cubic structures with space group $P2_13$, which indeed breaks inversion symmetry. Nakanishi *et al* [25] and Bak and Jensen [26] did a symmetry analysis of the $P2_13$ structure and showed that a helical magnetic structure can indeed occur in crystals of this structure as a consequence of the Dzyaloshinskii-Moriya mechanism. Historically, MnSi has received much more attention than FeGe, and in this dissertation we will also focus on MnSi, which has a lattice structure shown in Fig.2.1..

Below its critical temperature $T_c \approx 28K$, MnSi displays long-range helical magnetic order with the wavelength of the spiral about 180 $\mathring{A}$, which is much larger than the lattice spacing. This separation of length scales reflects the small coupling constant g_{so} of the spin-orbit interaction which causes the helical order.

The spiral propagates along the equivalent $\langle 1,1,1\rangle$ directions. The pinning of the helix pitch vector to specific directions in the lattice is the effect of the crystal field, which also originates from the spin-orbit interaction, with the pinning effects of order g_{so}^2.

We thus see in MnSi a hierarchy of energy or length scales that can be classified according to their dependence on the powers of the spin-orbit interaction amplitude g_{so}. To zeroth order of g_{so} the system is ferromagnetic, to linear order in g_{so} the system acquires a helical order, and to the second order in g_{so} the helix is pinned by the underlying lattice crystal. Also, an external magnetic field provides another energy scale, which is continuously tunable.

Phase Diagram of MnSi

The hierarchy of energy scales in MnSi leads to an interesting phase diagram, which in the H-T-plane is schematically displayed in Fig. 2.2., where H is the magnetic field and T is the temperature. From the phase diagram we see that MnSi displays a helical magnetic order below the critical temperature T_c. When there is no external magnetic field, the helix is pinned to the $\langle 1,1,1\rangle$ directions by the crystal-field effects. An external magnetic field not in one of the $\langle 1,1,1\rangle$ directions will tilt the helix away from the $\langle 1,1,1\rangle$ directions until the pitch vector $\mathbf{q}$ aligns with the direction of the magnetic field at a critical field strength H_{c1}. The external magnetic field will induce a homogeneous component of the magnetization, which is superimposed onto the helical order and leads to the so-called conical

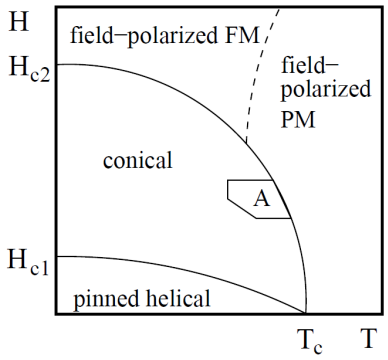

Figure 2.2. Schematic phase diagram of MnSi in the $H - T$ plane. In zero magnetic field, the system is in helical phase when temperature is below the Curie temperature. from [29].

phase [27]. As the magnetic field continues to increase from H_{c1}, the amplitude of the helix decreases and finally goes to zero continuously at another critical field H_{c2}, where the system enters a field-polarized ferromagnetic phase. We also see in the phase diagram a region called "A phase" which is inside the conical phase and at intermediate fields near T_c. The A phase was thought to represent a helix with a pitch vector perpendicular to the magnetic field, but more recently has been interpreted as a topological phase where three helices with co-planar **q**-vectors form a skyrmion-like structure [28].

LGW Functional

To explain the phase diagram of MnSi, we consider a LGW functional for a three-dimensional order parameter (OP) field $\boldsymbol{M} = (M_1, M_2, M_3)$, whose expectation value is proportional to the magnetization. We organize the various terms in the action according to their dependence on powers of the spin-orbit coupling constant

g_{so}. At zeroth order of g_{so} we have the microscopic scale, which is represented by the Fermi energy and the Fermi wave number k_F. This is renormalized by fluctuations to the critical scale, which is represented by the magnetic critical temperature T_c and the corresponding length scales. The physics at these scales is that of a classical Heisenberg ferromagnet, whose action we denote by S_H, see Eq. (II.2). The energy scale at first order in g_{so} is the chiral scale, given by the microscopic scale times g_{so}. The parameters of the helix are determined by this scale, in particular the helical pitch wave number q is proportional to g_{so}, which we will see later by explicit calculation. In MnSi, this scale is about 100 times smaller than the microscopic scale. We describe the physics at this scale by the action S_{DM} in conjunction with S_H. At second order in g_{so}, the crystal-field effects which are smaller than the chiral scale by another factor of g_{so} show up and they pin the helix to specific directions of the lattice.

In this chapter we will focus on the properties of the Goldstone mode in the conical phase, and will not discuss properties related to the crystal-field pinning effects. That is, for our purpose we only keep the energy scales up to linear order in g_{so}, which is equivalent to ignoring the lattice structures and only keeping in mind that the system does not have a spatial inversion symmetry. We will also ignore the A phase in this dissertation. More details about the properties related to crystal-field pinning effects and the A phase are given in reference [29]. Within

the scheme we just described, and keeping terms to linear order in g_{so}, we have the action

$$S = S_H + S_{DM} \tag{II.1}$$

where S_H describes an isotropic classical Heisenberg ferromagnet in a homogeneous external magnetic field $\boldsymbol{H}$,

$$\begin{aligned} S_H = \int_V d\boldsymbol{x} [& \frac{t}{2}\mathbf{M}^2(\boldsymbol{x}) + \frac{a}{2}(\nabla \mathbf{M}(\boldsymbol{x}))^2 \\ & + \frac{d}{2}(\nabla \cdot \mathbf{M}(\boldsymbol{x}))^2 + \frac{u}{4}(\mathbf{M}^2(\boldsymbol{x}))^2 \\ & - \mathbf{H} \cdot \mathbf{M}(\boldsymbol{x})] \end{aligned} \tag{II.2}$$

where $\int_V d\boldsymbol{x}$ denotes a real-space integral over the system volume. $(\nabla \boldsymbol{M})^2$ is $\sum_{i,j=1}^{3} \partial_i M_j \partial_i M_j$ with $\partial_i \equiv \partial/\partial x_i$ the components of the gradient operator $\boldsymbol{\nabla} \equiv (\partial_1, \partial_2, \partial_3) \equiv (\partial_x, \partial_y, \partial_z)$. t, a, d and u are the parameters of the LGW theory. They are of zeroth order in the spin-orbit coupling constant g_{so} as we mentioned above, and are thus related to the microscopic energy and length scales.

Equation (II.2) contains all analytic terms invariant under simultaneous rotations of real space and the magnetic order-parameter space up to quartic order in $\boldsymbol{M}$ and bi-quadratic order in $\boldsymbol{M}$ and $\boldsymbol{\nabla}$. The term $(\boldsymbol{\nabla} \cdot \boldsymbol{M})^2$, when combined with the term $(\nabla \boldsymbol{M})^2$, is equivalent to a term $(\boldsymbol{\nabla} \times \boldsymbol{M})^2$, which together with a stronger one, $|\boldsymbol{k} \cdot \boldsymbol{M}(\boldsymbol{k})|^2/k^2$ in Fourier space, results from the classical dipole-dipole interaction. The classical dipole-dipole interaction in turn results from the

coupling of the order-parameter field to the electromagnetic vector potential [30]. The coefficients of these terms are thus small due to the relativistic nature of the dipole-dipole interaction, and these terms are usually neglected when discussing isotropic classical Heisenberg ferromagnets.

We are interested in the helical magnetism that is caused by terms of linear order in the spin-orbit coupling constant g_{so}, so it is less obvious whether these terms can be ignored. We have studied the effects of the dipole-dipole interaction on the phase transition properties of classical helical magnets using the same method as used by Bak and Jensen [26], and did not find anything interesting. This conclusion, although it needs to be confirmed by further studies, lends support to the notion that we can neglect the terms resulting from the dipole-dipole interaction. Also, for the field configuration we are considering here, the terms from the dipole-dipole interaction are not different from the term $(\nabla \mathbf{M})^2$, so we neglect them from now on.

The Dzyaloshinskii-Moriya (DM) term that favors a nonvanishing curl of the magnetization has the form

$$S_{DM} = \frac{c}{2} \int_V d\boldsymbol{x}\ \mathbf{M}(\boldsymbol{x}) \cdot (\nabla \times \mathbf{M}(\boldsymbol{x})) \tag{II.3}$$

This term depends on the spin-orbit coupling and can only exist when there is no spatial inversion symmetry, since it depends linearly on the gradient operator.

The coupling constant c is linear in g_{so}, and on dimensional ground we have,

$$c = ak_F g_{so} \tag{II.4}$$

where k_F is the Fermi wave number which serves as the microscopic inverse length scale. In our context, this can be considered as the definition of g_{so}.

In all, by keeping only terms that are of interest to us, we get for the action of a rotational invariant helical magnet

$$\begin{aligned} S = \int_V d\boldsymbol{x}[&\frac{t}{2}\mathbf{M}^2(\boldsymbol{x}) + \frac{a}{2}(\nabla\mathbf{M}(\boldsymbol{x}))^2 \\ &+ \frac{c}{2}\mathbf{M}(\boldsymbol{x})\cdot(\nabla\times\mathbf{M}(\boldsymbol{x})) + \frac{u}{4}(\mathbf{M}^2(\boldsymbol{x}))^2 \\ &- \mathbf{H}\cdot\mathbf{M}(\boldsymbol{x})] \end{aligned} \tag{II.5}$$

Phase Diagram

We now derive the mean-field phase diagram for systems described by the action given in Eq. (II.5). From Ref. [28] we know that field configurations of the form

$$\boldsymbol{M}(\boldsymbol{x}) = \boldsymbol{m}_0 + m_1\hat{\boldsymbol{e}}_1\cos(\boldsymbol{q}\cdot\boldsymbol{x}) + m_2\hat{\boldsymbol{e}}_2\sin(\boldsymbol{q}\cdot\boldsymbol{x}) \tag{II.6}$$

yield a global minimum of the action S in Eq. (II.5). Here $\boldsymbol{m}_0$ is the homogeneous component of the magnetization, $m_{1,2}$ are amplitudes of Fourier components with wave vector $\boldsymbol{q}$, and $\hat{\boldsymbol{e}}_{1,2}$ are two unit vectors that form a right-handed *dreibein* together with $\boldsymbol{q}$:

$$\hat{\boldsymbol{e}}_1\times\hat{\boldsymbol{e}}_2 = \hat{\boldsymbol{q}}, \quad \hat{\boldsymbol{e}}_2\times\hat{\boldsymbol{q}} = \hat{\boldsymbol{e}}_1, \quad \hat{\boldsymbol{q}}\times\hat{\boldsymbol{e}}_1 = \hat{\boldsymbol{e}}_2 \tag{II.7}$$

where $\hat{\boldsymbol{q}} = \boldsymbol{q}/q$. The sinusoidal terms in Eq.II.6 describe a helix with pitch vector $\boldsymbol{q}$. In general, the helix is elliptically polarized. Here we will consider only the circularly polarized case, i.e., $m_1 = m_2$. A more general description can be found in Ref.[29].

Now we can derive the phase digram. We will follow the hierarchy of energy scales described above; that is, we always discuss ferromagnets first and then helimagnets.

Ferromagnets

We first consider terms to zeroth order in g_{so}, in which case the system is approximated by a ferromagnet. From the action S_H in Eq. (II.2) we see that for $H = 0$ there is a second-order phase transition at $t = 0$ in mean-field approximation. When $H \neq 0$, there is a crossover from a field-polarized paramagnetic state to a field-polarized ferromagnetic state at $t = 0$. In the field-polarized paramagnetic state, the magnetization extrapolates to zero for $H \to 0$ while in the field-polarized ferromagnetic state it extrapolates to $\boldsymbol{m}_0 = \sqrt{-t/u}\,\hat{\boldsymbol{H}}$. The free energy density in mean-field approximation and in a zero field is,

$$f = S/V = -t^2/4u \tag{II.8}$$

In a nonzero field, we get the free energy density as,

$$f = \frac{t}{2}m_0^2 + \frac{u}{4}m_0^4 - Hm_0 \tag{II.9}$$

where m_0 is the solution of the mean-field equation of state,

$$tm_0 + um_0^3 = H \tag{II.10}$$

This is just the well-known classic Heisenberg model.

Helimagnets, Conical Phase

We next include in the action the DM term which is of linear order of g_{so}. The DM terms favors a nonzero curl of the magnetization, and the direction of the curl depends on the sign of c. The DM term itself would favor an arbitrarily large curl of the magnetization, however, the other gradient term in the action, $(\boldsymbol{\nabla M})^2$, limits the magnitude of the curl. We thus expect a spatial modulation of $\boldsymbol{M}$ on a length scale on the order of a/c. We will check this by showing that the ansatz in Eq. (II.6) with a circular polarization, i.e., $m_1 = m_2 \equiv m_1$ indeed solves the saddle-point equations for the action S in Eq. (II.5). Putting the ansatz into the action we get the free energy as

$$f = \frac{t}{2}(m_0^2 + m_1^2) + \frac{1}{2}aq^2 m_1^2 - \frac{1}{2}cqm_1^2 + \frac{1}{4}u(m_0^2 + m_1^2)^2 - Hm_0 \tag{II.11}$$

By extremizing this free energy with respect to m_0 and m_1 we get

$$\boldsymbol{q} = q\hat{\boldsymbol{H}}, \tag{II.12}$$

$$\boldsymbol{m}_0 = m_0\hat{\boldsymbol{H}}, \tag{II.13}$$

and

$$m_0 = H/(cq - aq^2), \tag{II.14}$$

$$m_1^2 = -(t + aq^2 - cq)/u - H^2/(cq - aq^2)^2 \tag{II.15}$$

To determine the value of q, we again extremize the free energy with respect to q and get $q = c/2a$ for all values of H, which agrees with our previous analysis. We still need to ascertain that the solution is a minimum, which turns out to be true when $t < aq^2$ and $H < aq^2\sqrt{(aq^2 - t)/u}$. We thus conclude that the field configuration

$$\mathbf{M}(\boldsymbol{x}) = m_0\hat{\boldsymbol{H}} + m_1(\hat{\boldsymbol{e}}_1 \cos(q\hat{\boldsymbol{H}} \cdot \boldsymbol{x}) + \hat{\boldsymbol{e}}_2 \sin(q\hat{\boldsymbol{H}} \cdot \boldsymbol{x})) \tag{II.16}$$

with $\hat{\boldsymbol{e}}_1$,$\hat{\boldsymbol{e}}_2$, $\hat{\boldsymbol{H}}$ forming a *dreibein*, and

$$q = c/2a, \quad m_0 = H/aq^2, \quad m_1 = \sqrt{-r/u}(1 - (H/H_{c2})^2) \tag{II.17}$$

with

$$r = t - aq^2, \quad H_{c2} = aq^2\sqrt{-r/u} \tag{II.18}$$

minimizes the free energy in the parameter range $r < 0$ and $H < H_{c2}$. We thus confirmed that Eqs. (II.16)-(II.18) describe the helical phase for $H = 0$ and the conical phase for $0 < H < H_{c2}$. The mean-field free energy density in this range is

$$f = -r^2/4u - H^2/(2aq^2) \tag{II.19}$$

By comparing Eq. (II.19) with Eq. (II.8) we see that the helical transition pre-empts the ferromagnetic one. The amplitude m_1 of the helix decreases with increasing H for $H < H_{c2}$ and vanishes at H_{c2}, and the free energy Eq. (II.19) approaches that of

the ferromagnet, Eq. (II.9) and Eq. (II.10) as $H \to H_{c2}$. For $H > H_{c2}$ the equation of state and the free energy for the DM action S are the same as for a ferromagnet S_H. Thus we get the phase diagram shown in Fig. 2.2.. Here we have ignored energy scales to second order in g_{so}, and hence the pinning of the helix.

The Nature of the Goldstone Modes in Classical Helimagnets

Physically, a Goldstone mode represents a long-ranged correlation function and thus a diverging susceptibility. The susceptibility of a material describes its response to an applied field, so it is reasonable to say that a diverging susceptibility means a soft mode. Goldstone's theorem states that if a continuous symmetry of the Hamiltonian is spontaneously broken by the state the system is in, then there will be one or more Goldstone modes. The number of Goldstone modes is determined by the dimensions of the original symmetry group of the system and the remaining subgroup in the broken symmetry phase, more specifically, the number of the Goldstone modes equals the dimension of the coset space G/H, where G is the symmetry group of the Hamiltonian and H subgroup of the ordered phase.

A well-known example of Goldstone modes are the so-called ferromagnons in ferromagnets. The rotational symmetry of a ferromagnetic system whose magnetization has three components is described by the rotational group SO(3). In the ordered phase, the magnetization chooses a specific direction and breaks the rotational symmetry. The system in the ordered phase is only invariant

under rotations around the axis in the direction of the magnetization, that is, the system is now described by the group SO(2). By Goldstone's theorem, there exist dim(SO(3)/SO(2)) =2 Goldstone modes in the ordered phase of a ferromagnetic system with a three-component magnetization.

To see this more explicitly, we present an argument given by Ma [12]. Consider a ferromagnet in its ordered state with magnetization $\boldsymbol{m}$. If one applies a small external magnetic field $\boldsymbol{h}$, the magnetization will align with the direction of the external field. If we change the magnetic field to $\boldsymbol{h} + \delta\boldsymbol{h}$, the magnetization will become $\boldsymbol{m}+\delta\boldsymbol{m}$. If $\delta\boldsymbol{h} \parallel \boldsymbol{h}$, the ratio $\delta m/\delta h$ is called the longitudinal susceptiblity, where δm and δh are the magnitudes of $\delta\boldsymbol{m}$ and $\delta\boldsymbol{h}$, respectively. If $\delta\boldsymbol{h} \perp \boldsymbol{h}$, the ratio $\delta m/\delta h$ is called the transverse susceptibility. Now we rotate the magnetic field by an infinitesimal angle $\delta h/h$, which is equivalent to applying an infinitesimally small field $\delta\boldsymbol{h}$ perpendicular to $\boldsymbol{h}$. This results in the magnetization rotating by the same angle, which equals $\delta m/m$. We thus get

$$\delta m/m = \delta h/h \tag{II.20}$$

where $\delta\boldsymbol{m} \perp \boldsymbol{m}$. As a result, we have

$$\delta m/\delta h = m/h \tag{II.21}$$

Now if we let $h \to 0$ in the ordered phase, where $m \neq 0$, the transverse susceptiblity $\delta m/\delta h$ diverges. This says that below the Curie temperature T_c, when

$h = 0$, the transverse fluctuations of ferromagnets are soft, *i.e.* it costs no energy to rotate the magnetization. More generally, for a ferromagnetic system with an n-component magnetization, there are $n - 1$ Goldstone modes.

In the ordered phase of helical magnets, the helical order spontaneously breaks the translational symmetry, and thus according to Goldstone's theorem there exists one Goldstone mode in the helically orderered phase. In the following sections we calculate the Goldstone modes explicitly from the Hamiltonian.

Classical Ferromagnons

To calculate the Goldstone mode in the helical phase of MnSi we again follow the hierarchy of energy scales according to their dependences on orders of g_{so}, and first calculate the Goldstone modes in ferromagnets, *i.e.*, the ferromagnons, explicitly.

A standard method to derive the ferromagnons is to use the nonlinear σ-model (NLσM) [31]. Consider the fluctuations about the mean-field or saddle-point solution for the classical Heisenberg ferromagnet whose action is given by Eq. (II.2), with the term $\frac{d}{2}(\nabla \cdot \mathbf{M}(\boldsymbol{x}))^2$ neglected as we did for helimagnets. One can parameterize the order parameter field as

$$\boldsymbol{M}(\boldsymbol{x}) = m_0 \begin{pmatrix} \pi_1(\boldsymbol{x}) \\ \pi_2(\boldsymbol{x}) \\ \sqrt{1 - \pi_1^2(\boldsymbol{x}) - \pi_2^2(\boldsymbol{x})} \end{pmatrix} \tag{II.22}$$

where we have chosen $\boldsymbol{m}_0$ to be in the z-direction and have neglected the fluctuations of the magnetization amplitude m_0, which is massive. The latter

statement can be shown to be true by an explicit calculation, but it also follows from Ma's argument reproduced above. We then expand the action to bilinear order in $\pi_{1,2}$,

$$S_H = S_{sp} + \int_V d\boldsymbol{x}(\frac{1}{2}am_0^2[(\boldsymbol{\nabla}\pi_1(\boldsymbol{x}))^2 + (\boldsymbol{\nabla}\pi_2(\boldsymbol{x}))^2] + \frac{1}{2}Hm_0[(\pi_1(\boldsymbol{x}))^2 + (\pi_2(\boldsymbol{x}))^2]) \tag{II.23}$$

After a Fourier transform it is easy to see there are two identical eigenvalues in momentum space,

$$\lambda = \frac{m_0}{2}(am_0\boldsymbol{k}^2 + H) \tag{II.24}$$

It is then obvious that for $H = 0$, $\lambda(\boldsymbol{k} \to 0) \to 0$, which reveals the two Goldstone modes, the well-known ferromagnons. This is the static manifestation of the spontaneously broken symmetry. To determine the dynamics one needs to solve an appropriate kinetic equation within a classical context [12] or treat the problem quantum mechanically [17, 32].

We now discuss the dynamics using the time dependent Ginzburg-Landau (TDGL) theory for ferromagnets, where the kinetic equation for the time-dependent generalization of the magnetization field $\boldsymbol{M}$ reads,

$$\partial_t \boldsymbol{M}(\boldsymbol{x},t) = -\gamma \boldsymbol{M}(\boldsymbol{x},t) \times \frac{\delta S}{\delta \boldsymbol{M}(\boldsymbol{x})}|_{\boldsymbol{M}(\boldsymbol{x},t)} - \int d\boldsymbol{y} D(\boldsymbol{x}-\boldsymbol{y}) \frac{\delta S}{\delta \boldsymbol{M}(\boldsymbol{y})}|_{\boldsymbol{M}(\boldsymbol{y},t)} + \zeta(\boldsymbol{x},t) \tag{II.25}$$

where γ is a constant and the first terms describes the precession of the magnetic moment in the magnetic field generated by all other magnetic moments. The

damping operator D describes the dissipation. In the case of a conserved order parameter, D is proportional to a gradient squared. ζ is a random Langevin force with zero mean, $\langle\zeta(\boldsymbol{x},t)\rangle = 0$, and a second moment consistent with the fluctuation-dissipation theorem, which requires

$$\langle\zeta(\boldsymbol{x},t)\zeta(\boldsymbol{y},t)\rangle = D(\boldsymbol{x}-\boldsymbol{y}) \tag{II.26}$$

We now consider deviations from the equilibrium state as in Eq. (II.22), with $\pi_{1,2}$ now also time dependent. Our main goal is to find the dynamical dispersion relation of the Goldstone modes, so we neglect the dissipative term for the time being and consider $H = 0$. We now calculate the average deviations $\langle\pi_i(\boldsymbol{x},t)\rangle$ using the kinetic equation Eq. (II.25) and get,

$$\partial_t\pi_i(\boldsymbol{x},t) = -\gamma\frac{1}{2}am_0\boldsymbol{\nabla}^2\pi_i(\boldsymbol{x},t) \tag{II.27}$$

where $i = 1,2$ and I have suppressed the averaging brackets in the notation for simplicity. Fourier transforming this we get the dispersion relation of the ferromagnons for small wave numbers,

$$\omega_{FM}(\boldsymbol{k}) = D\boldsymbol{k}^2 \tag{II.28}$$

where $D = \gamma\, a\, m_0/2$ is the spin wave stiffness, which vanishes linearly as the magnetization goes to zero.

Classical Helimagnons

Now we keep the terms of first order in the spin-orbit coupling constant g_{so}, which lead to the helical and conical phases when the magnetic field is zero and nonzero, respectively. For these phases the relevant symmetry is the translational one. If we denote the Lie group of one-dimensional translations by T, then the action is invariant under $T \otimes T \otimes T \equiv T^3$. The helical and conical states discussed in Sec.II.2.2 break the T^3 symmetry down to T^2 since the system is no longer translational invariant along the direction of the pitch vector in the helical or conical phases, so there should be one Goldstone mode in these ordered phases according to the Goldstone theorem. The dispersion relation of the Goldstone mode in the helical phase has been given in Ref. [11] as $\omega_{HM}(\boldsymbol{k}) = \sqrt{c_{\parallel} k_{\parallel}^2 + c_{\perp} \boldsymbol{k}_{\perp}^4 / q^2}$, where $k_{\parallel}$ and $\boldsymbol{k}_{\perp}$ are the components of the wave vector parallel and perpendicular to the helix pitch vector $\boldsymbol{q}$, respectively. This anisotropic dispersion relation of the Goldstone mode can be seen by simple physical arguments. At first guess one might think that the soft fluctuations in the helical phase are phase fluctuations of the form,

$$\mathbf{M}(\boldsymbol{x}) = m(\cos(qz + \phi(\boldsymbol{x})), \cos(qz + \phi(\boldsymbol{x})), 0) \tag{II.29}$$

where we have chosen a coordinate system such that $\{\hat{\boldsymbol{e}}_1, \hat{\boldsymbol{e}}_2, \hat{\boldsymbol{q}}\} = \{\hat{x}, \hat{y}, \hat{z}\}$ for convenience. By putting this parameterization of the order parameter field into Eq. (II.5) and keeping to Gaussian order of the fluctuations, with zero magnetic

field, we get an effective action,

$$S_{eff}[\phi] = const. \int d\boldsymbol{x} (\nabla\phi(\boldsymbol{x}))^2 \tag{II.30}$$

However, this cannot be true, as can be seen from the following argument [33]. Consider an infinitesimal rotation of the planes containing the spins such that their normal changes from $(0, 0, q)$ to $(\alpha_1, \alpha_2, \sqrt{q^2 - \alpha_1^2 - \alpha_2^2})$. To linear order in α_i $(i = 1, 2)$, this corresponds to a phase fluctuation $\phi(\boldsymbol{x}) = \alpha_1 x + \alpha_2 y$. This rotation does not cost any energy; however, $(\nabla\phi(\boldsymbol{x}))^2 = \alpha_1^2 + \alpha_2^2 \neq 0$ for this particular fluctuation, so this cannot be the correct answer. The problem is that the effective action cannot depend directly on $\nabla_\perp\phi$, where $\nabla = (\nabla_\perp, \nabla_z)$. So the lowest-order term allowed by the rotational symmetry that involves the gradients perpendicular to $\boldsymbol{q}$ is of the form $(\nabla_\perp^2 u)^2$, with u a generalized phase variable. We thus expect the effective action to have a form,

$$S_{eff}[u] = \frac{1}{2} \int d\boldsymbol{x} \left[c_z (\partial_z u(\boldsymbol{x}))^2 + c_\perp (\boldsymbol{\nabla}_\perp^2 u(\boldsymbol{x}))^2 / q^2 \right] \tag{II.31}$$

where c_z and $c_\perp$ are elastic constants. The Goldstone mode in the helically ordered phase thus has an anisotropic dispersion relation: it is softer in the direction perpendicular to the pitch vector of the helix than in the longitudinal direction. The factor $1/q^2$ in the transverse term in Eq. (II.31) serves to make sure that c_z and $c_\perp$ have the same dimension. Since the nonzero pitch wave number is the reason for the anisotropy, it is a natural length scale to enter here, which will later be shown to be correct by an explicit calculation. We thus get an inverse order-

parameter susceptibility proportional to $c_z k_z^2 + c_\perp \boldsymbol{k}_\perp^4/q^2$, with k_z and $\boldsymbol{k}_\perp$ wave vector components parallel and perpendicular, respectively, to the helical pitch vector $\boldsymbol{q}$.

When the external magnetic field is nonzero, the ground state is the conical phase, where the pitch vector is aligned with the direction of the magnetic field, so there is no longer rotational symmetry for the pitch vector. Our previous argument for why the effective action cannot depend on $(\boldsymbol{\nabla}_\perp u(\boldsymbol{x}))^2$ is no longer true in the conical phase. We thus expect a $\beta \boldsymbol{k}_\perp^2$ term in the inverse order parameter susceptiblity, with β a prefactor depending on the magnetic field. The prefactor is expected to be an analytic function of H and the natural guess would be $\beta \propto H^2$ under this condition. We therefore expect the Goldstone mode in the conical phase to have a schematic form as $c_z k_z^2 + H^2 \boldsymbol{k}_\perp^2 + c_\perp \boldsymbol{k}_\perp^4/q^2$.

We now perform an explicit calculation for the Goldstone mode in the conical phase. We start from the saddle-point field configuration, Eq. (II.16) - Eq. (II.18), and go through the same process as we did for ferromagnets by parameterizing the order parameter and expanding the action to Gaussian order in the fluctuations. A

complete parameterization of the fluctuations about the saddle point has the form,

$$\begin{aligned}\mathbf{M}(\boldsymbol{x}) =&(m_0+\delta m_0(\boldsymbol{x}))\begin{pmatrix}\psi_3(\boldsymbol{x})\\ \psi_4(\boldsymbol{x})\\ \sqrt{1-\psi_3^2(\boldsymbol{x})-\psi_4^2(\boldsymbol{x})}\end{pmatrix}\\ &+\frac{m_1+\delta m_1(\boldsymbol{x})}{\sqrt{1+\psi^2(\boldsymbol{x})}}\begin{pmatrix}\cos(qz+\psi_0(\boldsymbol{x}))\\ \sin(qz+\psi_0(\boldsymbol{x}))\\ \psi(\boldsymbol{x})\end{pmatrix}\end{aligned} \tag{II.32}$$

where the first term describes fluctuations for a homogeneous magnetization. The second term parameterizes the fluctuations of the helix. The amplitude fluctuations are again expected to be massive (this can be confirmed by an explicit calculation), so we drop δm_0 and δm_1. Upon performing a Fourier transform, $\psi_0(\boldsymbol{k}=0)$ corresponds to taking $\mathbf{M}$ at $\boldsymbol{k}=\boldsymbol{q}$, while ψ and $\mathbf{M}$ have the same wave number, so we write,

$$\psi(\boldsymbol{x}) = \psi_1(\boldsymbol{x})\cos qz + \psi_2(\boldsymbol{x})\sin qz\ . \tag{II.33}$$

Here ψ_1 and ψ_2 are restricted to containing Fourier components with $|\boldsymbol{k}| \ll q$ to avoid overcounting. Putting this parameterization of the order parameter into the helical action S in Eq. (II.5) and expanding the action about the saddle point solution to bilinear order in fluctuations, we get an effective Gaussian action in momentum space:

$$S^{(2)} = \frac{a^2q^4}{2uV}\sum_{\boldsymbol{k}}\sum_{i,j=0}^{4}\psi_i(\boldsymbol{k})\gamma_{ij}(\boldsymbol{k})\psi_j(\boldsymbol{k}) \tag{II.34}$$

with

$$\gamma(\boldsymbol{k}) = \begin{pmatrix} \hat{m}_1^2\hat{k}^2 & -i\hat{m}_1^2\hat{k}_x & -i\hat{m}_1^2\hat{k}_y & 0 & 0 \\ i\hat{m}_1^2\hat{k}_x & \hat{m}_1^2(1+\hat{m}_0^2+\frac{1}{2}\hat{k}^2) & -i\hat{m}_1^2\hat{k}_z & \hat{m}_0^2\hat{m}_1^2 & 0 \\ i\hat{m}_1^2\hat{k}_y & i\hat{m}_1^2\hat{k}_z & \hat{m}_1^2(1+\hat{m}_0^2+\frac{1}{2}\hat{k}^2) & 0 & \hat{m}_0^2\hat{m}_1^2 \\ 0 & \hat{m}_0^2\hat{m}_1^2 & 0 & \hat{m}_0^2(1+\hat{m}_1^2+\hat{k}^2) & -2i\hat{m}_0^2\hat{k}_z \\ 0 & 0 & \hat{m}_0^2\hat{m}_1^2 & 2i\hat{m}_0^2\hat{k}_z & \hat{m}_0^2(1+\hat{m}_1^2+\hat{k}^2) \end{pmatrix} \tag{II.35}$$

where we have defined $\hat{\boldsymbol{k}} = \boldsymbol{k}/q$ and $\hat{m}_{0,1}^2 = um_{0,1}^2/aq^2$. Now we see that of the five eigenvalues of the matrix $\gamma(\boldsymbol{k})$ one goes to zero as $\boldsymbol{k} \to 0$, so there is one Goldstone mode, which agrees with our previous symmetry arguments. By solving the corresponding eigenvalue equation perturbatively we get the eigenvalues at nonzero wave vector $\boldsymbol{k}$,

$$\lambda_1 = \alpha\hat{k}_z^2 + \beta\hat{\boldsymbol{k}}_\perp^2 + \delta\hat{\boldsymbol{k}}_\perp^4 \tag{II.36}$$

with

$$\alpha = \hat{m}_1^2 \tag{II.37}$$

$$\beta = \frac{\hat{m}_0^2\hat{m}_1^2}{1+\hat{m}_0^2+\hat{m}_1^2} \tag{II.38}$$

$$\delta = \frac{1}{2}\hat{m}_1^2\frac{(1+\hat{m}_1^2)^3 - \hat{m}_0^2(1+\hat{m}_1^4) + 2\hat{m}_0^4\hat{m}_1^2}{(1+\hat{m}_0^2+\hat{m}_1^2)^3} \tag{II.39}$$

Here the prefactor β for $\boldsymbol{k}_\perp^2$ is proportional to $\hat{m}_0^2$, which is proportional to H^2, in agreement with our expectation. For $H = 0$, this reduces to the helimagnon result

in Ref.[11]. There are four massive eigenvalues that appear in pairs. At zero wave number, they are

$$\lambda_2 = \lambda_3 = \hat{m}_1^2(1 + \hat{m}_0^2 + O(\hat{m}_0^4)) \tag{II.40}$$

$$\lambda_4 = \lambda_5 = \hat{m}_0^2(1 + \hat{m}_1^2) + O(\hat{m}_0^4) \tag{II.41}$$

We recognize $\lambda_{2,3}$ as massive helimagnon modes modified by the presence of m_0, and $\lambda_{4,5}$ as massive ferromagnon modes, Eq. (II.24), modified by the presence of m_1.

To determine the dynamics one again needs some additional steps, which lead to a resonance frequency that is proportional to the square root of the inverse susceptibility, unlike the ferromagnetic one. For simplicity, we first consider the helical phase with $H = 0$, where the dispersion relation reads [11]

$$\omega_{HM} = \sqrt{c_z k_z^2 + c_\perp \boldsymbol{k}_\perp^4 / q^2} \tag{II.42}$$

We will derive this dispersion relation using the TDGL formalism, similar to what we did for the dynamics in ferromagnets. In zero magnetic field the equilibrium state in the helical phase is

$$\boldsymbol{M}_{sp}(\boldsymbol{x}) = M(\cos qz, \sin qz, 0) \tag{II.43}$$

where we have chosen the pitch vector to be in $\hat{z}$ direction as before. We now consider deviations from the equilibrium state. The generalized phase modes

at wave vector $\boldsymbol{k} = \boldsymbol{q}$ are soft since they are Goldstone modes as discussed above. Other than this, there are soft modes at zero wave vector due to the spin conservation; these we denote by $\boldsymbol{m}(\boldsymbol{x}, t)$. In all we get the time dependent magnetization field,

$$\boldsymbol{M}(\boldsymbol{x}, t) = \boldsymbol{M}_{sp}(\boldsymbol{x}) + \boldsymbol{m}(\boldsymbol{x}, t) + Mu(\boldsymbol{x}, t)(-\sin qz, \cos qz, 0) \tag{II.44}$$

The effective action for the fluctuations thus has a form,

$$S_{eff}[\boldsymbol{m}, u] = \frac{r_0}{2} \int d\boldsymbol{x}\ \boldsymbol{m}^2(\boldsymbol{x}, t) + S_{eff}[u] \tag{II.45}$$

where the action for $\boldsymbol{m}$ is a renormalized Ginzburg-Landau action which is kept to Gaussian order. The mass r_0 is assumed to be positive here. $S_{eff}[u]$ is given in Eq. (II.31). We can now calculate $\langle \boldsymbol{m}(\boldsymbol{x}, t) \rangle$ and $\langle u(\boldsymbol{x}, t) \rangle$ by using the kinetic equation, Eq. (II.25). As in the ferromagnetic case, we again neglect the damping term and suppress the average brackets and the explicit time dependence in our notation for simplicity. To linear order in the fluctuations we get

$$\begin{aligned}
\partial_t M_3(\boldsymbol{x}, t) &= \partial_t m_3(\boldsymbol{x}, t) \\
&= -\gamma \epsilon_{3ij} M^i_{sp}(\boldsymbol{x}) \frac{\delta S}{\delta M_j(\boldsymbol{x})} |_{\boldsymbol{M}(\boldsymbol{x},t)} \\
&= -\gamma \epsilon_{3ij} M^i_{sp}(\boldsymbol{x}) \int d\boldsymbol{y} \frac{\delta S}{\delta u(\boldsymbol{y})} \frac{\delta u(\boldsymbol{y})}{\delta M_j(\boldsymbol{x})} |_{\boldsymbol{M}(\boldsymbol{x},t)} \\
&= -\gamma M \int d\boldsymbol{y} \frac{\delta S}{\delta u(\boldsymbol{y})} \left[\cos qz \frac{\partial u(\boldsymbol{y})}{\partial M_y(\boldsymbol{x})} - \sin qz \frac{\partial u(\boldsymbol{y})}{\partial M_x(\boldsymbol{x})} \right] |_{\boldsymbol{M}(\boldsymbol{x},t)}
\end{aligned} \tag{II.46}$$

By using the identity

$$\delta(\boldsymbol{x} - \boldsymbol{y}) = \int d\boldsymbol{z} \frac{\delta u(\boldsymbol{x})}{\delta M_i(\boldsymbol{z})} \frac{\delta M_i(\boldsymbol{z})}{\delta u(\boldsymbol{y})} \tag{II.47}$$

for the time dependent magnetization field $\boldsymbol{M}(\boldsymbol{x},t)$ in Eq. (II.44) and using the result in Eq. (II.47) we get,

$$\begin{aligned}\partial_t m_3(\boldsymbol{x},t) &= -\gamma \frac{\delta S_{eff}}{\delta u(\boldsymbol{x})}|_{u(\boldsymbol{x},t)} \\ &= -\gamma(-c_z\partial_z^2 + c_\perp \boldsymbol{\nabla}_\perp^4/q^2)u(\boldsymbol{x},t)\end{aligned} \tag{II.48}$$

Another relation we have is,

$$\begin{aligned}\partial_t M_1(\boldsymbol{x},t) &= -\gamma\epsilon_{1ij}M^i_{sp}(\boldsymbol{x})\frac{\delta S}{\delta M_j(\boldsymbol{x})}|_{\boldsymbol{M}(\boldsymbol{x},t)} \\ &= -\gamma M \sin qz \frac{\delta S}{\delta M_3(\boldsymbol{x})}|_{\boldsymbol{M}(\boldsymbol{x},t)} \\ &= \gamma \int d\boldsymbol{y} \frac{\delta M_1(\boldsymbol{x},t)}{\delta u(\boldsymbol{y},t)} r_0 m_3(\boldsymbol{y},t)\end{aligned} \tag{II.49}$$

Combining this with the identity,

$$\partial_t M_1(\boldsymbol{x},t) = \int d\boldsymbol{y} \frac{\delta M_1(\boldsymbol{x},t)}{\delta u(\boldsymbol{y},t)} \partial_t u(\boldsymbol{y},t) \tag{II.50}$$

we get,

$$\partial_t u(\boldsymbol{x},t) = \gamma r_0 m_3(\boldsymbol{x},t) \tag{II.51}$$

Combining Eq. (II.48) and Eq. (II.51) we find a wave equation,

$$\partial_t^2 u(\boldsymbol{x},t) = -\gamma^2 r_0(-c_z\partial_z^2 + c_\perp \boldsymbol{\nabla}_\perp^4/q^2)u(\boldsymbol{x},t) \tag{II.52}$$

This is the equation of motion for a harmonic oscillator with a resonance frequency

$$\omega_0(\boldsymbol{k}) = \gamma\sqrt{r_0}\sqrt{c_z k_z^2 + c_\perp \boldsymbol{k}_\perp^4/q^2} \tag{II.53}$$

So we get the dispersion relation with the square root. The susceptibility is,

$$\chi_0 = \frac{1}{\omega_0^2(\boldsymbol{k}) - \omega^2} \tag{II.54}$$

We thus have a propagating mode, the helimagnon, with an anisotropic dispersion relation. It is worth noting that when discussing the static properties of the helimagnon it is enough to consider only the phase modes at wave vector $\boldsymbol{q}$, while the dynamics are generated by a coupling between the phase modes and the modes at zero wave vector. We will see this more clearly later while discussing quantum helimagnets.

The conical phase is a special case of the helical order, so we expect the dispersion relation in the conical phase to read,

$$\omega_{co}(\boldsymbol{k}) \propto \sqrt{c_z k_z^2 + \tilde{c}_\perp \boldsymbol{k}_\perp^2 + c_\perp \boldsymbol{k}_\perp^4/q^2} \tag{II.55}$$

where $\tilde{c}_\perp \propto H^2$.

Nature of Goldstone Modes in Quantum Helimagnets

We now turn to properties of Goldstone modes in quantum helimagnets. As in the classical case we still follow the hierarchy of energy scales and first talk about quantum ferromagnons and then go to linear order in g_{so} to obtain the quantum helimagnons.

Quantum Ferromagnons

To calculate the ferromagnons explicitly we need an effective action for the fluctuations as in the classical case. For itinerant ferromagnets, we follow Hertz's scheme[17], that is to start from a microscopic fermionic action, and derive a

quantum mechanical generalization of the classical Ginzburg-Landau theory. We start from a partition function,

$$Z = \int D[\bar{\psi}, \psi] e^{S[\bar{\psi}, \psi]} \tag{II.56}$$

where the electronic action $S[\bar{\psi}, \psi]$ is a functional of fermionic fields $\bar{\psi}$ and ψ. The spin-triplet interaction is what causes the ferromagnetic order, so we separate it out and write the action as

$$S[\bar{\psi}, \psi] = \tilde{S}_0[\bar{\psi}, \psi] + S^t_{int} \tag{II.57}$$

with S^t_{int} describing the spin triplet interaction,

$$S^t_{int} = \frac{1}{2}\Gamma_t \int dx \ \boldsymbol{n}_s(x) \cdot \boldsymbol{n}_s(x) \ . \tag{II.58}$$

Here $x \equiv (\boldsymbol{x}, \tau)$ is a four-vector notation for the position $\boldsymbol{x}$ and the imaginary time τ, and $\int dx \equiv \int d\boldsymbol{x} \int_0^\beta d\tau$ with $\beta = 1/T$. Γ_t is the spin-triplet coupling constant and $\boldsymbol{n}_s(x)$ is the electronic spin-density field,

$$n^i_s(x) = \bar{\psi}^\alpha(x) \sigma^i_{\alpha\beta} \psi^\beta(y) \tag{II.59}$$

where σ^i(i=1,2,3) are Pauli matrices. α and β are spin indices and Einstein summation convention is applied here and hereafter. $\tilde{S}_0[\bar{\psi}, \psi]$ contains all parts of the action other than the spin-triplet interaction. For simplicity we will neglect the spin-singlet interaction contained in $\tilde{S}_0$ since it is not important for our purpose. With this simplification, $\tilde{S}_0$ describes free electrons,

$$\tilde{S}_0[\bar{\psi}, \psi] = \int dxdy \ \bar{\psi}^\alpha(x) G^{-1}_{0\alpha\beta}(x, y) \psi^\beta(y) \tag{II.60}$$

where G_0^{-1} is the inverse Green function for free electrons,

$$G_0^{-1}(x,y) = (-\partial_\tau + \frac{1}{2m_e}\boldsymbol{\nabla}^2 + \mu)\delta(x-y)\sigma_0 \tag{II.61}$$

with m_e the effective electron mass, $\mu = \epsilon_F$ the chemical potential or Fermi energy, and σ_0 the 2×2 unit matrix. For later reference, we also define the Fermi wave number $k_F = \sqrt{2m_e\epsilon_F}$, the Fermi velocity $v_F = k_F/m_e$, and the density of states per spin on the Fermi surface $N_F = k_F m_e/2\pi^2$.

Now we perform a Hubbard-Stratonovich transformation to decouple the spin-triplet interaction and get an effective action in terms of the Hubbard-Stratonovich field $\boldsymbol{M}$, whose expectation value is proportional to the magnetization. The partition function can then be written

$$Z = \int D[\bar{\psi},\psi] e^{\tilde{S}_0[\bar{\psi},\psi]} \int D[\boldsymbol{M}] e^{-\frac{\Gamma_t}{2}\int dx \boldsymbol{M}^2(x) + \Gamma_t \int dx \boldsymbol{M}(x)\cdot\boldsymbol{n}_s(x)} \tag{II.62}$$

We now consider the ordered phase and write,

$$\boldsymbol{M}(x) = \boldsymbol{M}_{sp}(\boldsymbol{x}) + \delta\boldsymbol{M}(x) \tag{II.63}$$

where $\boldsymbol{M}_{sp}(\boldsymbol{x}) = (0,0,m_0)$ is the saddle-point configuration of the field $\boldsymbol{M}$, with m_0 to be determined. By substituting Eq. (II.63) and $M_{sp}(\boldsymbol{x})$ into Eq. (II.62), and formally integrating out the fermions, we get the partition function

$$Z = \int D[\delta\boldsymbol{M}] e^{-A[\delta\boldsymbol{M}]} \tag{II.64}$$

where A is the effective action for the order-parameter fluctuations,

$$A[\delta\boldsymbol{M}] = const. + \frac{\Gamma_t}{2}\int dx \boldsymbol{M}^2(x) - \ln\left\langle e^{\Gamma_t \int dx \delta\boldsymbol{M}(x)\cdot\boldsymbol{n}_s(x)}\right\rangle_{S_0} . \tag{II.65}$$

Here

$$S_0[\bar{\psi},\psi] = \tilde{S}_0[\bar{\psi},\psi] + \Gamma_t \int dx \boldsymbol{M}_{sp}(\boldsymbol{x}) \cdot \boldsymbol{n}_s(\boldsymbol{x}) \tag{II.66}$$

is a reference ensemble action for electrons described by $\tilde{S}_0$ in a effective external magnetic field

$$\boldsymbol{H}(\boldsymbol{x}) = \Gamma_t \boldsymbol{M}_{sp}(\boldsymbol{x}) \tag{II.67}$$

Only the Zeeman term due to the effective external magnetic field is included in the reference ensemble, and $\langle \cdots \rangle_{S_0}$ denotes an average with respect to the action S_0.

The effective action A can be expanded in a Landau expansion in powers of $\delta \boldsymbol{M}$. To quadratic order this yields

$$A[\delta \boldsymbol{M}] = \int dx \Gamma_i^{(1)}(x) \delta M_i(x) + \frac{1}{2} \int dx dy \delta M_i(x) \Gamma_{ij}^{(2)}(x,y) \delta M_j(y) + O(\delta M^3) \tag{II.68}$$

with vertices

$$\Gamma_i^{(1)}(x) = \Gamma_t (M_{sp}^i(x) - \left\langle n_s^i(x) \right\rangle_{S_0}) \tag{II.69}$$

and

$$\Gamma_{ij}^{(2)}(x,y) = \delta_{ij}\delta(x-y)\Gamma_t - \Gamma_t^2 \chi_0^{ij}(x,y) \tag{II.70}$$

where

$$\chi_0^{ij}(x,y) = \left\langle n_s^i(x) n_s^j(y) \right\rangle_{S_0}^c \tag{II.71}$$

is the spin susceptibility in the reference ensemble. The superscript c in Eq. (II.71) indicates that only connected diagrams contribute to this correlation function. The equation of state is determined by

$$\langle \delta \boldsymbol{M}(x) \rangle = 0 \tag{II.72}$$

where $\langle \cdots \rangle$ denotes an average with respect to the effective action A in Eq. (II.68). To zerp-loop order this condition reads,

$$\boldsymbol{M}(\boldsymbol{x}) = \langle \boldsymbol{n}_s(x) \rangle_{S_0} \tag{II.73}$$

which is what one would expect.

We need calculate the Green function, which is the building block for the correlation functions of the reference ensemble. The action of the reference ensemble S_0 reads explicitly

$$S_0[\bar{\psi}, \psi] = \int dxdy \; \bar{\psi}_\alpha(x) G^{-1}_{\alpha\beta}(x,y) \psi_\beta(y) \tag{II.74}$$

with the inverse Green function

$$G^{-1}(x,y) = \left[(-\partial_\tau + \frac{1}{2m_e} \boldsymbol{\nabla}^2 + \mu)\sigma_0 + m_0 \Gamma_t \sigma_3 \right] \delta(x-y) \tag{II.75}$$

where σ_3 is the third Pauli matrix. A Fourier transformation yields

$$G^{-1}(\boldsymbol{k}, i\omega_n) = G_0^{-1}(\boldsymbol{k}, i\omega_n)\sigma_0 + m_0 \Gamma_t \sigma_3 \delta(\boldsymbol{k}) \tag{II.76}$$

with $\omega_n = 2\pi T(n + 1/2)$ a fermionic Matsubara frequency, and

$$\xi_{\boldsymbol{k}} = \boldsymbol{k}^2/2m_e - \mu \tag{II.77}$$

So we get the Green function

$$G(\boldsymbol{k}, i\omega_n) = \sigma_{+-}/(i\omega_n - \xi_{\boldsymbol{k}} + \lambda\delta(\boldsymbol{k})) + \sigma_{-+}/(i\omega_n - \xi_{\boldsymbol{k}} - \lambda\delta(\boldsymbol{k})) \tag{II.78}$$

where $\lambda \equiv m_0\Gamma_t$ is the exchange splitting or Stoner gap. Here we have defined $\sigma_{+-} = \sigma_+\sigma_-$ and $\sigma_{-+} = \sigma_-\sigma_+$, with $\sigma_\pm = (\sigma_1 \pm i\sigma_2)/2$.

Now we can calculate the spin susceptibility. Since the reference ensemble describes noninteracting electrons, the reference-ensemble spin susceptibility factorizes into a product of two Green functions. Applying Wick's theorem to Eq. (II.71) we get

$$\chi_0^{ij}(x, y) = -tr\left(\sigma_i G(x, y)\sigma_j G(y, x)\right) \tag{II.79}$$

or, after a Fourier transform,

$$\chi_0^{ij}(\boldsymbol{k}, i\Omega_n) = -\frac{1}{V}\sum_{\boldsymbol{p}} T\sum_{i\omega_n} tr\left(\sigma_i G(\boldsymbol{p}+\boldsymbol{k}, i\omega_n + i\Omega_n)\sigma_j G(\boldsymbol{p}, i\omega_n)\right) \tag{II.80}$$

Here the trace is over the spin degrees of freedom, and $\Omega_n = 2\pi Tn$ is a bosonic Matsubara frequency.

Now we can parameterize the fluctuations of the order parameter as in the classical case, Eq. (II.22), and allow the fields $\pi_i (i = 1, 2)$ to depend on imaginary time or Matsubara frequency. To linear order in the fluctuations we have

$$\delta\boldsymbol{M}(x) = m_0\left(\pi_1(x), \pi_2(x), 0\right) \tag{II.81}$$

where we have neglected the massive fluctuations of the magnitude of the order parameter as in the classical case. Now we can get the effective action Eq. (II.68)

in terms of the fluctuations π_i. The term linear in $\delta \boldsymbol{M}$ vanishes due to the saddle-point condition. To Gaussian order in the fluctuations we get the effective action

$$A^{(2)}[\pi_1, \pi_2] = \frac{1}{2} N_F \Gamma_t^2 \sum_{\boldsymbol{k}, i\Omega_n} \sum_{i,j=1}^{2} \pi_i(\boldsymbol{k}, i\Omega_n) \tilde{\gamma}_{ij}(\boldsymbol{k}, i\Omega_n) \pi_j(-\boldsymbol{k}, -i\Omega_n) \tag{II.82}$$

where the matrix $\tilde{\gamma}$ reads

$$\tilde{\gamma}_{ij}(\boldsymbol{k}, i\Omega_n) = \begin{pmatrix} k^2/12k_F^2 & i(i\Omega_n)/2\lambda \\ -i(i\Omega_n)/2\lambda & k^2/12k_F^2 \end{pmatrix} . \tag{II.83}$$

We see that the relation between the resonance frequency and the momentum is $\omega(\boldsymbol{k}) \propto \boldsymbol{k}^2$, which agrees with what we get using the TDGL theory.

Quantum Helimagnons

We now consider the helical case by keeping terms to linear order in the spin-orbit coupling g_{so}. The spin-triplet interaction part of the action has a form,

$$S_{int}^t = \frac{1}{2} \int d\boldsymbol{x} d\boldsymbol{y} \int_0^\beta d\tau \; n_s^i(\boldsymbol{x}, \tau) A_{ij}(\boldsymbol{x} - \boldsymbol{y}) n_s^j(\boldsymbol{y}, \tau) \tag{II.84}$$

For simplicity we first consider the zero magnetic field case, the treatment of the conical phase in the presence of an external magnetic field will be similar. The interaction amplitude A for helical magnets is given by

$$A_{ij}(\boldsymbol{x} - \boldsymbol{y}) = \delta_{ij} \Gamma_t \delta(\boldsymbol{x} - \boldsymbol{y}) + \epsilon_{ijk} C_k(\boldsymbol{x} - \boldsymbol{y}) \tag{II.85}$$

The first term is the usual Hubbard interaction. The second term is the Dzyaloshinsky-Moriya term, which arises from the spin-orbit interaction in lattices lacking inversion symmetry and favors a nonzero curl of the spin density. In an

effective theory that is valid at length scales large compared to the lattice spacing, the vector $\boldsymbol{C}(\boldsymbol{x}-\boldsymbol{y})$ can be expanded in powers of gradients. The lowest-order term in the gradient expansion is

$$\boldsymbol{C}(\boldsymbol{x}-\boldsymbol{y}) = c\Gamma_t \delta(\boldsymbol{x}-\boldsymbol{y})\boldsymbol{\nabla} + O(\nabla^2) \tag{II.86}$$

with c a constant. We now follow the same steps as in the ferromagnetic case and first perform a Hubbard-Stratonovich transformation to decouple the spin-triplet interaction. To linear order in the gradients, the inverse of the matrix A has the same form as A itself,

$$A_{ij}^{-1} = \frac{\delta_{ij}}{\Gamma_t}\delta(\boldsymbol{x}-\boldsymbol{y}) - \epsilon_{ijk}\frac{c}{\Gamma_t}\delta(\boldsymbol{x}-\boldsymbol{y})\partial_k + O(\nabla^2) \tag{II.87}$$

The Hubbard-Stratonovich transformation then gives a action

$$\begin{aligned} Z = \int D[\bar{\psi},\psi] e^{\tilde{S}_0[\bar{\psi},\psi]} \int D[\boldsymbol{M}] e^{-\frac{\Gamma_t}{2}\int dx \boldsymbol{M}^2(x) + \Gamma_t \int dx \boldsymbol{M}(x)\cdot\boldsymbol{n}_s(x)} \\ \times\, e^{-c(\Gamma_t/2)\int dx \boldsymbol{M}(x)\cdot(\boldsymbol{\nabla}\times\boldsymbol{M}(x))} \end{aligned} \tag{II.88}$$

Again we consider the ordered phase as in Eq. (II.63), with the $\boldsymbol{M}_{sp}$ in the helical phase now given by

$$\boldsymbol{M}_{sp}(\boldsymbol{x}) = M(\cos qz, \sin qz, 0) \tag{II.89}$$

We then get the effective action for the order parameter fluctuations in the helical

phase as

$$A[\delta \boldsymbol{M}] = const. + \frac{\Gamma_t}{2} \int dx \boldsymbol{M}^2(x) + \frac{c\Gamma_t}{2} \int dx \boldsymbol{M}(x) \cdot (\boldsymbol{\nabla} \times \boldsymbol{M}(x)) - \ln \left\langle e^{\Gamma_t \int dx \delta \boldsymbol{M}(x) \cdot \boldsymbol{n}_s(x)} \right\rangle_{S_0} . \tag{II.90}$$

Compared to the ferromagnetic case there is an extra $\boldsymbol{M} \cdot (\boldsymbol{\nabla} \times \boldsymbol{M})$ term, and now the action S_0 describes a reference ensemble of free electrons in an effective external magnetic field that has the form

$$\boldsymbol{H}(\boldsymbol{x}) = M\Gamma_t(\cos qz, \sin qz, 0) \tag{II.91}$$

The Landau expansion in powers of $\delta \boldsymbol{M}$ of the effective action A still has the same form as in Eq. (II.68), only now the vertices have the form

$$\Gamma_i^{(1)}(x) = \Gamma_t(1 - cq) M_{sp}^i(x) - \Gamma_t \left\langle n_s^i(x) \right\rangle_{S_0} \tag{II.92}$$

and

$$\Gamma_{ij}^{(2)}(x, y) = \delta_{ij}\delta(x - y)\Gamma_t - \epsilon_{ijk}\delta(x - y)\Gamma_t c\partial_k - \Gamma_t^2 \chi_0^{ij}(x, y) . \tag{II.93}$$

We now calculate the Green function for the reference ensemble described by the action S_0. With the helical effective external magnetic field, the inverse Green function reads

$$G^{-1}(x, y) = [(-\frac{\partial}{\partial \tau} + \frac{\boldsymbol{\nabla}^2}{2m_e} + \mu)\sigma_0 + \Gamma_t \boldsymbol{M}_{sp}(\boldsymbol{x}) \cdot \boldsymbol{\sigma}]\delta(x - y) \tag{II.94}$$

Here $\boldsymbol{\sigma} = (\sigma_1, \sigma_2, \sigma_3)$ are the Pauli matrices. In momentum space we have

$$G^{-1}_{\boldsymbol{k},\boldsymbol{p}}(i\omega_n) = \begin{pmatrix} \delta_{\boldsymbol{k},\boldsymbol{p}} G_0^{-1}(\boldsymbol{k}, i\omega_n) & \lambda\delta_{\boldsymbol{k}+\boldsymbol{q},\boldsymbol{p}} \\ \lambda\delta_{\boldsymbol{k}-\boldsymbol{q},\boldsymbol{p}} & \delta_{\boldsymbol{k},\boldsymbol{p}} G_0^{-1}(\boldsymbol{k}, i\omega_n) \end{pmatrix} \tag{II.95}$$

We thus get the Green function associated with S_0 as

$$\begin{aligned} G_{\boldsymbol{k}\boldsymbol{p}}(i\omega_n) =& \delta_{\boldsymbol{k},\boldsymbol{p}}[\sigma_{+-}a_+(\boldsymbol{k},\boldsymbol{q};i\omega_n) + \sigma_{-+}a_-(\boldsymbol{k},\boldsymbol{q};i\omega_n)] \\ &+ \delta_{\boldsymbol{k}+\boldsymbol{q},\boldsymbol{p}}\sigma_+ b_+(\boldsymbol{k},\boldsymbol{q};i\omega_n) + \delta_{\boldsymbol{k}-\boldsymbol{q},\boldsymbol{p}}\sigma_- b_-(\boldsymbol{k},\boldsymbol{q};i\omega_n) \end{aligned} \tag{II.96}$$

where

$$a_\pm(\boldsymbol{k},\boldsymbol{q};i\omega_n) = \frac{G_0^{-1}(\boldsymbol{k}\pm\boldsymbol{q},i\omega_n)}{G_0^{-1}(\boldsymbol{k},i\omega_n)G_0^{-1}(\boldsymbol{k}\pm\boldsymbol{q},i\omega_n) - \lambda^2} \tag{II.97}$$

$$b_\pm(\boldsymbol{k},\boldsymbol{q};i\omega_n) = \frac{-\lambda}{G_0^{-1}(\boldsymbol{k},i\omega_n)G_0^{-1}(\boldsymbol{k}\pm\boldsymbol{q},i\omega_n) - \lambda^2} \tag{II.98}$$

and $\lambda = M\Gamma_t$.

We will also need the reference ensemble spin susceptibility, which still factorizes into a product of two Green functions, as in Eq. (II.79). After a Fourier transformation, now we have

$$\chi_s^{ij}(\boldsymbol{k},\boldsymbol{p},i\Omega_n) = \frac{-1}{V}\sum_{\boldsymbol{k}',\boldsymbol{p}'} T\sum_{i\omega_n} tr(\sigma_i G_{\boldsymbol{k}',\boldsymbol{p}'}(i\omega_n)\sigma_j G_{\boldsymbol{p}'+\boldsymbol{p},\boldsymbol{k}'+\boldsymbol{k}}(i\omega_n + i\Omega_n)) \tag{II.99}$$

Now we consider the fluctuations. From the discussion in the classical case we know that the dynamics require considering fluctuations both at zero wave vector and at wave vector $\boldsymbol{q}$. The quantum mechanical case was discussed in [11]. These authors showed that keeping only fluctuations near the pitch vector $\boldsymbol{q}$ suffices to describe the static behavior, while the dynamics require fluctuations near $\boldsymbol{k} = 0$ as,

as in the classical case. Taking into account fluctuation near both $\boldsymbol{k} = 0$ and $\boldsymbol{k} = \boldsymbol{q}$ we get the magnetization fluctuations as,

$$\delta \boldsymbol{M}(x) = M \begin{pmatrix} -\phi(x)\sin(\boldsymbol{q}\cdot\boldsymbol{x}) \\ \phi(x)\cos(\boldsymbol{q}\cdot\boldsymbol{x}) + \pi_2(x) \\ \varphi_1(x)\sin(\boldsymbol{q}\cdot\boldsymbol{x}) + \varphi_2(x)\cos(\boldsymbol{q}\cdot\boldsymbol{x}) + \pi_1(x) \end{pmatrix} \tag{II.100}$$

From [11] we know that π_2 does not couple to ϕ, and its couplings to φ_1 and φ_2 produce only higher order corrections, so we drop π_2 and consider a 4x4 problem given by the three phase modes plus π_1. Putting this back into the effective action, Eq. (II.90), using the spin susceptiblity χ_s above, and using the saddle-point condition, we obtain the Gaussian effective action in the form

$$\mathcal{A}^{(2)}[\varphi_i] = \frac{\lambda^2}{2} \sum_{\boldsymbol{p}} \sum_{i\Omega_n} \sum_{i=0}^{3} \varphi_i(\boldsymbol{p}, i\Omega_n) \gamma_{ij}^{(\boldsymbol{q},0)}(\boldsymbol{p}, i\Omega_n) \varphi_j(-\boldsymbol{p}, -i\Omega_n) \tag{II.101}$$

with

$$\gamma^{(\boldsymbol{q},0)}(k) = \begin{pmatrix} & & -ih_{\phi 1}(k) \\ & \gamma^{(\boldsymbol{q})}(k) & 0 \\ & & 0 \\ ih_{\phi 1}(k) & 0\ \ 0 & 1/\Gamma_t - g_{11}(k) \end{pmatrix} \tag{II.102}$$

Here we have defined $\varphi_3 \equiv \pi_1$,m and $\gamma^{(\boldsymbol{q})}(k)$ is a 3×3 matrix which couples the $\boldsymbol{k} = \boldsymbol{q}$ modes with each other. It reads

$$\gamma^{(q)}(k) = \begin{pmatrix} (1-cq)/\Gamma_t - f_{\phi\phi}(k) & -ick_y/2\Gamma_t & -ick_x/2\Gamma_t \\ ick_y/2\Gamma_t & 1/2\Gamma_t - f_{11}(k) & -f_{12}(k) \\ ick_x/2\Gamma_t & f_{12}(k) & 1/2\Gamma_t - f_{11}(k) \end{pmatrix} \tag{II.103}$$

Here

$$\begin{aligned} f_{\phi\phi}(k) &= \varphi_{\phi\phi}(k) + \varphi_{\phi\phi}(-k) \\ f_{11}(k) &= \varphi_{11}(k) + \varphi_{11}(-k) \\ f_{12}(k) &= i[\varphi_{11}(k) - \varphi_{11}(-k)] \end{aligned} \tag{II.104}$$

and

$$\varphi_{\phi\phi}(k) = -\frac{1}{V}\sum_{\boldsymbol{p}} T\sum_{i\omega_m} \frac{G_0^{-1}(\boldsymbol{p}-\boldsymbol{k}, i\omega_m - i\Omega_n)G_0^{-1}(\boldsymbol{p}-\boldsymbol{q}, i\omega_m) - \lambda^2}{u_-(\boldsymbol{p},\boldsymbol{k})} \tag{II.105}$$

$$\varphi_{11}(k) = -\frac{1}{4V}\sum_{\boldsymbol{p}} T\sum_{i\omega_m} \frac{G_0^{-1}(\boldsymbol{p}-\boldsymbol{k}, i\omega_m - i\Omega_n)G_0^{-1}(\boldsymbol{p}+\boldsymbol{q}, i\omega_m) - \lambda^2}{u_+(\boldsymbol{p},\boldsymbol{k})} \tag{II.106}$$

$$g_{11}(\boldsymbol{k}, i\Omega_n) = 4\varphi_{11}(\boldsymbol{k}-\boldsymbol{q}, i\Omega_n) \tag{II.107}$$

$$h_{\phi 1}(\boldsymbol{k}, i\Omega_n) = \eta_{\phi 1}(\boldsymbol{k}, i\Omega_n) - \eta_{\phi 1}(-\boldsymbol{k}, -i\Omega_n) \tag{II.108}$$

with

$$\begin{aligned} u_\pm = \; & [G_0^{-1}(\boldsymbol{p}-\boldsymbol{k}, i\omega_m - i\Omega_n)G_0^{-1}(\boldsymbol{p}-\boldsymbol{k}-\boldsymbol{q}, i\omega_m - i\Omega_n) - \lambda^2] \\ & \times[G_0^{-1}(\boldsymbol{p}, i\omega_m)G_0^{-1}(\boldsymbol{p}\pm\boldsymbol{q}, i\omega_m) - \lambda^2] \end{aligned} \tag{II.109}$$

$$\eta_{\phi 1}(k) = \frac{\lambda}{V}\sum_{\boldsymbol{p}} T\sum_{i\omega_m} \frac{G_0^{-1}(\boldsymbol{p}-\boldsymbol{k}, i\omega_n - i\Omega_n) - G_0^{-1}(\boldsymbol{p}-\boldsymbol{q}, i\omega_n)}{u_-(\boldsymbol{p},\boldsymbol{k})} \tag{II.110}$$

The complete calculations are rather complicated, and we restrict ourselves to the limit $\lambda > qv_F$. In this limit we get,

$$\gamma^{(\boldsymbol{q},0)}(k) = 2N_F \begin{pmatrix} \kappa^2 + c_\phi |\omega| \frac{\kappa_z^2}{\boldsymbol{\kappa}} & -iQ\kappa_y & -iQ\kappa_x & i(i\omega) \\ iQ\kappa_y & Q^2 + \frac{1}{2}\boldsymbol{\kappa}_\perp^2 & iQ\kappa_z & 0 \\ iQ\kappa_z & -iQ\kappa_z & Q^2 + \frac{1}{2}\boldsymbol{\kappa}_\perp^2 & 0 \\ -i(i\omega) & 0 & 0 & Q^2 \end{pmatrix} \tag{II.111}$$

where we have defined $\boldsymbol{\kappa} = \sqrt{1/3}\boldsymbol{k}/2k_F$, $\boldsymbol{Q} = \sqrt{1/3}\boldsymbol{q}/2k_F$, $\omega = \Omega_n/2\lambda$ and $c_\phi = \sqrt{3}\pi(qv_F)^2/(16\lambda\epsilon_F)$. In the small wave number and small frequency limit we find for the smallest eigenvalue

$$\mu(\boldsymbol{\kappa} \to 0, \omega \to 0) = \kappa_z^2 + \frac{\omega^2}{Q^2} + \frac{\boldsymbol{\kappa}_z^2}{2Q^2} + c_\phi |\omega| \frac{\kappa_z^2}{|\boldsymbol{\kappa}|} + O(\kappa_z^3) \tag{II.112}$$

The corresponding eigenvector reads

$$v(\boldsymbol{k}, i\Omega_n) = \phi(\boldsymbol{k}, i\Omega_n) - i(\kappa_y/Q)\varphi_1(\boldsymbol{k}, i\Omega_n) - i(\kappa_x/Q)\varphi_2(\boldsymbol{k}, i\Omega_n) + (4\omega/Q^2)\pi_1(\boldsymbol{k}, i\Omega_n) \tag{II.113}$$

so we get the Goldstone mode as

$$g(\boldsymbol{k}, i\Omega_n) = (\sqrt{2N_F}\sqrt{3}k_F/q)v(\boldsymbol{k}, i\Omega_n) \tag{II.114}$$

and

$$\langle g(\boldsymbol{k}, i\Omega_n) g(-\boldsymbol{k}, -i\Omega_n) \rangle = \frac{1}{-(i\Omega_n)^2 + \omega_0^2(\boldsymbol{k})} \tag{II.115}$$

where

$$\omega_0(\boldsymbol{k}) = \lambda \frac{q}{3k_F} \sqrt{k_z^2/(2k_F)^2 + \frac{1}{2}\boldsymbol{k}_\perp^4/(2qk_F)^2} \tag{II.116}$$

Here we have kept terms to first order in qv_F/λ only, and thus have neglected the weak damping term, which is smaller than the resonance frequency by a factor of $(qv_f/\lambda)(q/k_F)$. In Section II.3.2 we have shown that the Goldstone mode changes from $c_z k_z^2 + c_\perp k_\perp^4/q^2$ to $c_z k_z^2 + \tilde{c}_\perp k_\perp^2 + c_\perp k_\perp^4/q^2$ with $\tilde{c}_\perp \propto H^2$ when a magnetic field is tuned on. The quantum case must have the same dispersion relation as the classical case, thus we get the general dispersion relation for helimagnons as

$$\omega_0(\boldsymbol{k}) = \sqrt{c_z k_z^2 + \tilde{c}_\perp \boldsymbol{k}_\perp^2 + c_\perp \boldsymbol{k}_\perp^4/q^2} \tag{II.117}$$

Effects of Goldstone Modes on Electronic Properties

The Goldstone mode derived in the preceding section influence the electronic properties of the helical magnet via a coupling to the conduction electrons. In

this section, we consider the effects of the Goldstone modes on the specific heat, the single-particle relaxation rate or the thermal resistivity, and the electrical resistivity. We consider only the contributions from the Goldstone mode; all of these observables have other contributions that come in addition to those from the Goldstone mode.

Specific Heat

Any well-defined (i.e., not overdamped) excitation with a dispersion relation $\omega_0(\boldsymbol{k})$ contributes to the internal energy density a term

$$u(T) = \frac{1}{V}\sum_{\boldsymbol{k}} \omega_0(\boldsymbol{k}) n_B(\omega_0(\boldsymbol{k})) \tag{II.118}$$

Therefore, the contribution of the helimagnon to the specific heat C is given by

$$C(T) = \frac{\partial}{\partial T}\frac{1}{V}\sum_{\boldsymbol{k}} \omega_0(\boldsymbol{k}) n_B(\omega(\boldsymbol{k})) \tag{II.119}$$

where $n_B(x) = \dfrac{1}{e^{x/T}-1}$ is the Bose distribution function, and V is the system volume. Here we use units such that $\hbar = k_B = 1$. Using this formula, we can determine the contribution of the Goldstone mode in helical magnets to the specific heat.

We have the dispersion relation for generalized helimagnon mode has the form

$$\omega_0(\boldsymbol{k}) = \sqrt{c_z k_z^2 + \tilde{c}_\perp \boldsymbol{k}_\perp^2 + c_\perp \boldsymbol{k}_\perp^4} \tag{II.120}$$

where $\tilde{c}_\perp = O(H^2) \ll c_z, c_\perp$, and for simplicity we have chosen coordinates such that the pitch vector is in the $\hat{z}$ direction. We also have absorbed a factor $1/q^2$ into

the prefactor $c_\perp$ for the $\boldsymbol{k}_\perp^4$ term. From this dispersion relation we can calculate its effects on the specific heat.

In the context of the magnetic Goldstone mode coupling to the electronic degrees of freedom the resonance frequency ω_0 always scales as the temperature T, $\omega_0 \sim T$. So we scale k_z with $T/\sqrt{c_z}$ and $k_\perp$ with $\sqrt{T}/c_\perp^{1/4}$, and then write

$$\omega_0(\boldsymbol{k}) = T\sqrt{k_z^2 + \frac{\tilde{c}_\perp/\sqrt{c_\perp}}{T}\boldsymbol{k}_\perp^2 + \boldsymbol{k}_\perp^4} \tag{II.121}$$

where k now denotes the scaled dimensionless wave number. It is now easy to see that when $T \gg \tilde{c}_\perp/\sqrt{c_\perp}$ the symmetry breaking $\boldsymbol{k}_\perp^2$ term is negligible, and the Goldstone mode effectively has the same form as in a rotationally invariant system. Thus in this regime the crystal-field effects due the external magnetic field play a very small role and the physics is dominated by universal hydrodynamic effects. In the opposite limit $T \ll \tilde{c}_\perp/\sqrt{c_\perp}$, the effects due to the magnetic field dominate and the Goldstone mode has the same functional form as anisotropic acoustic phonons. We will discuss the contribution of the Goldstone mode to the specific heat in these two regimes and will do the same for electronic transport properties.

When $T \gg \tilde{c}_\perp/\sqrt{c_\perp}$, we have effectively

$$\omega_0(\boldsymbol{k}) \cong \sqrt{c_z k_z^2 + c_\perp \boldsymbol{k}_\perp^4} \tag{II.122}$$

where k_z scales as T and $k_\perp$ scales as $\sqrt{T}$, so now we can calculate the temperature

dependence of the Goldstone mode contribution to the specific heat

$$\begin{aligned} C(T) &\cong \frac{\partial}{\partial T}\frac{1}{V}\sum_{\boldsymbol{k}}\sqrt{c_z k_z^2 + c_\perp \boldsymbol{k}_\perp^4}\, n_B(\sqrt{c_z k_z^2 + c_\perp \boldsymbol{k}_\perp^4}) \\ &= \frac{1}{(2\pi)^3}\frac{\partial}{\partial T}\int dk_z d\boldsymbol{k}_\perp^2 \frac{\sqrt{c_z k_z^2 + c_\perp \boldsymbol{k}_\perp^4}}{e^{\sqrt{c_z k_z^2 + c_\perp \boldsymbol{k}_\perp^4}/T} - 1} \\ &= \frac{1}{(2\pi)^3}\frac{\partial}{\partial T}\frac{T^3}{\sqrt{c_z c_\perp}}\int dk_z d\boldsymbol{k}_\perp^2 \frac{\sqrt{k_z^2 + \boldsymbol{k}_\perp^4}}{e^{\sqrt{k_z^2 + \boldsymbol{k}_\perp^4}} - 1} \end{aligned} \tag{II.123}$$

In the hydrodynamic regime, and for $T \gg \tilde{c}_\perp/\sqrt{c_\perp}$, we thus find that the Goldstone mode contributes to the specific heat a term

$$C(T) = const. \times T^2/\sqrt{c_z c_\perp} \tag{II.124}$$

In the opposite limit an analogous calculation yields

$$\begin{aligned} C(T) &\cong \frac{\partial}{\partial T}\frac{1}{V}\sum_{\boldsymbol{k}}\sqrt{c_z k_z^2 + \tilde{c}_\perp \boldsymbol{k}_\perp^2}\, n_B(\sqrt{c_z k_z^2 + \tilde{c}_\perp \boldsymbol{k}_\perp^2}) \\ &= \frac{1}{(2\pi)^3}\frac{\partial}{\partial T}\int dk_z d\boldsymbol{k}_\perp^2 \frac{\sqrt{c_z k_z^2 + \tilde{c}_\perp \boldsymbol{k}_\perp^2}}{e^{\sqrt{c_z k_z^2 + \tilde{c}_\perp \boldsymbol{k}_\perp^2}/T} - 1} \\ &= \frac{1}{(2\pi)^3}\frac{\partial}{\partial T}\frac{T^4}{\sqrt{c_z}\tilde{c}_\perp}\int dk_z d\boldsymbol{k}_\perp^2 \frac{\sqrt{k_z^2 + \boldsymbol{k}_\perp^2}}{e^{\sqrt{k_z^2 + \boldsymbol{k}_\perp^2}} - 1} \end{aligned} \tag{II.125}$$

For the Goldstone mode contribution to the specific heat in the case $T \ll \tilde{c}_\perp/\sqrt{c_\perp}$ we thus find

$$C(T) = const. \times T^3/\sqrt{c_z}\tilde{c}_\perp \ . \tag{II.126}$$

The universal hydrodynamic result $C(T) \propto T^2$ is subleading to, but distinct from, the Fermi-liquid result $C(T) \propto T + O(T^3 \ln T)$. At asymptotically low temperature it crosses over to a T^3 behavior consistent with the acoustic-phonon-like dispersion relation in the conical phase with a external magnetic field at asymptotically small wave numbers.

Single-particle Relaxation Time

In this subsection we will calculate the temperature dependence of the single-particle relaxation time, that is, the life time of an electron state on the Fermi surface due to scattering by helimagnon fluctuations. It is given by the imaginary part of the self energy. To get the self energy we need an purely electronic effective action. The external magnetic field does not make a difference for the functional form of the relaxation time except for changing the dispersion relation of the Goldstone mode, so we consider the zero magnetic field case first.

We start from the electronic action in Eq. (II.57) with the spin-triplet interaction given by Eq. (II.84), and replace one of the spin density field by a classical field that represents the effective field seen by the electrons due to the magnetic order. For representational simplicity, we first explain this procedure for an ordinary Hubbard interaction. The chiral case we are interested is exactly analogous. We will use the identity

$$\boldsymbol{n}_s(x) = \langle \boldsymbol{n}_s(x) \rangle + \delta \boldsymbol{n}_s(x) \tag{II.127}$$

By keeping terms to linear order in the fluctuation we thus get

$$\begin{aligned} \boldsymbol{n}_s^2(x) &= 2\boldsymbol{n}_s(x) \langle \boldsymbol{n}_s(x) \rangle - \langle \boldsymbol{n}_s(x) \rangle^2 + \delta \boldsymbol{n}_s^2(x) \\ &\approx 2\boldsymbol{n}_s(x) \langle \boldsymbol{n}_s(x) \rangle - \langle \boldsymbol{n}_s(x) \rangle^2 \end{aligned} \tag{II.128}$$

The action with an ordinary Hubbard interaction can be written

$$\begin{aligned} S[\bar{\psi},\psi] &= \tilde{S}_0[\bar{\psi},\psi] + \frac{\Gamma_t}{2}\int dx \boldsymbol{n}_s(x)\cdot\boldsymbol{n}_s(x) \\ &= \tilde{S}_0[\bar{\psi},\psi] + \frac{\Gamma_t}{2}\int dx (2\boldsymbol{n}_s(x)\langle \boldsymbol{n}_s(x)\rangle - \langle \boldsymbol{n}_s(x)\rangle^2) \\ &= \tilde{S}_0[\bar{\psi},\psi] + \int dx \boldsymbol{H}_0(\boldsymbol{x})\cdot\boldsymbol{n}_s(\boldsymbol{x}) + const. \end{aligned} \tag{II.129}$$

where

$$\boldsymbol{H}_0(\boldsymbol{x}) = \Gamma_t \langle \boldsymbol{n}_s(x)\rangle \tag{II.130}$$

is effective magnetic field due to the magnetic order. The form of the magnetic order is given by $\boldsymbol{M}_{sp}(\boldsymbol{x}) = (0,0,m_0)$ for ferromagnets and has the form given in Eq. (II.89) for helical magnets.

We now replace $\boldsymbol{H}_0(\boldsymbol{x})$ by a fluctuating classical field $\boldsymbol{H}(x) = \Gamma_t \boldsymbol{M}(x) = \boldsymbol{H}_0(\boldsymbol{x}) + \Gamma_t \delta\boldsymbol{M}(x)$, where $\boldsymbol{M}(x)$ represents the spin density averaged over the quantum mechanical degrees of freedom. Neglecting a constant contribution to the action we thus have

$$\begin{aligned} S[\bar{\psi},\psi,\delta\boldsymbol{M}] &= \tilde{S}_0[\bar{\psi},\psi] + \int dx \boldsymbol{H}_0(\boldsymbol{x})\cdot\boldsymbol{n}_s(x) + \Gamma_t\int dx \delta\boldsymbol{M}(x)\cdot\delta\boldsymbol{n}_s(x) \\ &= S_0[\bar{\psi},\psi] + \Gamma_t\int dx \delta\boldsymbol{M}(x)\cdot\delta\boldsymbol{n}_s(x) \end{aligned} \tag{II.131}$$

with S_0 the action associated with the reference ensemble that describes noninteracting electrons in an effective magnetic field given by the magnetization. If the expectation value of $\boldsymbol{M}$ is to respresent the exact magnetization, a supplemental term in the action that governs $\delta\boldsymbol{M}$ has the form

$$A[\delta\boldsymbol{M}] = -\frac{1}{2}\int dx dy \delta M_i(x)(\chi_0^{-1})_{ij}(x,y)\delta M_j(y) \tag{II.132}$$

with χ_0 given by Eq. (II.71). Now we can integrate out $\delta\boldsymbol{M}$,

$$e^{S_{eff}[\bar{\psi},\psi]} = \int D[\delta\boldsymbol{M}] e^{S[\bar{\psi},\psi]+A[\delta\boldsymbol{M}]} \tag{II.133}$$

where the purely electronic effective action S_{eff} has the form

$$S_{eff}[\bar{\psi},\psi] = S_0[\bar{\psi},\psi] + \frac{1}{2}\Gamma_t^2 \int dxdy\delta n_s^i(x)\chi_0^{ij}(x,y)\delta n_s^j(y) \tag{II.134}$$

Now we come back to helimagnets. In the helical phase, where the reference ensemble is described by S_0 with the effective field $\boldsymbol{H}_0$ now has form

$$\begin{aligned} \boldsymbol{H}_0(\boldsymbol{x}) &= \Gamma_t \boldsymbol{M}_{sp}(\boldsymbol{x}) \\ &= \lambda(\cos(\boldsymbol{q}\cdot\boldsymbol{x}), \sin(\boldsymbol{q}\cdot\boldsymbol{x}), 0) \end{aligned} \tag{II.135}$$

Now we are ready to calculate the self energy Σ of the single-particle Green function to linear order in the perturbing potential $\tilde{\chi}_s \equiv \Gamma_t^2\chi_0$. Only the exchange or Fock contribution has an imaginary part and contributes to the scattering rate, so we consider only the exchange self energy, which is given by

$$\Sigma^{ex}_{\boldsymbol{kp}}(i\omega_n) = \frac{1}{V}\sum_{\boldsymbol{k}',\boldsymbol{p}'} T\sum_{i\Omega_n} \sigma_i G_{\boldsymbol{k}'+\boldsymbol{k},\boldsymbol{p}'+\boldsymbol{p}}(i\Omega_n + i\omega_n)\sigma_i\tilde{\chi}_s^{ij}(\boldsymbol{k}',\boldsymbol{p}';i\Omega_n) \tag{II.136}$$

The self energy Σ has a structure very similar to that of the inverse Green function, and we can write

$$\begin{aligned} \Sigma_{\boldsymbol{kp}}(i\omega_n) =& \delta_{\boldsymbol{k},\boldsymbol{p}}[\sigma_{+-}\Sigma_{++}(\boldsymbol{k},i\omega_n) + \sigma_{-+}\Sigma_{--}(\boldsymbol{k},i\omega_n)] \\ &+ \delta_{\boldsymbol{k}+\boldsymbol{q},\boldsymbol{p}}\sigma_+\Sigma_{+-}(\boldsymbol{k},i\omega_n) + \delta_{\boldsymbol{k}-\boldsymbol{q},\boldsymbol{p}}\sigma_-\Sigma_{-+}(\boldsymbol{k},i\omega_n) \end{aligned} \tag{II.137}$$

The renormalized Green function $\mathcal{G}$ is given by the Dyson equation

$$\mathcal{G}^{-1}_{\boldsymbol{kp}}(i\omega_n) = G^{-1}_{\boldsymbol{kp}}(i\omega_n) - \Sigma_{\boldsymbol{kp}}(i\omega_n) \tag{II.138}$$

It then follows that $\mathcal{G}$ has the same structure as G,

$$\begin{aligned}\mathcal{G}_{\boldsymbol{kp}}(i\omega_n) =&\delta_{\boldsymbol{k},\boldsymbol{p}}[\sigma_{+-}A_+(\boldsymbol{k},\boldsymbol{q};i\omega_n)+\sigma_{-+}A_-(\boldsymbol{k},\boldsymbol{q};i\omega_n)]\\ &+\delta_{\boldsymbol{k}+\boldsymbol{q},\boldsymbol{p}}\sigma_+B_+(\boldsymbol{k},\boldsymbol{q};i\omega_n)+\delta_{\boldsymbol{k}-\boldsymbol{q},\boldsymbol{p}}\sigma_-B_-(\boldsymbol{k},\boldsymbol{q};i\omega_n)\end{aligned} \tag{II.139}$$

where

$$A_\pm(\boldsymbol{k},\boldsymbol{q};i\omega_n)=\frac{f_\mp^{-1}(\boldsymbol{k}\pm\boldsymbol{q},i\omega_n)}{f_\pm^{-1}(\boldsymbol{k},i\omega_n)f_\mp^{-1}(\boldsymbol{k}\pm\boldsymbol{q},i\omega_n)-\lambda_\pm(\boldsymbol{k},i\omega_n)\lambda_\mp(\boldsymbol{k}\pm\boldsymbol{q},i\omega_n)} \tag{II.140}$$

$$B_\pm(\boldsymbol{k},\boldsymbol{q};i\omega_n)=\frac{-\lambda_\pm(\boldsymbol{k},i\omega_n)}{f_\pm^{-1}(\boldsymbol{k},i\omega_n)f_\mp^{-1}(\boldsymbol{k}\pm\boldsymbol{q},i\omega_n)-\lambda_\pm(\boldsymbol{k},i\omega_n)\lambda_\mp(\boldsymbol{k}\pm\boldsymbol{q},i\omega_n)} \tag{II.141}$$

with

$$f_\pm^{-1}(\boldsymbol{k},i\omega_n)=G^{-1}(\boldsymbol{k},i\omega_n)-\Sigma_{\pm\pm}(\boldsymbol{k},i\omega_n) \tag{II.142}$$

$$\lambda_\pm(\boldsymbol{k},i\omega_n)=\lambda-\Sigma_{\pm\mp}(\boldsymbol{k},i\omega_n) \tag{II.143}$$

The quasi-particle relaxation time is determined by the imaginary parts of the poles of the Green function $\mathcal{G}$, that is, by the imaginary part of the self energy. Thus for a vanishing self energy, the resonance frequencies do not have imaginary parts, and the quasi-particles are infinitely long lived. We verify this by explicit calculation. The poles of the Green function G are at,

$$\omega_{1,2}^\pm(\boldsymbol{k})=\frac{1}{2}\left(\xi_{\boldsymbol{k}}+\xi_{\boldsymbol{k}\pm\boldsymbol{q}}\pm\sqrt{(\xi_{\boldsymbol{k}}-\xi_{\boldsymbol{k}\pm\boldsymbol{q}})^2+4\lambda^2}\right) \tag{II.144}$$

The two possible signs of the square root reflect the Stoner splitting of the Fermi surface into two sheets. On a given sheet, we have $\omega_i^-(\boldsymbol{k}+\boldsymbol{q})=\omega_i^+(\boldsymbol{k})(i=1,2)$.

So all poles can be expressed as

$$\omega_{1,2}(\boldsymbol{k}) = \frac{1}{2}\left(\xi_{\boldsymbol{k}} + \xi_{\boldsymbol{k}+\boldsymbol{q}} \pm \sqrt{(\xi_{\boldsymbol{k}} - \xi_{\boldsymbol{k}+\boldsymbol{q}})^2 + 4\lambda^2}\right) \tag{II.145}$$

These poles are indeed real for a vanishing self energy, that is to zeroth order in the effective potential χ_s. If we go to first order in χ_s, the resonance frequency will acquire an imaginary part, which corresponds to a finite relaxation time $\tau(\boldsymbol{k})$. The temperature dependence of the relaxation time on the two Fermi surface is the same, so it suffices to consider the resonance at $\omega_1(\boldsymbol{k})$.

To first order in χ_s we get

$$\begin{aligned}\frac{1}{\tau(\boldsymbol{k})} = \frac{1}{2} Im(&\Sigma_{++}(\boldsymbol{k}, z) + \Sigma_{--}(\boldsymbol{k}+\boldsymbol{q}, z) \\ &+ \frac{\xi_{\boldsymbol{k}} - \xi_{\boldsymbol{k}+\boldsymbol{q}}}{[(\xi_{\boldsymbol{k}} - \xi_{\boldsymbol{k}+\boldsymbol{q}})^2 + 4\lambda^2]^2}[\Sigma_{++}(\boldsymbol{k}, z) - \Sigma_{--}(\boldsymbol{k}+\boldsymbol{q}, z)] \\ &- \frac{2\lambda}{[(\xi_{\boldsymbol{k}} - \xi_{\boldsymbol{k}+\boldsymbol{q}})^2 + 4\lambda^2]^2}[\Sigma_{+-}(\boldsymbol{k}, z) + \Sigma_{-+}(\boldsymbol{k}+\boldsymbol{q}, z)])\end{aligned} \tag{II.146}$$

where $z = \omega_1(\boldsymbol{k}) + i0$.

We are interested in the relaxation rate for quasi-particles on the Fermi surface, which is defined by

$$\omega_1(\boldsymbol{k}) = \frac{1}{2}\left(\xi_{\boldsymbol{k}} + \xi_{\boldsymbol{k}+\boldsymbol{q}} + \sqrt{(\xi_{\boldsymbol{k}} - \xi_{\boldsymbol{k}\pm\boldsymbol{q}})^2 + 4\lambda^2}\right) = 0 \tag{II.147}$$

We now perform the frequency summation. With the condition Eq. (II.147), and by using Eq. (II.136) in Eq. (II.146), we obtain for the relaxation rate of a quasi-particle on the Fermi surface

$$\frac{1}{\tau(\boldsymbol{k})} = \frac{-2\lambda^2}{(\xi_{\boldsymbol{k}} + \xi_{\boldsymbol{k}+\boldsymbol{q}})^2} \frac{1}{V} \sum_{\boldsymbol{p}} \frac{v(\boldsymbol{k}, \boldsymbol{p})}{\sinh(\omega_1(\boldsymbol{p})/T)} \chi''(\boldsymbol{p} - \boldsymbol{k}, \omega_1(\boldsymbol{p})) \tag{II.148}$$

where χ'' is the spectrum of the phase susceptibility, which is given by Eq. (II.114) and Eq. (II.115) and explicitly reads

$$\chi(\boldsymbol{p}, i\Omega_n) = \frac{1}{2N_F}\frac{q^2}{3k_F^2}\frac{1}{\omega_0^2(\boldsymbol{p}) - (i\Omega_n)^2} \tag{II.149}$$

with $\omega_0(\boldsymbol{p})$ the helimagnon resonance frequency. So the spectrum is

$$\chi''(\boldsymbol{p}, \omega) = \frac{1}{2N_F}\frac{q^2}{3k_F^2}\frac{\pi}{2\omega_0(\boldsymbol{p})}[\delta(\omega - \omega_0(\boldsymbol{p})) - \delta(\omega + \omega_0(\boldsymbol{p}))] \tag{II.150}$$

The function $v(\boldsymbol{k}, \boldsymbol{p})$ is given by

$$v(\boldsymbol{k}, \boldsymbol{p}) = \omega_1(\boldsymbol{p})(\xi_{\boldsymbol{k}} + \xi_{\boldsymbol{k}+\boldsymbol{q}}) + \xi_{\boldsymbol{k}}(\xi_{\boldsymbol{k}+\boldsymbol{q}} - \xi_{\boldsymbol{p}+\boldsymbol{q}}) + \xi_{\boldsymbol{k}+\boldsymbol{q}}(\xi_{\boldsymbol{k}} - \xi_{\boldsymbol{p}}) \tag{II.151}$$

Now we can calculate the temperature dependence of the single-particle relaxation time on the Fermi surface. In a cubic lattice as in MnSi, the energy momentum relation has the form

$$\epsilon_k = \boldsymbol{k}^2/2m_e + \frac{\nu}{2m_e k_F^2}(k_x^2 k_y^2 + k_y^2 k_z^2 + k_z^2 k_x^2) \tag{II.152}$$

where ν is a dimensionless measure of deviations from a nearly-free electron model. Generally it is of order $O(1)$. We thus get the single-particle relaxation rate schematically as

$$\frac{1}{\tau} \sim \int dp_\parallel \int d\boldsymbol{p}_\perp^2 \frac{\boldsymbol{p}_\perp^2 + p_\parallel^2}{\sinh\left[\omega_0(\boldsymbol{p}/T)\right]} \frac{\delta\left[\omega_0(\boldsymbol{p}) - p_\perp - p_\parallel\right]}{\omega_0(\boldsymbol{p})} \tag{II.153}$$

As the we discussed before, the resonance frequency always scales as the temperature, so the temperature dependence of the relaxation rates is determined

by how the momentum components scale with temperature. Again we consider two temperature regimes. As we discussed in the specific heat section, at asymptotically low temperature, we have $p_{\parallel} \sim p_{\perp} \sim T$, while at intermediate temperature, we have $p_{\parallel} \sim T$ and $p_{\perp} \sim \sqrt{T}$. Thus we get the temperature dependence of the single-particle relaxation rate

$$\frac{1}{\tau} \sim \begin{cases} T^3 & if T \ll \tilde{c}_{\perp}/\sqrt{c_{\perp}} \\ T^{3/2} & if T \gg \tilde{c}_{\perp}/\sqrt{c_{\perp}} \end{cases} \tag{II.154}$$

The thermal resistivity ρ_{th} has the same temperature dependence as the single-partical relaxation rate [34].

Resistivity

The electrical resistivity is related to, but not the same as, the single-particle relaxation time. Physically, backscattering events contribute more strongly to the resistivity than forward scattering events, so the transport scattering rate is given by the single-particle relaxation rate with an extra factor of $(\boldsymbol{p} - \boldsymbol{k})^2$ in Eq. (II.148). Technically, the electrical resistivity can be calculated as the inverse of the conductivity, which can be obtained from the Kubo formula

$$\sigma_{ij}(i\Omega_n) = \frac{1}{i\Omega_n}[\pi_{ij}(i\Omega_n) - \pi_{ij}(i\Omega_n = 0)] \tag{II.155}$$

where the current-current susceptibility tensor is given by

$$\pi_{ij}(i\Omega_n) = -e^2 T \sum_{n_1,n_2} \frac{1}{V} \sum_{\boldsymbol{k},\boldsymbol{p}} \frac{\partial \epsilon_{\boldsymbol{k}}}{\partial k_i} \frac{\partial \epsilon_{\boldsymbol{p}}}{\partial p_j} \left\langle \bar{\psi}_{n_1,\sigma}(\boldsymbol{k}) \psi_{n_1+n,\sigma}(\boldsymbol{k}) \bar{\psi}_{n_2,\sigma'}(\boldsymbol{p}) \psi_{n_2-n,\sigma'}(\boldsymbol{p}) \right\rangle \tag{II.156}$$

The average denoted by $\langle \cdots \rangle$ is to be performed with the effective action given by Eq. (II.134). The calculation details have been given in [35–37], and here we only cite the result. The electrical resistivity, which is determined by the electrical transport relaxation time, is given by

$$\frac{1}{\tau_{el}^{tr}} = \frac{1}{N_F} \int_{-\infty}^{+\infty} \frac{du}{\sinh(u/T)} \frac{1}{V^2} \sum_{\boldsymbol{p},\boldsymbol{k}} \frac{(\boldsymbol{p}-\boldsymbol{k})^2}{k_F^2} v(\boldsymbol{k},\boldsymbol{p}) \chi''(\boldsymbol{p}-\boldsymbol{k};\boldsymbol{k},\boldsymbol{p};u) \delta[u-\omega_1(\boldsymbol{p})] \times \delta[\omega_1(\boldsymbol{k})] \tag{II.157}$$

For a nonspherical Fermi surface ($\nu \neq 0$), and for a generic wave vector $\boldsymbol{k}$, we thus find that the electrical resistivity ρ_{el} can be represented schematically by the expression

$$\rho_{el} \sim \int dp_{\parallel} \int d\boldsymbol{p}_{\perp}^2 \frac{(\boldsymbol{p}_{\perp}^2 + p_{\parallel}^2)^2}{\sinh[\omega_0(\boldsymbol{p})/T]} \frac{\delta[\omega_0(\boldsymbol{p}) - \boldsymbol{p}_{\perp} - p_{\parallel}]}{\omega_0(\boldsymbol{p})} \tag{II.158}$$

Again we consider the temperature dependence for two temperature regimes as we did for specific heat and the single-particle relaxation time. The electrical resistivity depends on the temperature as follows,

$$\rho_{el} \propto \begin{cases} T^5 & if T \ll \tilde{c}_\perp/\sqrt{c_\perp} \\ T^{5/2} & if T \gg \tilde{c}_\perp/\sqrt{c_\perp} \end{cases} \tag{II.159}$$

CHAPTER III

WEAK FERROMAGNETS

Introduction

In this chapter we will consider materials with true ferromagnetic order with none of the complications resulting from the spin-orbit interaction discussed in Chapter. II. Specifically, we will discuss the properties of "weak ferromagnets", which have a very low critical temperature and allow to study the quantum ferromagnetic phase transition. The latter is of fundamental interest in itself, and also helps understand more generally phase transitions that occur at very low temperature. The quantum ferromagnetic transition has been observed to be of first order in many metallic systems, such as $ZrZn_2$ [23], UGe_2 [38–40], and URhGe [41], and also in the helical magnetic MnSi which can be considered a ferromagnet if we neglect its long-wavelength helical order. These observations make the study of quantum ferromagnetic phase transition especially important since for a long time it had been thought to be a classic example of a second-order phase transition. Stoner [16] was the first to describe the ferromagnetic phase transition in metals for both the classical and the quantum case. He developed a mean-field theory that describes the ferromagnetic phase transition to be of second

order. Hertz later used renormalization-group methods to study quantum phase transitions at zero temperature [17], and Millis extended this work to nonzero temperatures [18]. These theories also concluded that the quantum ferromagnetic phase transition is of second order. They further concluded that the quantum phase transition is characterized by mean-field critical exponents in the physical dimensions $d = 2$ and $d = 3$ for both clean and disordered system. The observed first-order ferromagnetic transitions disagree with these theories. Later theories [19, 21, 42] concluded that the quantum ferromagnetic phase transition in clean systems is generically of first order. The reason is that at low temperatures soft fermionic particle-hole excitations that couple to the order-parameter fluctuations play an important role. In Hertz-Millis theory these soft excitations are treated in a tree approximation, which missed some qualitative effects. If these fermionic degrees of freedom are treated more carefully, they lead to a fluctuation-induced first order transition.

At zero temperature, the soft or gapless fermionic excitations that exist in any clean metal lead to an equation of state of the form (in $d = 3$) [19]

$$h = rm - vm^3 \ln(1/m) + um^3 \tag{III.1}$$

where m is the magnetization in suitable unit, h is the external field and r is the control parameter. u and v are Landau parameters. The nonanalytic term $m^3 \ln(1/m)$ results from the coupling of m to the soft fermionic excitations. In

generic dimensions, this term has the form m^d. The parameter v is greater than zero, which causes a first-order phase transition at $r > 0$. When the temperature is nonzero, the soft modes acquire a mass. This cuts off the nonanalytic $\ln m$ term, and thus leads to a tricritical point, as shown in Fig.1.4.. This theory concludes that a first-order transition is a generic property of quantum ferromagnets. While this agrees with many experimental observations, there also are ferromagnets in which the transition is observed to be of second order. These materials tend to be disordered, and indeed quenched disorder provides an explanation for these different observations. Quenched disorder exists in all real systems, and its strength varies over a wide range depending on the system and also the sample preparation processes. The properties of the ferromagnetic phase transitions in disordered itinerant ferromagnets were studied in [43], where it was found that in three-dimensional systems, with sufficiently strong disorder, the equation of state has the form

$$h = rm + \frac{w}{(k_F l)^{3/2}}\, m^{3/2} + um^3 \tag{III.2}$$

Here w is another parameter, k_F is the Fermi wavenumber, and l is the elastic mean-free path. From this equation of state, we see that the $m^{3/2}$ terms will lead to a continuous transition with non-mean-field exponents.

Both equations (III.1) and (III.2) represent renormalized Landau theories, where the fluctuating order-parameter field is replaced by its expectation value. Reference [20] concluded that this approximation does not qualitatively affect the

nature of the quantum phase transition, although in the disordered case the order-parameter fluctuations lead to non-power-law modifications of the leading scaling behavior[20, 44].

Coming back to the experimental observations, some metallic ferromagnets show a continuous transition with mean-field like exponents, in agreement with Hertz-Millis theory, which doesn't agree with either equation (III.1) or (III.2). A likely explanation is that equations (III.1) and (III.2) represent two extreme cases: ultraclean and very disordered system, respectively, while some experiments fall in between these two extremes. It therefore is important to study how the ferromagnetic phase transition properties evolve with increasing disorder, and this will be the subject of the current chapter.

Another issue is that the mechanism given in [19] is not the only possibility for a first-order transition. The coupling between the magnetization and phonons can also lead to a first-order transition, as is known from classical compressible magnets [45]. It has been argued that at least in the case of the pressure-tuned quantum ferromagnets the first-order transition can be explained by an adaptation of this mechanism to the quantum transition [46–48]. It thus is desirable to develop criteria that can descriminate between these different theoretical ideas. This is another reason to study how the phase diagram evolves with increasing disorder. Phonons are not qualitatively affected by disorder, so if the first-order transition is caused by magnetostriction effects, then the phase diagram should show only

small quantitative changes if disorder is introduced. However, if the mechanism is the one presented in [19], then the phase diagram will be crucially affected by the disorder, as the equation of state changes from Eq. (III.1) to Eq. (III.2).

In this chapter we will study the effects of disorder on the quantum ferromagnetic phase transitions. We will first review the derivation of the generalized mean-field theory (GMFT) that gives the equation of state shown in Eq. (III.1) at $T = 0$ for clean systems, following the method in reference [49]. The idea is to start from a microscopic fermionic theory and integrate out all of the massive modes to get a coupled field theory in terms of all soft modes, including both magnetization fluctuations and the soft spin-triplet particle-hole excitations. We then replace the order parameter with its expectation value and integrate out the soft fermionic degrees of freedom to get a generalized mean-field theory for the magnetization. We will also review the generalized mean-field theory for strongly disordered system using similar methods. The details of the calculation can be found in [20]. We then combine the two cases and derive a comprehensive generalized mean-field theory that interpolates between the clean and disordered cases.

We will see from the comprehensive generalized-mean field theory that there are three distinct disorder regimes. When the disorder is very weak, the transition at zero temperature is first order and there is a tricritical point. Increasing disorder will suppress the tricritical temperature until it vanishes at a critical disorder. This leads to an intermediate-disorder regime where the observable quantum

ferromagnetic phase transition is continuous with mean-field critical exponents, which agrees with Hertz theory. Asymptotically close to the transition there will be a crossover to the non-mean-field critical behavior given in [43], but this happens so close to the transition that it is not observable. When the disorder continues to increase, the crossover will move away from the transition and become observable. When the disorder is very strong, the non-mean-field critical behavior will be present everywhere in the critical region. When the disorder is that strong other effects, e.g., Griffiths-region effects, may come into play as well. These predictions can be tested by introducing disorder into any material that displays a first-order quantum phase transition and observing the change in the phase diagram with increasing disorder.

The theories quoted so far were formulated for isotropic ferromagnetic systems. In this chapter we will also generalize the theory to the case of anisotropic systems and apply it to the interesting case of URhGe. URhGe is an anisotropic ferromagnet with a Curie temperature $T_c \approx 9.5K$ and a spontaneous magnetization moment $0.42\mu_B/f.u.$ aligned with the c-axis of its orthorhombic crystal structure. The a-axis, perpendicular to the bc-plane, is a very hard magnetic direction and the magnetic moment can be considered to be confined to the bc-plane. The moment turns in the bc-plane in response to an applied magnetic field. The phase diagram of URhGe is depicted in Fig. 3.1.. In zero external magnetic field the ferromagnetic transition is of second order. If an external magnetic field in the b-direction is

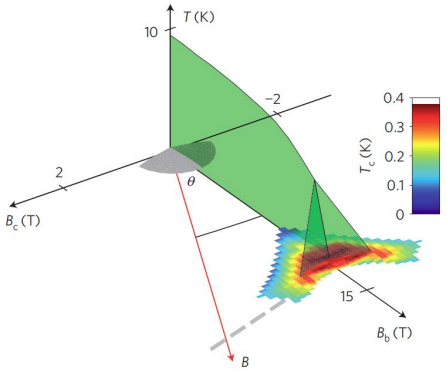

Figure 3.1. The field-temperature phase diagram for field directions in the easy magnetic plane. From [50].

applied, the transition temperature decreases. At zero temperature, there is a first-order transition at a critical magnetic field $h_{2c} \approx 12T$ in the b-direction. With increasing temperature, this critical magnetic field decreases. At intermediate temperature and magnetic field, the second-order transition and the first order one meet at a tricritical point (TCP), with the tricritical temperature $T_{tc} \approx 1K$. If a field in the c-direction is applied near h_{2c}, the first-order transition line will bifurcate into two first-order transition surfaces, across which the magnetization changes discontinuously.

This phase diagram has the same structure as the one in Fig.1.4.. The only difference is that here the transition temperate is tuned by a perpendicular magnetic field instead of hydrodynamic pressure, and the tuning is thus easier to implement experimentally. We will generalize the theory given in [19, 21] to explain this phase

diagram, and we will then predict its evolution with increasing disorder. These predictions should be relatively easy to test experimentally.

Generalized Mean Field Theory

In this section we will derive a generalized mean-field theory for both clean and disordered system, using the method of references [49, 51]. We start with reviewing the clean case.

Effective Field Theory for All Soft Modes

Consider a clean itinerant electron system, whose partition function is given by Eq. (II.56). The action S has the form

$$S[\bar{\psi},\psi] = S_0[\bar{\psi},\psi] + S_{int} \tag{III.3}$$

where S_0 describes free electrons and S_{int} describes an electron-electron interaction via a two-body potential $u(\boldsymbol{x})$,

$$S_{int} = -\frac{1}{2}\int_V d\boldsymbol{x}d\boldsymbol{y}\ u(\boldsymbol{x}-\boldsymbol{y})\ \bar{\psi}_a(\boldsymbol{x},\tau)\bar{\psi}_b(\boldsymbol{y},\tau)\psi_b(\boldsymbol{y},\tau)\psi_a(\boldsymbol{x},\tau)\ . \tag{III.4}$$

We are interested in the effects of the soft particle-hole excitations on the ferromagnetic phase transition properties, and for this purpose it is more suitable to describe our model in terms of composite bosonic variables instead of the basic fermionic fields. This will allow us to seperate the soft modes from the massive

modes explicitly [49, 51]. To introduce this bosonic formulation we first perform a Fourier transform from imaginary time τ to Matsubara frequencies $\omega_n = 2\pi T(n + 1/2)$,

$$\psi_{n,a}(\boldsymbol{x}) = \sqrt{T}\int_0^\beta d\tau e^{i\omega_n\tau}\psi_a(\boldsymbol{x},\tau), \tag{III.5}$$

$$\bar{\psi}_{n,a}(\boldsymbol{x}) = \sqrt{T}\int_0^\beta d\tau e^{-i\omega_n\tau}\bar{\psi}_a(\boldsymbol{x},\tau), \tag{III.6}$$

For later reference we also define a spatial Fourier transform

$$\psi_{n,a}(\boldsymbol{k}) = \frac{1}{\sqrt{V}}\int d\boldsymbol{x} e^{i\boldsymbol{k}\cdot\boldsymbol{x}}\psi_{n,a}(\boldsymbol{x}), \tag{III.7}$$

$$\bar{\psi}_{n,a}(\boldsymbol{k}) = \frac{1}{\sqrt{V}}\int d\boldsymbol{x} e^{-i\boldsymbol{k}\cdot\boldsymbol{x}}\bar{\psi}_{n,a}(\boldsymbol{x})\ . \tag{III.8}$$

Now we define a bispinor

$$\eta_n(\boldsymbol{x}) = \begin{pmatrix} \bar{\psi}_{n\uparrow}(\boldsymbol{x}) \\ \bar{\psi}_{n\downarrow}(\boldsymbol{x}) \\ \psi_{n\downarrow}(\boldsymbol{x}) \\ -\psi_{n\uparrow}(\boldsymbol{x}) \end{pmatrix} \tag{III.9}$$

with an adjoint

$$\begin{aligned} \eta_n^+(\boldsymbol{x}) &= i(C\eta)_n(\boldsymbol{x}) \\ &= \frac{i}{\sqrt{2}}(-\psi_{n\uparrow}(\boldsymbol{x}), -\psi_{n\downarrow}(\boldsymbol{x}), \bar{\psi}_{n\downarrow}(\boldsymbol{x}), -\bar{\psi}_{n\uparrow}(\boldsymbol{x})) \end{aligned} \tag{III.10}$$

where $C_{mn} = i(\tau_1 \otimes s_2)\delta_{mn}$ is the charge conjugation matrix in the spin-quarternion space spanned by $\tau_i \otimes s_j$ $(i,j = 0,1,2,3)$, where $\tau_0 = s_0 = I_2$ is the 2×2 unit

matrix and $\tau_j = -s_j = -i\sigma_j$ $(j = 1, 2, 3)$, with $\sigma_{1,2,3}$ the Pauli matrices. We then introduce a matrix of bilinear products of the fermionic fields,

$$B_{mn}(\boldsymbol{x}, \boldsymbol{y}) = \eta_m^+(\boldsymbol{x}) \otimes \eta_n(\boldsymbol{y})$$
$$= \frac{i}{2} \begin{pmatrix} -\psi_{m\uparrow}(\boldsymbol{x})\bar{\psi}_{n\uparrow}(\boldsymbol{y}) & -\psi_{m\uparrow}(\boldsymbol{x})\bar{\psi}_{n\downarrow}(\boldsymbol{y}) & -\psi_{m\uparrow}(\boldsymbol{x})\psi_{n\downarrow}(\boldsymbol{y}) & \psi_{m\uparrow}(\boldsymbol{x})\psi_{n\uparrow}(\boldsymbol{y}) \\ -\psi_{m\downarrow}(\boldsymbol{x})\bar{\psi}_{n\uparrow}(\boldsymbol{y}) & -\psi_{m\downarrow}(\boldsymbol{x})\bar{\psi}_{n\downarrow}(\boldsymbol{y}) & -\psi_{m\downarrow}(\boldsymbol{x})\psi_{n\downarrow}(\boldsymbol{y}) & \psi_{m\downarrow}(\boldsymbol{x})\psi_{n\uparrow}(\boldsymbol{y}) \\ \bar{\psi}_{m\downarrow}(\boldsymbol{x})\bar{\psi}_{n\uparrow}(\boldsymbol{y}) & \bar{\psi}_{m\downarrow}(\boldsymbol{x})\bar{\psi}_{n\downarrow}(\boldsymbol{y}) & \bar{\psi}_{m\downarrow}(\boldsymbol{x})\psi_{n\downarrow}(\boldsymbol{y}) & -\bar{\psi}_{m\downarrow}(\boldsymbol{x})\psi_{n\uparrow}(\boldsymbol{y}) \\ -\bar{\psi}_{m\uparrow}(\boldsymbol{x})\bar{\psi}_{n\uparrow}(\boldsymbol{y}) & -\bar{\psi}_{m\uparrow}(\boldsymbol{x})\bar{\psi}_{n\downarrow}(\boldsymbol{y}) & -\bar{\psi}_{m\uparrow}(\boldsymbol{x})\psi_{n\downarrow}(\boldsymbol{y}) & \bar{\psi}_{m\uparrow}(\boldsymbol{x})\psi_{n\uparrow}(\boldsymbol{y}) \end{pmatrix} \tag{III.11}$$

where we have used the notation $(\eta^+ \otimes \eta)_{ij} = \eta_i^+ \eta_j$. The Fourier transform of the B fields reads

$$B_{mn}(\boldsymbol{k}, \boldsymbol{p}) = \frac{1}{V} \int d\boldsymbol{x} d\boldsymbol{y} e^{-i\boldsymbol{k}\cdot\boldsymbol{x} + i\boldsymbol{p}\cdot\boldsymbol{y}} B_{mn}(\boldsymbol{x}, \boldsymbol{y}) \tag{III.12}$$

where the 4×4 matrix $B_{mn}(\boldsymbol{k}, \boldsymbol{p})$ can be expanded in the spin-quaternion basis defined above,

$$B_{mn}(\boldsymbol{k}, \boldsymbol{p}) = \sum_{i,r=0}^{3} (\tau_r \otimes s_i)\, {}_r^i B_{mn}(\boldsymbol{k}, \boldsymbol{p}) \tag{III.13}$$

It is further useful to define

$$B_{mn}(\boldsymbol{k}; \boldsymbol{q}) = B_{mn}(\boldsymbol{k} + \boldsymbol{q}/2, \boldsymbol{k} - \boldsymbol{q}/2) \tag{III.14}$$

It is easy to see that all bilinear products of ψ and $\bar{\psi}$ can be written in terms of B, and all of the interaction terms in the action can be written in terms of products of B. In the spin-quarternion basis, ${}_r^{i=0}B$ and ${}_r^{i=1,2,3}B$ describe the spin-singlet and spin-triplet, respectively. Explicit calculation reveals that ${}_{r=0,3}^{i}B$ corresponds to the

particle-hole channel (i.e., products $\bar{\psi}\psi$), while ${}_{r=1,2}^{\ \ i}B$ describes the particle-particle channel (i.e., products $\bar{\psi}\bar{\psi}$ or $\psi\psi$). The particle-particle channel is not important for describing magnetism, so from now on we will only keep the $r = 0, 3$ parts of the spin-quaternion basis.

The matrix elements of B commute with one another, and are therefore isomorphic to classical or number-valued fields. We thus can write the action of our electron system in terms of a classical matrix field Q. To do so, we first separate out the spin-triplet interaction given in Eq. (II.58), which is responsible for the ferromagnetism, by writing

$$S[\bar{\psi}, \psi] = S_0[\bar{\psi}, \psi] + S'_{int}[\bar{\psi}, \psi] + S^t_{int} \tag{III.15}$$

Here S'_{int} is the interaction part of the action with the spin-triplet interaction taken out. We then decouple S^t_{int} by means of a Hubbard-Stratonovich transformation as in Eq. (II.62) and write the rest part of the action in terms of bispinors and the bosonic field B. The partition function then reads

$$Z = \int D[M] e^{\frac{\Gamma_t}{2}\int dx M^2(x)} \int D[\bar{\psi}, \psi] e^{S_0[\bar{\eta},\eta] + S'_{int}[B] + \int dx \boldsymbol{M}(x)\cdot\boldsymbol{n}_s(x)} \tag{III.16}$$

We next constraint B to the isomorphic classical field Q by means of a Lagrange multiplier field $\tilde{\Lambda}$. The partition function now reads

$$Z = \int D[M] e^{\frac{\Gamma_t}{2}\int dx M^2(x)} \int D[\bar{\psi}, \psi] e^{S_0[\bar{\eta},\eta] + S'_{int}[B] + \int dx \boldsymbol{M}(x)\cdot\boldsymbol{n}_s(x)} \int D[Q, \tilde{\Lambda}] e^{Tr[\tilde{\Lambda}(Q-B)]} \tag{III.17}$$

where Tr denotes a trace over all degrees of freedom, including the continuous position in real space. Hereafter we will use it this way and use tr to denote a trace over all discrete degrees of freedom that are not explicitly shown. The fermion fields enter the action only bilinearly and can be integrated out exactly. We thus obtain a partition function that has the form

$$Z = \int D[M, Q, \tilde{\Lambda}] e^{\frac{\Gamma_t}{2} \int dx M^2(x) + A[M,Q,\tilde{\Lambda}]} \tag{III.18}$$

where A is an effective action in terms of Q and $\tilde{\Lambda}$ and the magnetization field $\boldsymbol{M}$,

$$A = \frac{1}{2} Tr(G_0^{-1} - i\tilde{\Lambda} - iM) + A_{int}[Q] + \int dx Tr[\tilde{\Lambda} Q] \tag{III.19}$$

Here G_0^{-1} is the inverse free electron Green function

$$G_0^{-1} = -\partial_\tau + \boldsymbol{\nabla}^2/2m + \mu \tag{III.20}$$

If a nontrivial band structure is desired, $\boldsymbol{\nabla}^2/2m$ can be replaced by an appropriate energy function $\epsilon(\boldsymbol{\nabla})$. This will not affect the physics at long wavelengths and small frequencies that we are interested in. From the Tr ln term in Eq. (III.19) we can see that the physical interpretation of the Lagrange multiplier field is a self-energy. $A_{int}[Q]$ is obtained by rewriting S'_{int} in Eq. (III.15) in terms of the B and constraining B to Q by means of the functional delta-constraint.

We now derive some useful properties of the matrix field Q. Since B, Eq. (III.11), is self-adjoint under the adjoint operation which is denoted by a superscript + and is defined in Eq. (III.10) , so is Q. We thus have

$$Q^+ = C^T Q^T C = Q \tag{III.21}$$

with C the charge conjugation matrix defined after Eq. (III.10). Similar to B, we can expand the fields Q in the spin-quaternion basis:

$$Q_{mn}(\boldsymbol{x}) = \sum_{i,r=0}^{3} (\tau_r \otimes s_i)\, {}^{i}_{r}Q_{mn}(\boldsymbol{x}) \tag{III.22}$$

$$\tilde{\Lambda}_{12}(\boldsymbol{x}) = \sum_{r,i=0}^{3} (\tau_r \otimes s_i)\, {}^{i}_{r}\tilde{\Lambda}_{12}(\boldsymbol{x}) \tag{III.23}$$

The Q fields also have the following properties [51]:

$${}^{0}_{r}Q_{mn} = (-1)^r\, {}^{0}_{r}Q_{nm}, \qquad (r = 0, 3) \tag{III.24}$$

$${}^{i}_{r}Q_{mn} = (-1)^{r+1}\, {}^{i}_{r}Q_{nm}, \qquad (r = 0, 3, i = 1, 2, 3) \tag{III.25}$$

$${}^{i}_{r}Q^{*}_{mn} = -\, {}^{i}_{r}Q_{-m-1,-n-1}, \qquad (r = 0, 3) \tag{III.26}$$

The physical degrees of freedom are now given by the matrix elements of the Q matrices, and the physical correlation functions of the number and spin density fluctuations can be expressed in terms of the Q-correlation functions. For example, the spin density has the form

$$\begin{aligned} n^i_s(\boldsymbol{x}, i\Omega_n) &= \sqrt{T} \sum_m \sum_{ab} \bar{\psi}^a_m(\boldsymbol{x}) \sigma^i_{ab} \psi^b_{m+n}(\boldsymbol{x}) \\ &= \sqrt{T} \sum_m \sum_{r=0,3} (\sqrt{-1})^r tr[(\tau_r \otimes s_i) Q_{m,m+n}(\boldsymbol{x})] \end{aligned} \tag{III.27}$$

with $i = 1, 2, 3$. $\Omega_n = 2\pi T n$ is a bosonic Matsubara frequency, and $\boldsymbol{n}_s(\boldsymbol{x}, i\Omega_n)$ is the Fourier transform of $\boldsymbol{n}_s(\boldsymbol{x}, \tau)$:

$$\boldsymbol{n}_s(\boldsymbol{x}, i\Omega_n) = \sqrt{T} \int_0^\beta d\tau e^{i\Omega_n \tau} \boldsymbol{n}_s(\boldsymbol{x}, \tau) \tag{III.28}$$

To get an effective field theory in terms of the matrix field Q only, we will want to integrate out the Lagrange multiplier field $\tilde{\Lambda}$. To do this, we first find Q and $\tilde{\Lambda}$ in a saddle-point approximation for the effective action A, and then expand the action to Gaussian order in the fluctuations. The calculational details are given in reference [49, 51] and we will only cite the results from these references. The next step is to separate out the soft modes and integrate out all massive modes that are not interesting for our purpose. An explicit calculation using a Ward identity shows that in a Fermi liquid, the Q fluctuations are massive if the two frequencies carried by the Q field have the same sign, while they are soft if the two frequencies have opposite signs [49, 51]. So we can separate the Q fluctuations into massless modes q_{mn} and massive modes P_{mn} by splitting the matrix Q into blocks in frequency space,

$$\begin{aligned} Q_{mn}(\boldsymbol{x}) =& \Theta(mn)P_{mn}(\boldsymbol{x}) \\ &+ \Theta(m)\Theta(-n)q_{mn}(\boldsymbol{x}) + \Theta(-m)\Theta(n)q^{\dagger}_{mn}(\boldsymbol{x}) \end{aligned} \tag{III.29}$$

with $\Theta(x)$ the Heaviside step function. From now on, we will incorporate the frequency constraints expressed by the step functions into the fields P and q. That is, the frequency indices of P must always have the same sign, and those of q and $q^{\dagger}$ will always have opposite signs.

The same thing can be done for $\tilde{\Lambda}$, and we separate the $\tilde{\Lambda}$ fluctuations into massless modes λ_{mn} and massive modes Λ_{mn}. We then integrate out all the massive modes. It turns out that the only effect of λ is to cancel out well-defined

contributions from other soft fluctuations [49]. Therefore, integrating out the soft modes λ will not cause any undesired features of the effective theory, such as nonlocality. We thus also integrate out λ. All of the calculational details are given in references [49, 51]; here we only cite the result for the soft-mode field theory in terms of the order-parameter field $\boldsymbol{M}$ and the soft modes q. The action reads

$$S[\mathbf{M}, q] = S_M + S_q + S_{M,q} \tag{III.30}$$

Here S_M is just a static, local, LGW functional for the magnetization fluctuations. No massless modes that couple to the magnetization have been integrated out, so it is local. It also can be chosen static, since the leading dynamics in the long-range and low-frequency limit will be provided by the coupling to the q fluctuations. S_M is thus given by

$$S_M = -\frac{1}{2}\int dx\ \mathbf{M}(x)\left[r - a\nabla^2\right]\mathbf{M}(x) - \frac{u}{4}\int dx\ \mathbf{M}^4(x) + \int dx \mathbf{H}\cdot\mathbf{M}(x) \tag{III.31}$$

where the four vector notation $x = (\boldsymbol{x}, \tau)$ has been used and we have included a Zeeman term for an external magnetic field $\mathbf{H}$. The expectation value of the order-parameter field $\mathbf{M}$ is proportional to the physical magnetization. r is the bare dimensionless distance from the critical point. a and u are positive Landau parameters.

S_q is the fermionic action. To Gaussian order it reads

$$S_q^{(2)} = -\frac{4}{G}\int d\boldsymbol{x} d\boldsymbol{y} \sum_{1,2,3,4}\sum_{r,i} {}^i_r q_{12}(\boldsymbol{x})\, {}^i_r \Gamma^{(2)}_{12,34}(\boldsymbol{x}-\boldsymbol{y})\, {}^i_r q_{34}(\boldsymbol{y}) \tag{III.32}$$

Before we discuss the vertex ${}^{i}_{r}\Gamma^{(2)}_{12,34}(\boldsymbol{x})$ and the coefficient G we consider the coupling term which coules $\mathbf{M}$ and q. This term originates from a term $S_{M,Q}$ that couples $\mathbf{M}$ and Q, which in turn originates from the Hubbard-Stratonovich decoupling of the spin-triplet interaction and has the form

$$S_{M,\hat{Q}} = c_1\sqrt{T}\int d\boldsymbol{x}\sum_n M^i_n(\boldsymbol{x})\sum_{r=0,3}(-1)^{r/2}\sum_m tr[\tau_r\otimes s_i Q^i_{m,m+n}(\boldsymbol{x})] \qquad \text{(III.33)}$$

The coupling constant $c_1 = \sqrt{2\pi\Gamma_t}$ is defined in terms of the spin-triplet interaction amplitude Γ_t. $\mathbf{M}_n(\boldsymbol{x})$ is the Fourier transform of the order parameter field $\mathbf{M}$,

$$\mathbf{M}_n(\boldsymbol{x}) = \sqrt{T}\int_0^\beta d\tau e^{i\Omega_n\tau}\mathbf{M}(\boldsymbol{x},\tau) \qquad \text{(III.34)}$$

For simplicity, we scale Q_{mn} with the density of states per spin at the Fermi surface, N_F, and define a dimensionless matrix field as $\hat{Q} = Q/N_F$. We then separate the dimensionless $\hat{Q}$ into soft modes q and massive modes P, where P and q now are dimensionless as well. By integrating out the massive modes, we get the coupling part of the action in the form

$$\begin{aligned} S_{M,q} =& -8ic_1N_F\sqrt{T} \\ &\times\int d\boldsymbol{x}\sum_n M^i_n(\boldsymbol{x})\sum_{mm'}({}^{1}_{0}q_{mm'}(\boldsymbol{x})\,{}^{2}_{3}q_{m+n,m'}(-\boldsymbol{x}) - {}^{1}_{3}q_{mm'}(\boldsymbol{x})\,{}^{2}_{0}q_{m+n,m'}(-\boldsymbol{x})) \end{aligned} \qquad \text{(III.35)}$$

An effective action $S_{eff}[\mathbf{M}]$ involving only the magnetization order parameter can now be obtained by integrating out the fermion fields. This is still the same strategy as Hertz's; however, Hertz treated the soft fermionic fluctuations at tree

level, which missed some qualitative effect. We keep the soft fermionic fluctuations explicitly to one-loop order, which preserves all of their qualitative effects. The final effective order-parameter action is then formally defined by

$$e^{S_{eff}[\mathbf{M}]} = \int D[q] e^{S[\mathbf{M},q]} \tag{III.36}$$

In general, the evaluation of this expression is very difficult. However, the integral can be evaluated exactly within a mean-field approximation for the order parameter which ignores the temporal and spatial variation of $\mathbf{M}$. Taking $\mathbf{M}$ in the 3-direction, we write

$$M_n^i(\boldsymbol{x}) \approx \delta_{i3}\delta_{n0} m/\sqrt{T} \tag{III.37}$$

It has been shown in Ref. [20] that this approximation does not change the nature of the quantum phase transition. For convenience we rescale m with c_1 and get $\mu = m/c_1$, where μ is the magnetization measured in μ_B per volume. We thus get the coupled action as functional of μ and dimensionless soft fermionic field q in the momentum space as

$$\begin{aligned} S[\mu, q] = &- \int dx (\frac{1}{2} r\mu^2 + \frac{1}{4} u\mu^4 - h\mu) \\ &- \frac{4}{G} \sum_{\boldsymbol{k}} \sum_{1,2,3,4} \sum_{r,i} {}^{i}_{r}q_{12}(\boldsymbol{k})\, {}^{i}_{r}\Gamma^{(2)}_{12,34}(\boldsymbol{k})\, {}^{i}_{r}q_{34}(-\boldsymbol{k}) \\ &- 8ic\mu \sum_{1,2} \sum_{\boldsymbol{k}} ({}^{1}_{0}q_{12}(\boldsymbol{k})\, {}^{2}_{3}q_{12}(-\boldsymbol{k}) - {}^{1}_{3}q_{12}(\boldsymbol{k})\, {}^{2}_{0}q_{12}(-\boldsymbol{k})) \end{aligned} \tag{III.38}$$

Here $1 \equiv n_1$, $2 \equiv n_2$, etc. $c = N_F c_1^2$ is a dimensionless coupling constant which is of order $O(1)$, and we have scaled r and u with c_1^2 and c_1^4, respectively. h is the accordingly rescaled magnetic field. It is now possible to integrate out q, as we will demonstrate in the following sections.

Generalized Mean Field Theory for Clean Systems

In this section, we will integrate out the soft fermionic field q in the coupled field theory given in Eq. (III.38), and obtain the generalized mean-field theory for a clean system. We then review the ferromagnetic phase transition properties using this generalized mean-field theory. In clean systems, the particle-hole excitations q have a linear dispersion relation, thus the vertex ${}^{i}_{r}\Gamma^{(2)}_{12,34}(\boldsymbol{k})$ has the form [52]

$$\begin{aligned} {}^{i}_{r}\Gamma^{(2)}_{12,34}(\boldsymbol{k}) =& \delta_{13}\delta_{24}(|\boldsymbol{k}| + GH\Omega_{n_1-n_2}) \\ &+ \delta_{1-2,3-4}\delta_{i0}2\pi TGK_s + \delta_{1-2,3-4}(1-\delta_{i0})2\pi TG\tilde{K}_t \end{aligned} \tag{III.39}$$

Here K_s is the coupling constant for the spin-singlet interaction, and $\tilde{K}_t$ is the coupling constant for the spin-triplet interaction that is generated under renormalization. In the absence of the latter, there is no coupling between the soft modes and the order parameter; however, as long as $K_s \neq 0$ the action will acquire a spin-triplet interaction under renormalization, and we therefore include one in the form of $\tilde{K}_t$. G and H are model dependent coefficients. For nearly free electrons, $G = \dfrac{12}{\pi N_F v_F}$ and $H = \pi N_F/4$ as in [52]. We next integrate out q to get

an effective action as a function of μ only,

$$e^{S_{eff}[\mu]} = \int D[q] e^{S[q,\mu]} \tag{III.40}$$

To do this, we denote the q-dependent part of the action by $S'[q]$, which reads

$$S'[q] = -\frac{1}{2} \sum_{i,j,r,s} \sum_{1234} \sum_{\boldsymbol{k}} {}^{i}_{r}q_{12}(\boldsymbol{k}) \, {}^{ij}_{rs}M_{12,34}(\boldsymbol{k}) \, {}^{j}_{s}q_{34}(-\boldsymbol{k}) \tag{III.41}$$

Here we have defined a matrix

$$\begin{aligned} {}^{ij}_{rs}M_{12,34}(\boldsymbol{k}) =& \frac{8}{G} \begin{pmatrix} {}^{0}_{r}\Gamma^{(2)}_{12,34} & 0 & 0 & 0 \\ 0 & {}^{1}_{r}\Gamma^{(2)}_{12,34} & 0 & 0 \\ 0 & 0 & {}^{2}_{r}\Gamma^{(2)}_{12,34} & 0 \\ 0 & 0 & 0 & {}^{3}_{r}\Gamma^{(2)}_{12,34} \end{pmatrix} \otimes \begin{pmatrix} 1 & 0 \\ 0 & 1 \end{pmatrix} \\ &+ 8ic\mu\delta_{13}\delta_{24} \otimes \begin{pmatrix} 0 & 0 & 0 & 0 \\ 0 & 0 & 1 & 0 \\ 0 & -1 & 0 & 0 \\ 0 & 0 & 0 & 0 \end{pmatrix} \otimes \begin{pmatrix} 0 & 1 \\ -1 & 0 \end{pmatrix} \end{aligned} \tag{III.42}$$

Now we have

$$\int D[q] e^{S'[q]} = e^{-\frac{1}{2} Tr \ln M} = e^{S'_{eff}} \tag{III.43}$$

where $S'_{eff} = -\frac{1}{2} Tr \ln M$ is the effective action that includes the coupling of the magnetization to the soft fermionic excitations. To calculate $Tr \ln M$, we write M as $\Gamma + X$, where the matrix Γ denotes the first term in Eq. (III.42), and X the second term. Since we are only interested in the μ-dependent terms and Γ is

independent of μ, we can write,

$$\begin{aligned} Tr\ln M &= Tr\ln(\Gamma + X) \\ &= O(\mu^0) + Tr\ln(I + \Gamma^{-1}X) \\ &= O(\mu^0) + \sum_{n=1}^{\infty} \frac{(-1)^{n+1}}{n} Tr(\Gamma^{-1}X)^n \\ &= O(\mu^0) - \frac{1}{2}\sum_{n=1}^{\infty} \frac{1}{n} Tr(\Gamma^{-1}X)^{2n} \end{aligned} \tag{III.44}$$

where we have used

$$tr \begin{pmatrix} 0 & 1 \\ -1 & 0 \end{pmatrix}^{2n+1} = 0 \tag{III.45}$$

Now we calculate $Tr((\Gamma^{-1}X)^2)^n$. The inverse of the vertex function reads (see Appendix A for details):

$${}^{i}_{r}\Gamma^{(2)-1}_{12,34}(\boldsymbol{k}) = \delta_{13}\delta_{24}D_{1-2}(\boldsymbol{k}) + \frac{\delta_{1-2,3-4}}{n_1 - n_2}\Delta\tilde{D}^t_{1-2}(\boldsymbol{k}) \tag{III.46}$$

with

$$D_n(\boldsymbol{k}) = 1/(|\boldsymbol{k}| + GH\Omega_n) \tag{III.47}$$

and

$$\tilde{D}^t_n(\boldsymbol{k}) = 1/(|\boldsymbol{k}| + G(H + \tilde{K}_t)\Omega_n) \tag{III.48}$$

as well as

$$\Delta\tilde{D}^t_n(\boldsymbol{k}) = \tilde{D}^t_n(\boldsymbol{k}) - D_n(\boldsymbol{k}) \tag{III.49}$$

the soft fermionic propagators. The only effect of the soft field λ, which we have dropped, is to cancel the noninteracting part of the q-propagator, Eq. (III.46) [49], thus we keep only the second term of Eq. (III.46). Keeping only the μ-dependent terms we get

$$\begin{aligned}
&Tr \ln M \\
&= \frac{-1}{2}\sum_{n=1}^{\infty}\frac{1}{n}(icG\mu)^{2n}Tr\left(\frac{\delta_{1-2,3-4}}{n_1-n_2}\Delta\tilde{D}^t_{1-2}(\boldsymbol{k})\otimes\begin{pmatrix}0 & 1\\ -1 & 0\end{pmatrix}\otimes\begin{pmatrix}0 & 1\\ -1 & 0\end{pmatrix}\right)^{2n} \\
&= 2\sum_{n=1}^{\infty}\frac{(-1)^{n+1}}{n}(cG\mu)^{2n}Tr\left(\frac{\delta_{1-2,3-4}}{n_1-n_2}\Delta\tilde{D}^t_{1-2}(\boldsymbol{k})\right)^{2n} \\
&= 2\sum_{n=1}^{\infty}\sum_{\boldsymbol{k}}\ln(1+c^2\mu^2G^2(\Delta\tilde{D}^t_n(\boldsymbol{k}))^2)
\end{aligned} \tag{III.50}$$

The effective action now reads,

$$\begin{aligned}
S'_{eff} &= -\sum_{n=1}^{\infty}\sum_{\boldsymbol{k}}\ln(1+c^2\mu^2G^2(\Delta\tilde{D}^t_n(\boldsymbol{k}))^2) \\
&= -\sum_{n=1}^{\infty}\sum_{\boldsymbol{k}}\ln(1+\frac{c^2\mu^2G^4\tilde{K}_t^2\Omega_n^2}{(k+GH\Omega_n)^2(k+G(H+\tilde{K}_t)\Omega_n)^2})
\end{aligned} \tag{III.51}$$

Combining this with the ordinary Landau action we get the effective action as

$$S_{eff}[\mu] = -\frac{V}{T}(\frac{1}{2}r\mu^2+\frac{1}{4}u\mu^4-h\mu) - \sum_{0<|\boldsymbol{k}|<\Lambda}\sum_{n}\ln N_{clean}(\boldsymbol{k},\Omega_n;T) \tag{III.52}$$

where

$$N_{clean} = (k+GH\Omega_n)^2(k+G(H+\tilde{K}_t)\Omega_n)^2 + c^2G^4\tilde{K}_t^2\mu^2\Omega_n^2 \tag{III.53}$$

We thus obtain the free energy density $f(\mu) = -TS_{eff}[\mu]/V$ in the form

$$f = f[\mu=0] + \frac{1}{2}r\mu^2+\frac{1}{4}u\mu^4-h\mu+\frac{1}{V}\sum_{0<|\boldsymbol{k}|<\Lambda}T\sum_{n}\ln N_{clean}(\boldsymbol{k},\Omega_n;T) \tag{III.54}$$

where $f[\mu = 0]$ is the contribution to the free energy density from degrees of freedom other than the magnetization. Λ is a momentum cutoff. r and u have dimensions of energy times volume and energy times cubic volume, respectively. Next we convert the sums over the wave number and the frequency to integrals. In d=3 this is accomplished by

$$\sum_{\boldsymbol{k}} \to V \int \frac{d^3\boldsymbol{k}}{(2\pi)^3} \tag{III.55}$$

and

$$\sum_{n} \to \int \frac{d\omega}{2\pi T} \tag{III.56}$$

A nonzero temperature we will model by an appropriate lower limit on the frequency integral.

It is convenient to make all variables in the model dimensionless. To do this, we scale the momentum and the frequency with the Fermi wave number k_F and the Fermi energy ϵ_F, respectively. That is, we define dimensionless variables $\hat{k} = \dfrac{k}{k_F}$ and $\hat{\Omega}_n = \dfrac{3\Omega_n}{2T_F}$. We also define a dimensionless magnetization as

$$\hat{\mu} = \mu / \frac{\pi n_e}{8c} \tag{III.57}$$

where $n_e = k_F^3/3\pi^2$ is the electron density, and the constant $\pi/8$ is for calculational convenience as we will see soon. Furthermore, we expect that $\tilde{K}_t$ is small compare to H, so we neglect $\tilde{K}_t$ when it appears additively to H. We thus approximate N_{clean} by

$$N_{clean} = (k + GH\Omega_n)^4 + c^2 G^4 \tilde{K}_t^2 \mu^2 \Omega_n^2 \tag{III.58}$$

We can furthur express N_{clean} in terms of the dimensionless magnetization $\hat{\mu}$ and dimensionless momentum $\hat{k}$ as well as dimensionless frequency $\hat{\Omega}_n$ as

$$N_{clean} = k_F^4[(\hat{k} + \hat{\Omega}_n)^4 + \tilde{\gamma}_t^2 \hat{\mu}^2 \hat{\Omega_n}^2] \tag{III.59}$$

where we have defined $\tilde{\gamma}_t \equiv \tilde{K}_t/H$. Inserting Eq. (III.59) into Eq. (III.54), and changing the sum into an integral, we get the free energy density in the form

$$\begin{aligned} f =& \frac{1}{2} r\hat{\mu}^2 + \frac{1}{4} u\hat{\mu}^4 - h\hat{\mu} \\ &+ \frac{1}{6\pi^3} k_F^3 T_F \int_0^{\Lambda/k_F} dk k^2 \int_{\frac{3\pi T}{T_F}}^{\infty} d\omega \ln((k+\omega)^4 + \tilde{\gamma}_t^2 \hat{\mu}^2 \omega^2) \end{aligned} \tag{III.60}$$

where we have discarded a constant contribution. The coefficients r and u as well as the magnetic field h have been rescaled, so now dimensionally they all are an energy per volume. For convenience, we further define a dimensionless free energy density as $\hat{f} = f/(\frac{T_F \pi n_e}{8c})$, so we get

$$\hat{f} = \frac{1}{2}\hat{r}\hat{\mu^2} + \frac{1}{4}\hat{u}\hat{\mu}^4 - \hat{h}\hat{\mu} + \frac{4}{\pi^2} c \int_0^1 dk k^2 \int_t^{\infty} d\omega \ln((k+\omega)^4 + \tilde{\gamma}_t^2 \hat{\mu}^2 \omega^2) \tag{III.61}$$

Here we have chosen the momentum cutoff Λ to be the Fermi momentum k_F, and we have defined a dimensionless temperature as $t = 3\pi T/T_F$. $\hat{r}$ and $\hat{u}$ are the appropriately scaled parameters r and u, which are now dimensionless. $\hat{h}$ is the properly scaled magnetic field, which is also dimensionless. Now we need to perform the integral. It is not easy to do so due to the ln-function in the integrand, so we differentiate the dimensionless free energy with respect to the dimensionless order

parameter $\hat{\mu}$ to get rid of the ln-function and get the equation of state

$$\begin{aligned}\frac{\partial \hat{f}}{\partial \hat{\mu}} &= \hat{r}\hat{\mu} + \hat{u}\hat{\mu}^3 - \hat{h} + \frac{8}{\pi^2} c\tilde{\gamma}_t^2 \hat{\mu} \int_0^1 dk k^2 \int_t^\infty d\omega \frac{\omega^2}{\tilde{\gamma}_t^2 \hat{\mu}^2 \omega^2 + (k+\omega)^4} \\ &= 0\end{aligned} \tag{III.62}$$

Now we can perform the integral in the equation of state. We denote the integral in Eq. (III.62) by I_1,

$$I_1(\hat{\mu}, t) = \int_0^1 dk k^2 \int_t^\infty d\omega \frac{\omega^2}{\tilde{\gamma}_t^2 \hat{\mu}^2 \omega^2 + (k+\omega)^4} \tag{III.63}$$

We only are interested in the magnetization dependence, so what we really want is $I_1(\hat{\mu}, t) - I_1(\hat{\mu} = 0, t)$, which we denote by I,

$$\begin{aligned} I(\hat{\mu}, t) &= I_1(\hat{\mu}, t) - I_1(\hat{\mu} = 0, t) \\ &= -\tilde{\gamma}_t^2 \hat{\mu}^2 \int_0^1 dk k^2 \int_t^\infty d\omega \frac{\omega^4}{(k+\omega)^4 (\tilde{\gamma}_t^2 \hat{\mu}^2 \omega^2 + (k+\omega)^4)} \end{aligned} \tag{III.64}$$

To perform this integral, we first rescale k and ω with $\tilde{\gamma}_t \hat{\mu}$ to get

$$I(\hat{\mu}, t) = -\tilde{\gamma}_t^2 \hat{\mu}^2 \int_0^{\frac{1}{\tilde{\gamma}_t \hat{\mu}}} dk k^2 \int_{\frac{t}{\tilde{\gamma}_t \hat{\mu}}}^\infty d\omega \frac{\omega^4}{(k+\omega)^4 (\omega^2 + (k+\omega)^4)} \tag{III.65}$$

It is still not easy to calculate the integral exactly, so we consider limiting cases. We first look at the zero temperature ($t = 0$) case,

$$\begin{aligned} I(\hat{\mu}, t) &= -\tilde{\gamma}_t^2 \hat{\mu}^2 \int_0^{\frac{1}{\tilde{\gamma}_t \hat{\mu}}} dk k^2 \int_0^\infty d\omega \frac{\omega^4}{(k+\omega)^4 (\omega^2 + (k+\omega)^4)} \\ &= -\tilde{\gamma}_t^2 \hat{\mu}^2 \int_0^{\frac{1}{\tilde{\gamma}_t \hat{\mu}}} dk k^{-1} \int_0^\infty d\omega \frac{\omega^4}{(1+\omega)^4 (\omega^2/k^2 + (1+\omega)^4)} \\ &\approx -\tilde{\gamma}_t^2 \hat{\mu}^2 \int_0^{\frac{1}{\tilde{\gamma}_t \hat{\mu}}} dk \frac{k}{3(1+35k^2)} \\ &= -\frac{\tilde{\gamma}_t^2 \hat{\mu}^2}{210} \ln(1 + 35(\frac{1}{\tilde{\gamma}_t \hat{\mu}})^2) \end{aligned} \tag{III.66}$$

Inserting Eq. (III.66) into Eq. (III.62) we get the equation of state at zero temperature as

$$\begin{aligned}\hat{h} &= \hat{r}\hat{\mu} + \hat{u}\hat{\mu}^3 - \frac{4}{105\pi^2} c\tilde{\gamma}_t^4 \hat{\mu}^3 \ln \frac{(\tilde{\gamma}\hat{\mu})^2 + 35}{(\tilde{\gamma}\hat{\mu})^2} \\ &\approx \hat{r}\hat{\mu} + \hat{u}\hat{\mu}^3 + \frac{4}{105\pi^2} c\tilde{\gamma}_t^4 \hat{\mu}^3 \ln(\frac{\hat{\mu}}{\sqrt{35}/\tilde{\gamma}_t})^2 \\ &= \hat{r}\hat{\mu} + \hat{u}\hat{\mu}^3 + \hat{v}\hat{\mu}^3 \ln(\hat{\mu}/\hat{\mu}_0)^2\end{aligned} \tag{III.67}$$

where we have defined $\hat{v} = \frac{4}{105\pi^2} c\tilde{\gamma}_t^4$ and $\hat{\mu}_0 = \sqrt{35}/\tilde{\gamma}_t$. We have taken into account that the dimensionless magnetization $\hat{\mu}$ and the dimensionless coefficient $\tilde{\gamma}_t$ are both small compared to one and thus have approximated $35 + (\tilde{\gamma}_t\hat{\mu})^2$ by 35. We see that Eq. (III.67) agrees with the equation of state for clean systems at zero temperature given in Eq. (III.1).

Next we consider the nonzero temperature situation. Let us go back to the integral in Eq. (III.65). If the dimensionless temperature is small compared to the dimensionless magnetization, $t/(\tilde{\gamma}_t\hat{\mu}) \ll 1$, we can still approximate the integral by its value at $t = 0$, which we have discussed above. The other limit is when the temperature is large compare to the dimensionless magnetization, that is, $t/\tilde{\gamma}_t\hat{\mu} \gg 1$. In this limit we get

$$\begin{aligned}I(\hat{\mu}, t) &\approx -\tilde{\gamma}_t^2 \hat{\mu}^2 \int_0^{\frac{1}{\tilde{\gamma}_t\hat{\mu}}} dk k^2 \int_{\frac{t}{\tilde{\gamma}_t\hat{\mu}}}^{\infty} d\omega \frac{\omega^4}{(k+\omega)^8} \\ &\approx -\frac{1}{105}\tilde{\gamma}_t^2 \hat{\mu}^2 \ln(1 + \frac{1}{t}) + O(\hat{\mu}^2)\end{aligned} \tag{III.68}$$

By combining the results of the two extreme cases, $t \ll \tilde{\gamma}_t\hat{\mu}$ and $t \gg \tilde{\gamma}_t\hat{\mu}$, given in

Eq. (III.66) and Eq. (III.68), respectively, we approximate the integral as

$$I(\hat{\mu},t) \approx -\frac{\tilde{\gamma}_t^2\hat{\mu}^2}{210}\ln\frac{1}{(\tilde{\gamma}_t\hat{\mu})^2/35+t^2} \tag{III.69}$$

Here we have taken into account the fact that the dimensionless temperature t is much less than 1, and we have neglected the uninteresting term of $O(\hat{\mu}^2)$ since it is just a modification of the $\hat{u}\hat{\mu}^4$ term in the free energy density. We now get the equation of state by inserting Eq. (III.69) into Eq. (III.62)

$$\hat{h} = \hat{r}\hat{\mu}^2 + \hat{u}\hat{\mu}^3 + \hat{v}\hat{\mu}^3\ln((\hat{\mu}/\hat{\mu}_0)^2+t^2) \tag{III.70}$$

We now take a look at the dimensionless coefficient $\hat{u}$. The original u in Eq. (III.31) is on the order of the second derivative of the density of states at the Fermi surface [17],

$$u = \frac{1}{12}\Gamma_t^2 N''(\epsilon_F) \tag{III.71}$$

so after the rescaling we have done we have the dimensionless $\hat{u}$ given by

$$\hat{u} = (c_1^4(\pi n_e/8c)^3/T_F)u = O(1) \tag{III.72}$$

Now we briefly discuss the equation of state given in Eq. (III.70) and show that it indeed gives a phase diagram as shown in Fig. 1.4.. Since the coefficient $\hat{v}$ of the ln-term is greater than zero, at zero temperature and for a small magnetization the ln-term will be negative. This will have the same effect as a negative $\hat{u}\hat{\mu}^4$ term in a regular Landau theory, namely, a first-order transition will pre-empt the second-order transition. For convenience, in the following discussion we neglect the hats,

which denotes dimensionlessness of the parameters in the equantion of state Eq. (III.70). An explicit calculation shows that at zero magnetic field, there is indeed a first order transition happens at $\hat{r} = \frac{1}{2}\hat{v}\hat{\mu}_1^2 > 0$ where $\hat{\mu}$ changes discontinuously from zero to $\hat{\mu}_1 = \hat{\mu}_0 e^{-\frac{1}{2}(1+\hat{u}/\hat{v})}$. One thus concludes that quantum ferromagnetic phase transitions are generally of first order for clean systems. If the temperature increases from zero the ln-term is cut off, and the first-order transition is weakened and finally completely suppressed at a sufficiently high temperature. There thus will be a tricritical point in the phase diagram. An explicit calculation shows that the tricritical temperature is $T_{tc} = \frac{T_F}{3\pi} e^{-u/2v}$. When an external magnetic field is present, the first order transition line will bifurcate into two first order transition planes [21]. So Eq. (III.70) does indeed yield the phase diagram as shown in Fig. 1.4..

Generalized Mean Field Theory for Disordered Systems

In this subsection we will discuss disordered ferromagnetic systems by using similar methods as in the preceding subsection for clean systems. In a disordered system, the action contains an extra term that represents the quenched disorder:

$$S_{dis} = -\int_0^\beta \int_V d\boldsymbol{x}\ v(\boldsymbol{x})\bar{\psi}(\boldsymbol{x},\tau)\psi(\boldsymbol{x},\tau) \tag{III.73}$$

where $v(\boldsymbol{x})$ is a random potential. For simplicity we assume that v is δ-correlated

and obeys a Gaussian distribution $P[v(\boldsymbol{x})]$ with second moment

$$\{v(\boldsymbol{x})v(\boldsymbol{y})\}_{dis} = \frac{1}{2\pi N_F \tau}\delta(\boldsymbol{x}-\boldsymbol{y}) \tag{III.74}$$

Here

$$\{\cdots\}_{dis} = \int D[v]P[v](\cdots) \tag{III.75}$$

denotes the disorder average, N_F is the bare density of states per spin at the Fermi level, and τ is the bare electron elastic mean-free time.

The classic way to deal with disorder is the replica trick [53, 54]. By performing the disorder average in Eq. (III.75), we get the disorder term in the action,

$$S_{dis} = \frac{1}{4\pi N_F \tau_{el}} \sum_{\alpha_1,\alpha_2=1}^{N} \int_0^\beta d\tau d\tau' \int d\boldsymbol{x} \bar{\psi}_a^{\alpha_1}(\boldsymbol{x},\tau)\psi_a^{\alpha_1}(\boldsymbol{x},\tau)\bar{\psi}_b^{\alpha_2}(\boldsymbol{x},\tau')\psi_b^{\alpha_2}(\boldsymbol{x},\tau') \tag{III.76}$$

where α_1 and α_2 are the replica indices, and N$\to$0 is the number of replicas. All other terms in the action are replicated N times. Next we can follow the same strategy as in the clean case, that is, we express the action in terms of the bosonic matrix field B. By constraining B to a number-valued matrix field Q, we get an action similar to Eq. (III.19), with an extra term $A_{dis}[Q]$ from S_{dis}. By finding the saddle point solution for the action and expanding about the saddle point solution, as well as integrating out the massive modes, we again get a coupled field theory which has a form similar to Eq. (III.30), with all field now carrying replica indices. The main difference is that in a clean system the particle-hole excitations

q are ballistic, that is the frequency scales linearly with the wave number, while in disordered system the dispersion relation is diffusive, i.e., the frequency scales with the wave number squared. So the vertex function $\Gamma^{(2)}$ has different forms in these two cases, as we mentioned before. Also the model-dependent coefficient G is different in the two cases: In the clean case, we used $G_{clean} = \dfrac{12}{\pi N_F v_F}$, while in the disordered case we have $G_{dis} = G_{clean}/l$ with $l = v_F\tau$ the mean-free path of the electrons. We obtain a coupled field theory which has a similar form as given in Eq. (III.38), only that now the indices also include the replica indices, *i.e.*, $1 = (n_1, \alpha_1)$, etc.

The vertex ${}^{i}_{r}\Gamma^{(2)}_{12,34}(\boldsymbol{k})$ in a disordered system has the form

$$\begin{aligned} {}^{i}_{r}\Gamma^{(2)}_{12,34}(\boldsymbol{k}) = \delta_{1-2,3-4}\{\delta_{13}(k^2 + GH\Omega_{n_1-n_2}) + (1-\delta_{i0})\delta_{\alpha_1\alpha_2}\delta_{\alpha_1\alpha_3}2\pi TG\tilde{K}_t\} \\ +\delta_{1-2,3-4}\delta_{i0}\delta_{\alpha_1\alpha_2}\delta_{\alpha_1\alpha_3}2\pi TGK_s \end{aligned} \tag{III.77}$$

As in the clean case, we integrate out the soft mode q to obtain a generalized Landau theory for the order parameter. In disordered systems, all Lagrange multiplier fields are soft, and the q-propagator therefore also includes the non-interacting part of

the inverse Γ^2 matrix [49]. The result of the Gaussian integration is

$$
\begin{aligned}
&Tr \ln M \\
&= 2\sum_{n=1}^{\infty} \frac{(-1)^{n+1}}{n} (cG\mu)^{2n} Tr \left(\delta_{13}\delta_{24} D_{n_1-n_2}(\boldsymbol{k}) + \frac{\delta_{1-2,3-4}\delta_{\alpha_1\alpha_2}\delta_{\alpha_1\alpha_3}}{n_1-n_2} \Delta\tilde{D}^t_{n_1-n_2}(\boldsymbol{k}) \right)^{2n} \\
&= 2\sum_{n=1}^{\infty} \sum_{\boldsymbol{k}} \ln \frac{1 + c^2\mu^2 G^2 (\Delta\tilde{D}^t_n(\boldsymbol{k}) + D_n(\boldsymbol{k}))^2}{1 + c^2\mu^2 G^2 D_n^2(\boldsymbol{k})}
\end{aligned}
\tag{III.78}
$$

with the propagators now having the form

$$
D_n(\boldsymbol{k}, \Omega_n) = \frac{1}{k^2 + G_{dis} H \Omega_n} \tag{III.79}
$$

$$
\tilde{D}^t_n(\boldsymbol{k}, \Omega_n) = \frac{1}{k^2 + G_{dis}(H + \tilde{K}_t)\Omega_n} \tag{III.80}
$$

and

$$
\Delta\tilde{D}^t_n(\boldsymbol{k}, \Omega_n) = \tilde{D}^t_n(\boldsymbol{k}, \Omega_n) - D_n(\boldsymbol{k}, \Omega_n) \tag{III.81}
$$

The action as a function of the magnetization only then is

$$
S[\mu] = -\frac{V}{T}(\frac{1}{2} r\mu^2 + \frac{1}{4} u\mu^4 - h\mu) - \sum_{|\boldsymbol{k}|<1/l} \sum_{n} \ln N_{disorder}(\boldsymbol{k}, \Omega_n; \mu) \tag{III.82}
$$

where

$$
N_{dis}(\boldsymbol{k}, \Omega_n; \mu) = \frac{1 + c^2\mu^2 G^2_{dis} (\tilde{D}^t_n)^2}{1 + c^2\mu^2 G^2_{dis} D^2_n} \tag{III.83}
$$

Note that the momentum integral in disordered system goes from 0 to $1/l$. Again we rescale the magnetization per volume μ by $\frac{\pi n_e}{8c}$ and define $\hat{k} = k/k_F$ as well as

$\hat{\Omega}_n = \dfrac{3\Omega_n}{2T_F}$ as we did in clean case. Now N_{dis} reads

$$N_{dis}(\hat{k}, \hat{\Omega}_n; \hat{\mu}) = \frac{(\hat{k}^2 + (1+\tilde{\gamma}_t)\frac{\hat{\Omega}_n}{lk_F})^2 + \frac{1}{(lk_F)^2}\hat{\mu}^2}{(\hat{k}^2 + \frac{\hat{\Omega}_n}{lk_F})^2 + \frac{1}{(lk_F)^2}\hat{\mu}^2} \times \frac{(\hat{k}^2 + \frac{\hat{\Omega}_n}{lk_F})^2}{(\hat{k}^2 + (1+\tilde{\gamma}_t)\frac{\hat{\Omega}_n}{lk_F})^2} \tag{III.84}$$

If we keep only the $\hat{\mu}$-dependent part of N_{dis} and rescale the free energy f by $\dfrac{\pi n_e}{8c}T_F$ we get the dimensionless free energy density in the form

$$\hat{f} = \frac{1}{2}\hat{r}\hat{\mu}^2 + \frac{1}{4}\hat{u}\hat{\mu}^4 - \hat{h}\hat{\mu} + \frac{4}{\pi^2}c\int_0^{1/lk_F} dkk^2 \int_t^\infty d\omega \ln \frac{(k^2 + (1+\tilde{\gamma}_t)\frac{\omega}{lk_F})^2 + \frac{\hat{\mu}^2}{(lk_F)^2}}{(k^2 + \frac{\omega}{lk_F})^2 + \frac{\hat{\mu}^2}{(lk_F)^2}} \tag{III.85}$$

where $\hat{r}$ and $\hat{u}$ as well as $\hat{h}$ are the same as in the clean case. To perform the integral we again first differentiate the free energy density with respect to the dimensionless magnetization to get the equation of state for the disordered system,

$$\begin{aligned}\frac{\partial \hat{f}}{\partial \hat{\mu}} &= \hat{r}\hat{\mu} + \hat{u}\hat{\mu}^3 - \hat{h} - \frac{16}{\pi^2}c\tilde{\gamma}_t \frac{\hat{\mu}}{(lk_F)^{3/2}} \int_0^{\frac{1}{\sqrt{lk_F}}} dkk^2 \int_t^\infty d\omega \frac{\omega(k^2+\omega)}{((k^2+\omega)^2 + \hat{\mu}^2)^2} \\ &= 0\end{aligned} \tag{III.86}$$

Here we have only kept terms to linear order in $\tilde{\gamma}_t$. We denote the integral by

$$I_1(\hat{\mu}, t) = \int_0^{\frac{1}{\sqrt{lk_F}}} dkk^2 \int_t^\infty d\omega \frac{\omega(k^2+\omega)}{((k^2+\omega)^2 + \hat{\mu}^2)^2} \tag{III.87}$$

and again consider

$$\begin{aligned} I(\hat{\mu}, t) &= I_1(\hat{\mu}, t) - I_1(\hat{\mu} = 0, t) \\ &= -\int_0^{\frac{1}{\sqrt{lk_F}}} dkk^2 \int_t^\infty d\omega \frac{\omega\hat{\mu}^2(2(k^2+\omega)^2 + \hat{\mu}^2)}{(k^2+\omega)^3((k^2+\omega)^2 + \hat{\mu}^2)^2} \\ &= -\hat{\mu}^{1/2} \int_0^{1/(lk_F\hat{\mu})} dx\sqrt{x} \int_{t/\hat{\mu}}^\infty d\omega \frac{\omega[2(x+\omega)^2 + 1]}{(x+\omega)^3[(x+\omega)^2+1]^2} \end{aligned} \tag{III.88}$$

For convenience we define

$$g(y,z) = \frac{1}{g_0}\int_0^{1/y} dx\sqrt{x}\int_z^{\infty} d\omega \frac{\omega[2(x+\omega)^2+1]}{(x+\omega)^3[(x+\omega)^2+1]^2} \tag{III.89}$$

where the normalization factor is defined by $g_0 = \pi/3\sqrt{2} \approx 0.74$, which makes $g(0,0) = 1$. The equation of state thus reads

$$\begin{aligned}\frac{\partial \hat{f}}{\partial \hat{\mu}} &= \hat{r}\hat{\mu} + \hat{u}\hat{\mu}^3 - \hat{h} + \frac{16}{3\sqrt{2}\pi} c\tilde{\gamma}_t \frac{\hat{\mu}^{3/2}}{(lk_F)^{3/2}} g(lk_F\hat{\mu}, t/\hat{\mu}) \\ &= \hat{r}\hat{\mu} + \hat{u}\hat{\mu}^3 - \hat{h} + \hat{w}\frac{\hat{\mu}^{3/2}}{(lk_F)^{3/2}} g(lk_F\hat{\mu}, t/\hat{\mu}) \\ &= 0\end{aligned} \tag{III.90}$$

where we have defined a dimensionless coefficient $\hat{w} = \frac{16}{3\sqrt{2}\pi} c\tilde{\gamma}_t \approx c\tilde{\gamma}_t$. With this equation of state we can discuss the quantum ferromagnetic phase transition in the presence of strong quenched disorder. When the temperature is zero, $g(y,0)$ is well approximated by

$$g(y,0) = \frac{1}{1 + y^{3/2}/(y/g_0 + 9g_0)} \tag{III.91}$$

Furthermore, when $lk_F\hat{\mu} \ll g_0$, we have $g(y,0) \approx 1 - y^{3/2}/9g_0$. The equation of state in this limit reads

$$\begin{aligned}\hat{h} &= \hat{r}\hat{\mu} + \hat{u}\hat{\mu}^3 + \hat{w}\frac{1}{(lk_F)^{3/2}}\hat{\mu}^{3/2}(1 - (lk_F\hat{\mu})^{3/2}/9g_0) \\ &= \hat{r}\hat{\mu} + (\hat{u} - \hat{w}/(9g_0))\hat{\mu}^3 + \hat{w}\frac{1}{(lk_F)^{3/2}}\hat{\mu}^{3/2} \\ &\equiv \hat{r}\hat{\mu} + \hat{w}\frac{1}{(lk_F)^{3/2}}\hat{\mu}^{3/2} + \hat{u}\hat{\mu}^3\end{aligned} \tag{III.92}$$

We recognize this as the equation of state given in Eq. (III.2). We have redefined $\hat{u} - \hat{w}/(9g_0)$ as $\hat{u}$, which just shifts the unknown Landau parameter u. From this

equation of state we see that there is a continuous phase transition characterized by non-mean-field critical exponents. When the quenched disorder is decreased, that is, when lk_F gets large, there will be a crossover from the non-mean-field critical behavior to ordinary mean-field critical behavior. This crossover happens when the last two terms in Eq. (III.92) have the same magnitude.

On the other hand, when $lk_F\hat{\mu} \gg 9g_0^2$, we have $g(y,0) \approx 1/(g_0\sqrt{y})$. In this limit the equation of state reads

$$\hat{h} = (\hat{r} + \frac{\hat{w}}{g_0(lk_F)^2})\hat{\mu} + \hat{u}\hat{\mu}^3 \tag{III.93}$$

This is an ordinary Landau model that has a second order phase transition characterized by mean-field critical exponents, which also agrees with our previous analysis.

In summary, we see that when the disorder is large enough there is a continuous ferromagnetic phase transition characterized by non-mean-field critical exponents, and when the disorder decreases, there is a crossover from the non-mean-field critical behavior to ordinary mean-field critical behavior.

Comprehensive Generalized Mean Field Theory

In the previous two sections we reviewed the equations of state and the quantum phase transition properties of very clean and strongly disordered ferromagnets. In reality, many systems fall in between these two extreme cases. In this section we

will construct a more realistic theory that interpolates between these two cases. In this way we will construct a comprehensive theory that is suitable for investigating how the phase diagram evolves with increasing disorder. The crucial point for the interpolation is that the soft fermionic modes are diffusive in a momentum range less than $1/l$, and ballistic outside of this range. With these in mind, we write a comprehensive action as follows,

$$\begin{aligned} S = -\frac{V}{T}(\frac{1}{2}r\mu^2 + \frac{1}{4}u\mu^4) - \sum_{1/l<|\boldsymbol{k}|<\Lambda}\sum_n \ln N_{clean}(\boldsymbol{k},\Omega_n;\mu) \\ - \sum_{|\boldsymbol{k}|<1/l}\sum_n \ln N_{disorder}(\boldsymbol{k},\Omega_n;\mu) \end{aligned} \tag{III.94}$$

with N_{clean} and $N_{disorder}$ given by Eq. (III.53) and Eq. (III.83), respectively. We see that the momentum sum in the clean term is over momenta from $1/l$, rather than zero, to the cutoff; this determines the effects of the disorder on the first-order transition. The disorder term is the same as before. We rescale all quantities to get a dimensionless magnetization and free energy density as we did in previous sections, and obtain the free energy density in the form

$$\begin{aligned} \hat{f} = \frac{1}{2}\hat{r}\hat{\mu}^2 + \frac{1}{4}\hat{u}\hat{\mu}^4 + \frac{4}{\pi^2}c\int_{1/lk_F}^{1} dk k^2 \int_t^\infty d\omega \ln(\tilde{\gamma}_t^2\hat{\mu}^2\omega^2 + (k+\omega)^4) \\ + \frac{4}{\pi^2}c\int_0^{1/lk_F} dk k^2 \int_t^\infty d\omega \ln \frac{(k^2 + (1+\tilde{\gamma}_t)\frac{\omega}{lk_F})^2 + \frac{\hat{\mu}^2}{(lk_F)^2}}{(k^2+\frac{\omega}{lk_F})^2 + \frac{\hat{\mu}^2}{(lk_F)^2}} \end{aligned} \tag{III.95}$$

To perform the integral we differentiate the free energy with respect to the magnetization as we did before. For the diffusive term we get the same answer as

before. From the clean term we have

$$\begin{aligned}\frac{\partial \hat{f}_{clean}}{\partial \hat{\mu}} &= \frac{8}{\pi^2} c\tilde{\gamma}_t^2 \hat{\mu} \int_{1/lk_F}^{1} dk k^2 \int_t^{\infty} d\omega \frac{\omega^2}{(k+\omega)^4 + \tilde{\gamma}_t^2 \hat{\mu}^2 \omega^2} \\ &= \frac{8}{\pi^2} c\tilde{\gamma}_t^2 \hat{\mu} I_1(\hat{\mu}, t)\end{aligned} \tag{III.96}$$

where we have denoted the third term in Eq. (III.95) by $\hat{f}_{clean}$. What we are really interested in is again the $\hat{\mu}$-dependent part

$$\begin{aligned}I(\hat{\mu}, t) &= I_1(\hat{\mu}, t) - I_1(\hat{\mu} = 0, t) \\ &= -\tilde{\gamma}_t^2 \hat{\mu}^2 \int_{\frac{1}{lk_F \tilde{\gamma}_t \hat{\mu}}}^{\frac{1}{\tilde{\gamma}_t \hat{\mu}}} dk k^2 \int_{\frac{t}{\tilde{\gamma}_t \hat{\mu}}}^{\infty} d\omega \frac{\omega^4}{(k+\omega)^4 [(k+\omega)^4 + \omega^2]}\end{aligned} \tag{III.97}$$

For $t \ll \tilde{\gamma}_t \hat{\mu}$ we get

$$I(\hat{\mu}, t) = -\tilde{\gamma}_t^2 \hat{\mu}^2 \times \frac{1}{210} \ln \frac{1 + \frac{35}{(\tilde{\gamma}_t \hat{\mu})^2}}{1 + \frac{35}{(lk_F \tilde{\gamma}_t \hat{\mu})^2}} \tag{III.98}$$

and for $t \gg \tilde{\gamma}_t \hat{\mu}$,

$$I(\hat{\mu}, t) = -\tilde{\gamma}_t^2 \hat{\mu}^2 \times \frac{1}{105} \ln \frac{1 + \frac{1}{t}}{1 + \frac{1}{lk_F t}} \tag{III.99}$$

$I(\hat{\mu}, t)$ can thus be approximated by

$$I(\hat{\mu}, t) = -\tilde{\gamma}_t^2 \hat{\mu}^2 \times \frac{1}{210} \ln \frac{1}{(\tilde{\gamma}_t \hat{\mu})^2/35 + (t + \frac{1}{lk_F})^2} \tag{III.100}$$

The equation of state from the comprehensive theory now reads

$$\begin{aligned}\frac{\partial \hat{f}}{\partial \hat{\mu}} &= \hat{r}\hat{\mu} + \hat{w} \frac{1}{(lk_F)^{3/2}} g(lk_F \hat{\mu}, t/\hat{\mu}) \hat{\mu}^{3/2} + \hat{u}\hat{\mu}^3 - \hat{h} - \hat{v}\hat{\mu}^3 \ln \frac{1}{\hat{\mu}^2/\hat{\mu}_0^2 + (t + \frac{1}{lk_F})^2} \\ &= 0\end{aligned} \tag{III.101}$$

where $g(x, y)$ has been given in Eq. (III.89), $\hat{w}$ is defined below Eq. (III.90), $\hat{u}$ is discussed in Eq. (III.72), $\hat{v}$ and μ_0 are given under Eq. (III.67).

However, we need to keep in mind that these results for the coefficients $\hat{w}$, $\hat{v}$, and $\hat{\mu}_0$ come from a very simple model calculation that is valid at best for weakly correlated systems, where $\tilde{\gamma}_t << 1$. In realistic systems the values may be very different. For notational convenience we now discard the carets in the equation of state and denote the dimensionless magnetization by m. The generalized equation of state then has the form

$$h = rm + \frac{w}{(lk_F)^{3/2}}\, g(lk_F m, t/m) m^{3/2} - vm^3 \ln\left(\frac{1}{m^2/m_0^2 + (1/lk_F + t)^2}\right) + um^3 \tag{III.102}$$

As mentioned above, m_0 in Eq. (III.102) should be considered an independent microscopic parameter that sets the scale of the magnetic moment and depends on the details of the band structure and other microscopic details. Similarly, we need to introduce one more parameter to free ourselves from the nearly-free-electron model we used for the original derivation of the equation of state. We will denote this by σ_0, and it sets the disorder scale. We thus generalize the equation of state to

$$h = rm + \frac{w}{(lk_F)^{3/2}} g(lk_F m, t/m) m^{3/2} - vm^3 \ln\left(\frac{1}{m^2/m_0^2 + (\sigma_0/lk_F + t)^2}\right) + um^3 \tag{III.103}$$

σ_0 depends on the correlation strength and is ≤ 1. Its physical origin is as follows. In a strongly correlated material two electrons with opposite spins cannot

simultaneously take advantage of a disorder-induced downward fluctuation of the local potential energy, because of the strong repulsion between the electrons. This is consistent with the fact that in the absence of symmetry-breaking fields, interactions cause the disorder to get renormalized downward [52, 55]. Correlations will thus weaken the effects of the disorder. When there is no correlation, $\sigma_0 = 1$. For strong correlation systems, $\sigma_0 = 0.1$ is a reasonable estimate based on the RG flow equations of Ref. [55].

We now use this equation of state to discuss the dependence of the phase diagram and the related critical phenomena on the disorder. We will refer the second and third term on the right-hand side of the equation of state (III.103) as the diffusive and ballistic nonanalyticity, respectively.

We start with the clean case. Our first step is to find values for the parameters in Eq. (III.103) that give a reasonable description of the experiments for clean systems that show a first-order transition and a tricritical point. In the clean case, Eq. (III.103) recovers Eq. (III.70). As we have discussed at the end of Section III.2.2, in this case the quantum ferromagnetic phase transition is of first order with the magnetization at the transition give by $m_1 = m_0 e^{-(1+u/v)/2}$, and there exists a tricritical point with tricritical temperature $T_{tc} = \dfrac{T_F}{3\pi} e^{-u/2v}$. We now consider the weak ferromagnets $ZrZn_2$, MnSi, URhGe and UGe_2, where first order ferromagnetic transitions and tricritical temperatures have been observed. The magnetic moments per formula unit for these materials are about 0.17 [23], 0.4 [56], 0.4 [57] and $1.5\mu_B$

[58], respectively. A typical value of the Fermi wavenumber in a good metal is about $1\mathring{A}^{-1}$, and the formula unit volume for these materials is about $50\mathring{A}^3$ [56–59]. With these values, the dimensionless saturation magnetization is about 0.25, 0.6, 0.6 and 2.3, respectively, for these four materials. If we choose u to be 1, $\tilde{\gamma}_t = 0.5$, which represents fairly strong correlation, and $c = 1$, we get $v \approx 0.06$. With a Fermi temperature $T_F = 10^5 K$, the tricritical temperature T_{tc} is then around $10K$, which is the right order of magnitude for the tricritical temperature in $ZrZn_2$, MnSi, and UGe_2. If the value of $\tilde{\gamma}_t$ is slightly lower, say, 0.45, we get a tricritical temperature of about $1K$, as observed in URhGe. If the value of m_0 is between 75 (for $ZrZn_2$) and 350 (for UGe_2), this gives values of m_1 that range from 0.05 to 0.25, which is a reasonable fraction of the saturation magnetization in these materials. If an external magnetic field is applied, there will be two wings of first order transitions that extend from the tricritical point and end at the two quantum critical points in the zero-temperature plane. The critical magnetic field at the tips of the tricritical wings is [21] $h_c = (4/3)e^{-13/4} m_0^3 v e^{-3u/2v}$. With the same parameters given above, this yields critical magnetic fields that range from 0.1T to 10T, which agrees with the experimental observations [23, 39, 60].

Now that we have determined the parameter values that yield reasonable numbers for the clean phase diagram, we take into account the quenched disorder. In the Drude model, the residual resistivity is $\rho_0 = \dfrac{3\pi^2 \hbar e^2 / k_F}{l k_F}$. A typical Fermi temperature for a good metal is about $10^5 K$, so we have $l k_F \approx 1000 \mu\Omega cm / \rho_0$.

In the cleanest samples of weak ferromagnets, the residual resistivity ρ_0 is about $0.1\mu\Omega cm$, while in poor metals the residual resistivity is about $100\mu\Omega cm$, thus lk_F ranges from 10 to 10^4. This implies that values of $lk_F m$ between roughly 2 and 2×10^4 are realizable. From Eq. (III.103) we see thant $lk_F m \approx 5$ is the demarcation between two different regimes, which falls well within this range.

From Eq. (III.103) we can distinguish three different regimes according to the values of lk_F (clean vs. dirty samples) and m (weak vs. strong magnetism). They follow from the observation that at zero temperature the diffusive and ballistic nonanlyticities are operative (inoperative) for $lk_F m \leq 5$ ($lk_F m \geq 5$) and $lk_F m \geq m_0\sigma_0$ ($lk_F m \leq m_0\sigma_0$), respectively. Next we look at these different regimes in detail.

Regime I (clean/strong): $lk_F m \geq m_0\sigma_0$; that is, the magnetism is strong and the sample is very clean. In this regime, the diffusive nonanalycity is inoperative and just renormalizes r, and the equation of state is given by Eq. (III.70). As we have discussed, in this case there is a first order transition with $m_1 = m_0 e^{-(1+u/v)/2} \leq m$. To stay in this regime, we must have $lk_F m_1 \geq m_0\sigma_0$. With u and v chosen as above, and $\sigma_0 \approx 1/5$, this yields $lk_F \geq 300$, or $\rho \approx$ a few $\mu\Omega$cm.

Regime IIa (intermediate): $5 \leq lk_F m \leq m_0\sigma_0$. In this regime both the ballistic and diffusive non-analyticities is inoperative, so the transition is continuous with mean-field component in a range of m-values. When m decreases to the point that $lk_F m \leq 5$, the system enters Regime IIb or Regime III.

Regime IIb (intermediate): $lk_F m \leq 5$ and $lk_F \geq (lk_F)^*$ (with $(lk_F)^*$ defined below). In this regime the diffusive nonanalyticity becomes operative and the equation of state is given by Eq. (III.2). The transition is second order with asymptotic critical behavior characterized by non-mean-field exponents as we discussed in Section III.2.3. However, far away from the transition this behavior will cross over to ordinary mean-field behavior at a disorder-dependent value r^* of r. The crossover happens when the last two terms of Eq. (III.2) are about equal in magnitude. Having the crossover occur at $r = r^*$ thus requires a disorder given by $lk_F = (lk_F)^* = \omega^{2/3}/u^{1/6}\,|r^*|^{1/2}$. If we choose $\tilde{\gamma}_t = 0.5$ and $u = 1$ as before, we have $(lk_F)^* \approx 6$ or $\rho^* \approx 150\mu\Omega$cm. Thus, when $lk_F \geq (lk_F)^*$ and $lk_F m \leq 5$, the system is in a regime where the transition is continuous with effective exponents that have their usual mean-field values.

Regime III (Dirty/weak): $lk_F \leq (lk_F)^*$ and $lk_F m \leq 5$. In this regime the equation of state is dominated by the diffusive nonanalyticity and the transition is continuous with non-mean-field critical exponents in the entire critical region. This requires $\rho_0 \gg \rho_0^*$, with ρ_0^* ranging from approximately $100\mu\Omega$cm for strong correlated materials to hundreds of $\mu\Omega$cm for weakly correlated ones.

Next we look at the nonzero temperature case. From the Eq. (III.103), we see that a disorder resulting in $k_F l = \sigma_0 T_F/3\pi T_{tc}$ has the same effects as a temperature equal to T_{tc} in a clean system. That is, $\rho_0 \geq 10^4 T_{tc}/\sigma_0 T_F \approx$ a few $\mu\Omega$cm will suppress the tricritical temperature to zero, which is consistent with the above

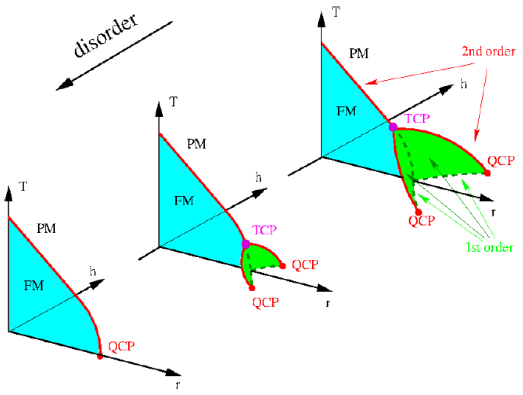

Figure 3.2. Evolution of the phase diagram of a metallic quantum ferromagnet in the space spanned by temperature T and magnetic field h and the control parameter r with increasing disorder. Shown are the ferromagnetic and paramagnetic phases, lines of second-order transitions, the tricritical point and surfaces of first-order transitions that end in quantum critical points. With increasing disorder the tricritical temperature decreases, the wings shrink and above a critical disorder strength a quantum critical point is realized in zero field. (From Ref. [61].)

estimate for the destruction of the first-order transition at zero temperature. The tricritical wings shrink, and eventually disappear, commensurate with the suppression of T_{tc}. These predictions are shown in Fig. 3.2..

Now we can summarize the effects of quenched disorder on typical strongly correlated quantum ferromagnets that in the clean limit have a first-order zero-temperature transition and a tricritical point in the phase diagram. Disorder will decrease T_{tc}, and suppress it to zero for a residual resistivity ρ_0 on the order of several $\mu\Omega$cm. For larger disorder, the quantum phase transition will be continuous and appear mean-field-like in a substantial disorder range, $\rho_0 \leq 100\mu\Omega$cm, with a crossover to non-mean-field behavior only extremely close to the transition. For even larger disorder, the critical behavior is characterized by the non-mean-field

exponents discussed in Section III.2.3. However, for disorder that strong it is to be expected that quantum Griffiths effects will be present and may compete with the critical behavior [62]. In order to distinguish between the two, measuring the critical behavior of the magnetization is crucial. All of the these predictions are semi-quantitative, and the disorder strengths that delineate the three different regimes are expected to show substantial variation from material to material.

Generalized Mean Field Theory for URhGe

Structure and Properties of URhGe

URhGe is a good example of a material that displays a first order quantum ferromagnetic phase transition and a tricritical point [50]. Its critical temperature can be tuned by an external magnetic field applied in the b-direction of its orthorhombic lattice, which is easy to implement in experiments. URhGe is thus a good candidate for testing our theory by experiments. The magnetization of URhGe is confined to the bc-plane, so in this section we will generalize the comprehensive generalized mean-field theory from the previous section to anisotropic materials and apply it to URhGe.

Generalized Mean Field Theory for URhGe

To derive an anisotropic generalized mean-field theory applicable to URhGe, we will generalize our derivation for isotropic systems by introducing a two-component

magnetization, and an anisotropic coupling between the magnetization and the fermionic fluctuations. Before getting into the details of the coupling between the magnetization fluctuations and the soft particle-hole excitations that causes a first-order quantum phase transition, we first look at an anisotropic Landau theory with a transverse magnetic field to see that an increasing transverse field will indeed decrease the critical temperature. A Landau free-energy density for a two-component magnetization such as in URhGe, with a magnetic field in the b- or 2-direction, has the form

$$f_L = \frac{1}{2} r_2 \mu_2^2 + \frac{1}{2} r_3 \mu_3^3 + \frac{1}{4} u (\mu_2^2 + \mu_3^2)^2 - h_2 \mu_2 \tag{III.104}$$

We assume the mass parameters r_2 and r_3 have the property $r_3 < r_2$, which makes 3, or c, the easy axis, as is the case in URhGe. By minimizing the free-energy density, we get

$$\frac{\partial f}{\partial \mu_2} = \mu_2 (r_2 + u(\mu_2^2 + \mu_3^2)) - h_2 = 0 \tag{III.105}$$

$$\frac{\partial f}{\partial \mu_3} = \mu_3 (r_3 + u(\mu_2^2 + \mu_3^2)) = 0 \tag{III.106}$$

We can see that at zero magnetic field, the spontaneous magnetization below a Curie temperature T_{c3} with $r_3(T_{c3}) = 0$ is indeed along the c-direction. As a transverse magnetic field is increased from zero, the 3-component of the magnetization m_3

decreases according to

$$\mu_3 = \sqrt{\frac{-r_3}{u} - \frac{h_2^2}{(r_2 - r_3)^2}} \tag{III.107}$$

From Eq. (III.107) we see that μ_3 goes to zero continuously as the magnetic field in 2-direction is increased to a critical value $h_2 = (r_2 - r_3)\sqrt{-r_3/u}$. In the ordered phase near the transition we have that $r_3 \propto (T_c - T)$, thus we get T_c decreases with increasing h_2. To describe the first-order transition at zero temperature, we need to take into account the soft particle-hole excitations and their coupling to the order parameter fluctuations, as we did for the isotropic theory.

The starting point is again an effective action as given in Eq. (III.30), where now S_M is the anisotropic Landau theory which gives the anisotropic free energy density given in Eq. (III.104). The Gaussian part of S_q has a similar structure as in the isotropic case,

$$\begin{aligned} S_q^{(2)} =& -\frac{4}{G}\sum_{\boldsymbol{k}}\sum_{1,2,3,4}\sum_{r,i} {}^i_r q_{12}(\boldsymbol{k})\, {}^i_r\Gamma^{(2)}_{12,34}(\boldsymbol{k})\, {}^i_r q_{34}(-\boldsymbol{k}) \\ =& -\frac{4}{G_{clean}}\sum_{1/l<|\boldsymbol{k}|<\Lambda}\sum_{1,2,3,4}\sum_{r,i} {}^i_r q_{12}(\boldsymbol{k})\, {}^i_r\Gamma^{(2)}_{cle12,34}(\boldsymbol{k})\, {}^i_r q_{34}(-\boldsymbol{k}) \\ & -\frac{4}{G_{dis}}\sum_{0<|\boldsymbol{k}|<1/l}\sum_{1,2,3,4}\sum_{r,i} {}^i_r q_{12}(\boldsymbol{k})\, {}^i_r\Gamma^{(2)}_{dis12,34}(\boldsymbol{k})\, {}^i_r q_{34}(-\boldsymbol{k}) \end{aligned} \tag{III.108}$$

The vertex functions now contain an anisotropy which is represented by different values of the RG-generated interaction amplitudes $\tilde{K}_t^i (i = 0, 1, 2, 3)$. The vertex function for the ballistic part thus has the form

$$
\begin{aligned}
{}^{i}_{r}\Gamma^{(2)}_{cle12,34}(\boldsymbol{k}) =& \delta_{13}\delta_{24}(|\boldsymbol{k}| + GH\Omega_{n_1-n_2}) \\
&+ \delta_{1-2,3-4}\delta_{i0}2\pi TGK_s + \delta_{1-2,3-4}(1-\delta_{i0})2\pi TG\tilde{K}^i_t
\end{aligned}
\tag{III.109}
$$

where $i = 1, 2, 3$. The vertex function for the diffusive part reads

$$
\begin{aligned}
{}^{i}_{r}\Gamma^{(2)}_{dis12,34}(\boldsymbol{k}) = \delta_{1-2,3-4}\{\delta_{13}(k^2 + GH\Omega_{n_1-n_2}) + (1-\delta_{i0})\delta_{\alpha_1\alpha_2}\delta_{\alpha_1\alpha_3}2\pi TG\tilde{K}^i_t\} \\
+\delta_{1-2,3-4}\delta_{i0}\delta_{\alpha_1\alpha_2}\delta_{\alpha_1\alpha_3}2\pi TGK_s
\end{aligned}
\tag{III.110}
$$

The indices 1,2,3,4 comprise both the frequency index and the replica index, as in the isotropic case.

The coupling part of the action, $S_{M,q}$, now contains two components since the magnetization is anisotropic,

$$
\begin{aligned}
A_{M-Q} =& \sum_i c'_i\sqrt{T}\int d\boldsymbol{x}\sum_n M^i_n(\boldsymbol{x})\sum_{r=0,3}(-1)^{r/2}\sum_m tr[\tau_r\otimes s_i Q^i_{m,m+n}(\boldsymbol{x})] \\
=& -8ic'_3N_F\sqrt{T}\int d\boldsymbol{x}\sum_n M^3_n(\boldsymbol{x}) \\
&\times\sum_{mm'}({}^{1}_{0}q_{mm'}(\boldsymbol{x})\,{}^{2}_{3}q_{m+n,m'}(-\boldsymbol{x}) - {}^{1}_{3}q_{mm'}(\boldsymbol{x})\,{}^{2}_{0}q_{m+n,m'}(-\boldsymbol{x})) \\
&-8ic'_2N_F\sqrt{T}\int d\boldsymbol{x}\sum_n M^2_n(\boldsymbol{x}) \\
&\times\sum_{mm'}({}^{1}_{0}q_{mm'}(\boldsymbol{x})\,{}^{3}_{3}q_{m+n,m'}(-\boldsymbol{x}) - {}^{1}_{3}q_{mm'}(\boldsymbol{x})\,{}^{3}_{0}q_{m+n,m'}(-\boldsymbol{x}))
\end{aligned}
\tag{III.111}
$$

Here $c'_i = \sqrt{2\pi\Gamma^i_t}$ $(i = 2, 3)$ represents the coupling constants for the coupling of the magnetization to the soft fermionic fluctuations in the 2- and 3-directions,

respectively, with $\Gamma_i (i = 2, 3)$ the anisotropic spin-triplet interaction. As in the isotropic case, we replace the fluctuating order parameter by its average value

$$M_n^i(\boldsymbol{x}) \approx \delta_{i2}\delta_{n0} m_2/\sqrt{T} + \delta_{i3}\delta_{n0} m_3/\sqrt{T} \tag{III.112}$$

We further define $\mu_i = m_i/c_i'$, and $c_i = N_F c_i'^2$ $(i = 2, 3)$. We thus get a q-dependent part of the action hat has the same structure as Eq. (III.41), but the coupling matrix M now is anisotropic,

$$\begin{aligned} {}^{ij}_{rs}M_{12,34}(\boldsymbol{k}) =& \frac{8}{G} \begin{pmatrix} {}^0\Gamma^{(2)}_{12,34} & 0 & 0 & 0 \\ 0 & {}^1\Gamma^{(2)}_{12,34} & 0 & 0 \\ 0 & 0 & {}^2\Gamma^{(2)}_{12,34} & 0 \\ 0 & 0 & 0 & {}^3\Gamma^{(2)}_{12,34} \end{pmatrix} \otimes \begin{pmatrix} 1 & 0 \\ 0 & 1 \end{pmatrix} \\ &+ 8i\delta_{13}\delta_{24} \otimes \begin{pmatrix} 0 & 0 & 0 & 0 \\ 0 & 0 & c_3\mu_3 & c_2\mu_2 \\ 0 & -c_3\mu_3 & 0 & 0 \\ 0 & -c_2\mu_2 & 0 & 0 \end{pmatrix} \otimes \begin{pmatrix} 0 & 1 \\ -1 & 0 \end{pmatrix} \end{aligned} \tag{III.113}$$

We now again integrate out the soft modes q. According to Eq. (III.43) we need to calculate $Tr \ln M$, which has a similar structure as the isotropic case,

$$
\begin{aligned}
Tr\ln M =& 2\sum_{1/l<|\boldsymbol{k}|<k_F}\sum_{n=1}^{\infty}\ln N_{clean}(\boldsymbol{k},\Omega_n;\mu_2,\mu_3) \\
&+2\sum_{0<|\boldsymbol{k}|<1/l}\sum_{n=1}^{\infty}\ln N_{diff}(\boldsymbol{k},\Omega_n;\mu_2,\mu_3)
\end{aligned}
\tag{III.114}
$$

where N_{clean} has the form

$$
\begin{aligned}
N_{clean}(\boldsymbol{k},\Omega_n;\mu_2,\mu_3) = 1 &+ c_2^2\mu_2^2\tilde{K}_{t1}\tilde{K}_{t3}G^4D_n^2(\boldsymbol{k},\Omega_n)\tilde{D}_n^{t1}(\boldsymbol{k},\Omega_n)\tilde{D}_n^{t3}(\boldsymbol{k},\Omega_n)\Omega_n^2 \\
&+ c_3^2\mu_3^2\tilde{K}_{t1}\tilde{K}_{t2}G^4D_n^2(\boldsymbol{k},\Omega_n)\tilde{D}_n^{t1}(\boldsymbol{k},\Omega_n)\tilde{D}_n^{t2}(\boldsymbol{k},\Omega_n)\Omega_n^2
\end{aligned}
\tag{III.115}
$$

with $D_n(\boldsymbol{k},\Omega_n)$ given in Eq. (III.47) and $D_n^{ti}(\boldsymbol{k},\Omega_n)(i=1,2,3)$ reads

$$
\tilde{D}_n^{ti}(\boldsymbol{k}) = 1/(|\boldsymbol{k}| + G(H+\tilde{K}_{ti})\Omega_n) \tag{III.116}
$$

As we have discussed in the isotropic case, the $\tilde{K}_{ti}$ are smaller than $H=\pi N_F/4$, so we only keep terms to $O(\tilde{\gamma}_{ti}^2)$ with $\tilde{\gamma}_{ti}=\tilde{K}_{ti}/H$. In this approximation we get

$$
N_{clean} = 1 + \frac{(c_2^2\mu_2^2\tilde{K}_{t1}\tilde{K}_{t3} + c_3^2\mu_3^2\tilde{K}_{t1}\tilde{K}_{t2})G_{clean}^4\Omega_n^2}{(k+G_{clean}H\Omega_n)^4} \tag{III.117}
$$

The diffusive part N_{diff} has the form

$$
\begin{aligned}
&N_{diff}(\boldsymbol{k},\Omega_n;\mu_2,\mu_3) \\
&= \frac{1 + c_2^2\mu_2^2G_{dis}^2\tilde{D}_n^{t1}(\boldsymbol{k},\Omega_n)\tilde{D}_n^{t3}(\boldsymbol{k},\Omega_n) + c_3^2\mu_3^2G_{dis}^2\tilde{D}_n^{t1}(\boldsymbol{k},\Omega_n)\tilde{D}_n^{t2}(\boldsymbol{k},\Omega_n)}{1+(c_2^2\mu_2^2+c_3^2\mu_3^2)G_{dis}^2D_n^2(\boldsymbol{k},\Omega_n)}
\end{aligned}
\tag{III.118}
$$

with $D_n(\boldsymbol{k}, \Omega_n)$ given in Eq. (III.79) and $\tilde{D}_n^{ti}(\boldsymbol{k}, \Omega_n)$ has the form

$$\tilde{D}_n^{ti}(\boldsymbol{k}, \Omega_n) = \frac{1}{k^2 + G_{dis}(H + \tilde{K}_{ti})\Omega_n} \tag{III.119}$$

For convenience we again rescale the momentum and frequency by $\hat{k} = k/k_F$ and $\hat{\Omega}_n = \dfrac{3\Omega_n}{2T_F}$, which makes $\hat{k}$ and $\hat{\Omega}_n$ dimensionless. We also define a dimensionless magnetization $\hat{\mu}_i = \dfrac{\mu_i}{\pi n_e/8c_i}$. After rescaling, we get

$$N_{clean} = 1 + \frac{(\tilde{\gamma}_{t1}\tilde{\gamma}_{t3}\hat{\mu}_2^2 + \tilde{\gamma}_{t1}\tilde{\gamma}_{t2}\hat{\mu}_3^2)\hat{\Omega}_n^2}{(\hat{k} + \hat{\Omega}_n)^4} \tag{III.120}$$

and

$$N_{diff} = \frac{1 + \frac{\hat{\mu}_2^2/(lk_F)^2}{(\hat{k}^2+(1+\tilde{\gamma}_{t1})\hat{\Omega}_n/(lk_F))(\hat{k}^2+(1+\tilde{\gamma}_{t3})\hat{\Omega}_n/(lk_F))} + \frac{\hat{\mu}_3^2/(lk_F)^2}{(\hat{k}^2+(1+\tilde{\gamma}_{t1})\hat{\Omega}_n/(lk_F))(\hat{k}^2+(1+\tilde{\gamma}_{t2})\hat{\Omega}_n/(lk_F))}}{1 + \frac{(\hat{\mu}_2^2+\hat{\mu}_3^2)/(lk_F)^2}{(\hat{k}^2+\hat{\Omega}_n/(lk_F))^2}} \tag{III.121}$$

Next we need to perform the integral given in Eq. (III.114). To do this we again first differentiate the free energy with respect to the magnetization to obtain the equation of state which does not contain the ln-function in the integrand. We first look at the ballistic part. Before doing the differentiation we first rescale the free energy density with $\pi n_e T_F/8$ and denote the ballistic part of the free energy density by $\hat{f}_{clean}$

$$\hat{f}_{clean} = \frac{8}{\pi n_e T_F}\frac{T}{V}\sum_{1/l<|\boldsymbol{k}|<k_F}\sum_{n=1}^{\infty}\ln N_{clean}(\hat{\boldsymbol{k}},\hat{\Omega}_n;\hat{\mu}_2,\hat{\mu}_3) \tag{III.122}$$

Differentiating this dimensionless free energy density with respect to $\hat{\mu}_2$ and $\hat{\mu}_3$ yields

$$\frac{\partial \hat{f}_{clean}}{\partial \hat{\mu}_2} = \frac{8}{\pi^2}\tilde{\gamma}_{t1}\tilde{\gamma}_{t3}\hat{\mu}_2\int_{1/lk_F}^{1}k^2dk\int_t^{\infty}d\omega\frac{\omega^2}{(k+\omega)^4+(\tilde{\gamma}_{t1}\tilde{\gamma}_{t3}\hat{\mu}_2^2+\tilde{\gamma}_{t1}\tilde{\gamma}_{t2}\hat{\mu}_3^2)\omega^2} \tag{III.123}$$

$$\frac{\partial \hat{f}_{clean}}{\partial \hat{\mu}_3} = \frac{8}{\pi^2}\tilde{\gamma}_{t1}\tilde{\gamma}_{t2}\hat{\mu}_3\int_{1/lk_F}^{1}k^2dk\int_t^{\infty}d\omega\frac{\omega^2}{(k+\omega)^4+(\tilde{\gamma}_{t1}\tilde{\gamma}_{t3}\hat{\mu}_2^2+\tilde{\gamma}_{t1}\tilde{\gamma}_{t2}\hat{\mu}_3^2)\omega^2} \tag{III.124}$$

where k and ω are the dimensionless wave number and frequency, respectively, and $t = \dfrac{3\pi T}{T_F}$ as in the previous section. The integral in Eq. (III.123) and Eq. (III.124) similar to the integral in Eq. (III.96), and we get the ballistic part of the equations of state as

$$\frac{\partial \hat{f}_{clean}}{\partial \hat{\mu}_2} = -\frac{4}{105\pi^2}\tilde{\gamma}_{t1}\tilde{\gamma}_{t3}\hat{\mu}_2(\tilde{\gamma}_{t1}\tilde{\gamma}_{t3}\hat{\mu}_2^2+\tilde{\gamma}_{t1}\tilde{\gamma}_{t2}\hat{\mu}_3^2)\ln\frac{1}{(\tilde{\gamma}_{t1}\tilde{\gamma}_{t3}\hat{\mu}_2^2+\tilde{\gamma}_{t1}\tilde{\gamma}_{t2}\hat{\mu}_3^2)/35+(t+\frac{1}{lk_F})^2} \tag{III.125}$$

and

$$\frac{\partial \hat{f}_{clean}}{\partial \hat{\mu}_3} = -\frac{4}{105\pi^2}\tilde{\gamma}_{t1}\tilde{\gamma}_{t2}\hat{\mu}_3(\tilde{\gamma}_{t1}\tilde{\gamma}_{t3}\hat{\mu}_2^2 + \tilde{\gamma}_{t1}\tilde{\gamma}_{t2}\hat{\mu}_3^2)\ln\frac{1}{(\tilde{\gamma}_{t1}\tilde{\gamma}_{t3}\hat{\mu}_2^2 + \tilde{\gamma}_{t1}\tilde{\gamma}_{t2}\hat{\mu}_3^2)/35 + (t+\frac{1}{lk_F})^2} \tag{III.126}$$

Next we look at the diffusive part. The corresponding contribution to the dimensionless free energy is

$$\hat{f}_{dis} = \frac{8}{\pi n_e T_F}\frac{T}{V}\sum_{0<|\boldsymbol{k}|<1/l}\sum_{n=1}^{\infty}\ln N_{dis}(\hat{\boldsymbol{k}}, \hat{\Omega}_n; \hat{\mu}_2, \hat{\mu}_3) \tag{III.127}$$

To perform the integral we again differentiate the dimensionless free energy density with respect to $\hat{\mu}_2$ and $\hat{\mu}_3$ to avoid integrating over a logarithm,

$$\frac{\partial \hat{f}_{dis}}{\partial \hat{\mu}_2} = -\frac{8}{\pi^2}(\tilde{\gamma}_{t1}+\tilde{\gamma}_{t3})\frac{\hat{\mu}_2}{(lk_F)^2}\int_0^{1/lk_F} dk k^2 \int_t^{\infty} d\omega \frac{\frac{\omega}{lk_F}(k^2+\frac{\omega}{lk_F})}{[(k^2+\frac{\omega}{lk_F})^2 + \frac{\hat{\mu}_2^2+\hat{\mu}_3^2}{(lk_F)^2}]^2} \tag{III.128}$$

and

$$\frac{\partial \hat{f}_{dis}}{\partial \hat{\mu}_3} = -\frac{8}{\pi^2}(\tilde{\gamma}_{t1}+\tilde{\gamma}_{t2})\frac{\hat{\mu}_3}{(lk_F)^2}\int_0^{1/lk_F} dk k^2 \int_t^{\infty} d\omega \frac{\frac{\omega}{lk_F}(k^2+\frac{\omega}{lk_F})}{[(k^2+\frac{\omega}{lk_F})^2 + \frac{\hat{\mu}_2^2+\hat{\mu}_3^2}{(lk_F)^2}]^2} \tag{III.129}$$

As in the isotropic case, we have kept terms to linear order in $\tilde{\gamma}_{ti}$ and we have dropped terms that are independent of the magnetization. The integrals in Eq. (III.128) and Eq. (III.129) are similar to the one in Eq. (III.86). We find

$$\frac{\partial \hat{f}_{dis}}{\partial \hat{\mu}_2} = \frac{8}{3\sqrt{2}\pi}(\tilde{\gamma}_{t1}+\tilde{\gamma}_{t3})\frac{\hat{\mu}_2\sqrt{\hat{\mu}_2^2+\hat{\mu}_3^2}}{(lk_F)^{3/2}} g(lk_F\sqrt{\hat{\mu}_2^2+\hat{\mu}_3^2}, t/\sqrt{\hat{\mu}_2^2+\hat{\mu}_3^2}) \tag{III.130}$$

and

$$\frac{\partial \hat{f}_{dis}}{\partial \hat{\mu}_3} = \frac{8}{3\sqrt{2}\pi}(\tilde{\gamma}_{t1} + \tilde{\gamma}_{t2})\frac{\hat{\mu}_3\sqrt{\hat{\mu}_2^2 + \hat{\mu}_3^2}}{(lk_F)^{3/2}} g(lk_F\sqrt{\hat{\mu}_2^2 + \hat{\mu}_3^2}, t/\sqrt{\hat{\mu}_2^2 + \hat{\mu}_3^2}) \qquad \text{(III.131)}$$

Combining the ballistic and diffusive nonanalytic parts as well as the normal analytic parts of the euqations of state, we get the full equations of state in the form

$$\begin{aligned}
\frac{\partial \hat{f}}{\partial \hat{\mu}_2} &= \hat{r}_2\hat{\mu}_2 + \hat{u}\hat{\mu}_2(\hat{\mu}_2^2 + \hat{\mu}_3^2) - \hat{h}_2 \\
&- \frac{4}{105\pi^2}\tilde{\gamma}_{t1}\tilde{\gamma}_{t3}\hat{\mu}_2(\tilde{\gamma}_{t1}\tilde{\gamma}_{t3}\hat{\mu}_2^2 + \tilde{\gamma}_{t1}\tilde{\gamma}_{t2}\hat{\mu}_3^2)\ln\frac{1}{(\tilde{\gamma}_{t1}\tilde{\gamma}_{t3}\hat{\mu}_2^2 + \tilde{\gamma}_{t1}\tilde{\gamma}_{t2}\hat{\mu}_3^2)/35 + (t + \frac{1}{lk_F})^2} \\
&+ \frac{8}{3\sqrt{2}\pi}(\tilde{\gamma}_{t1} + \tilde{\gamma}_{t3})\frac{\hat{\mu}_2\sqrt{\hat{\mu}_2^2 + \hat{\mu}_3^2}}{(lk_F)^{3/2}} g(lk_F\sqrt{\hat{\mu}_2^2 + \hat{\mu}_3^2}, t/\sqrt{\hat{\mu}_2^2 + \hat{\mu}_3^2}) \\
&= 0
\end{aligned} \qquad \text{(III.132)}$$

and

$$\begin{aligned}
\frac{\partial \hat{f}_{dis}}{\partial \hat{\mu}_3} &= \hat{r}_3\hat{\mu}_3 + \hat{u}\hat{\mu}_3(\hat{\mu}_2^2 + \hat{\mu}_3^2) \\
&- \frac{4}{105\pi^2}\tilde{\gamma}_{t1}\tilde{\gamma}_{t2}\hat{\mu}_3(\tilde{\gamma}_{t1}\tilde{\gamma}_{t3}\hat{\mu}_2^2 + \tilde{\gamma}_{t1}\tilde{\gamma}_{t2}\hat{\mu}_3^2)\ln\frac{1}{(\tilde{\gamma}_{t1}\tilde{\gamma}_{t3}\hat{\mu}_2^2 + \tilde{\gamma}_{t1}\tilde{\gamma}_{t2}\hat{\mu}_3^2)/35 + (t + \frac{1}{lk_F})^2} \\
&+ \frac{8}{3\sqrt{2}\pi}(\tilde{\gamma}_{t1} + \tilde{\gamma}_{t2})\frac{\hat{\mu}_3\sqrt{\hat{\mu}_2^2 + \hat{\mu}_3^2}}{(lk_F)^{3/2}} g(lk_F\sqrt{\hat{\mu}_2^2 + \hat{\mu}_3^2}, t/\sqrt{\hat{\mu}_2^2 + \hat{\mu}_3^2}) \\
&= 0
\end{aligned} \qquad \text{(III.133)}$$

For notational convenience, we again discard the carets in the equations of state and denote the dimensionless magnetization by m. As in the isotropic case, we keep in mind that the parameter values one gets from simple model calculations are oversimplified, and that the parameter values for real materials may be quite different. It is crucial, however, to keep qualitative features, such as the anisotropy. As in the isotropic case, we introduce the independent constants m_0 and σ_0 which set the scales for the magnetic moment and the disorder, respectively. With these points in mind, and denoting $\beta = \tilde{\gamma}_{t3}/\tilde{\gamma}_{t2}$, we can write the equations of state as,

$$\begin{aligned}\frac{\partial f}{\partial m_2} &= r_2 m_2 + u m_2(m_2^2 + m_3^2) - h_2 \\ &+ \frac{w}{(lk_F)^{3/2}} m_2 \sqrt{m_2^2 + m_3^2}\, g(lk_F\sqrt{m_2^2 + m_3^2}, t/\sqrt{m_2^2 + m_3^2}) \\ &+ \beta v m_2(\beta m_2^2 + m_3^2)\ln(\frac{\beta m_2^2 + m_3^2}{m_0^2} + (\frac{\sigma_0}{lk_F} + t)^2) \\ &= 0\end{aligned} \tag{III.134}$$

and

$$\begin{aligned}\frac{\partial f}{\partial m_3} &= r_3 m_3 + u m_3(m_2^2 + m_3^2) \\ &+ \frac{w}{(lk_F)^{3/2}} m_3 \sqrt{m_2^2 + m_3^2}\, g(lk_F\sqrt{m_2^2 + m_3^2}, t/\sqrt{m_2^2 + m_3^2}) \\ &+ v m_3(\beta m_2^2 + m_3^2)\ln(\frac{\beta m_2^2 + m_3^2}{m_0^2} + (\frac{\sigma_0}{lk_F} + t)^2) \\ &= 0\end{aligned} \tag{III.135}$$

with the function $g(x, y)$ given by Eq. (III.89). w is proportional to $\tilde{\gamma}_{ti}$, and v is

proportional to $\tilde{\gamma}_{ti}^4$, as in the isotropic case. From Eq. (III.134) and Eq. (III.135) we see that both the diffusive and ballistic nonanalytic terms are similar to those in an isotropic system. Therefore, if the anisotropic model describes the experimentally observed phase diagram in the clean case, then the evolution of the phase diagram with increasing disorder will also be similar to that of an isotropic systems. Thus our discussion of three distinct regimes in the isotropic case will also apply to URhGe. What remains to be done is show that in the clean case our equations of state yield a phase diagram as shown in Fig. 3.1..

Accordingly, we now discuss the clean limit of our model. Again we start from the zero-temperature case, where the equations of state have the form

$$\begin{aligned}\frac{\partial f}{\partial m_2} &= r_2 m_2 + u m_2(m_2^2 + m_3^2) - h_2 + \beta v m_2(\beta m_2^2 + m_3^2) \ln \frac{\beta m_2^2 + m_3^2}{m_0^2} \\ &= 0\end{aligned} \tag{III.136}$$

$$\begin{aligned}\frac{\partial f}{\partial m_3} &= r_3 m_2 + u m_3(m_2^2 + m_3^2) + v m_3(\beta m_2^2 + m_3^2) \ln \frac{\beta m_2^2 + m_3^2}{m_0^2} \\ &= 0\end{aligned} \tag{III.137}$$

Contrary to the isotropic case, it is not obvious that these equations describe a first-order transition. We therefore verify that they do by means of numerical calculations. From the solutions of these two equations we obtain the free-energy density of a clean system at zero temperature in the form

$$f = \frac{1}{2} r_2 m_2^2 + \frac{1}{2} r_3 m_3^3 + \frac{1}{4} v(\beta m_2^2 + m_3^2)^2 \ln \frac{\beta m_2^2 + m_3^2}{m_0^2} + \frac{1}{4} u(m_2^2 + m_3^2)^2 - h_2 m_2 \tag{III.138}$$

Here we have ignored terms of the form $(\beta m_2^2 + m_3^2)^2$,which we have verified to not qualitatively affect our result. From the two equations of state, we can express m_2 as a function of m_3, which we then insert into the free energy to get a free-energy density which has the form $f(m_2(m_3), m_3)$. Minimizing this free-energy density as a function of m_3, we can now verify that there is a first-order transition at a critical transverse magnetic field. At zero magnetic field, the model must describe a second-order transition at a critical temperature T_c. This is an ordinary thermal ferromagnetic phase transition, so we have $r_3(T_c) = 0$. Below T_c, we will have $r_3 < 0$. Our constraint is that $r_3 < r_2$, so for simplicity we can assume r_2 to be positive, and at zero temperature we assume $r_3(T = 0) = -r_2(T = 0)$, with r_3 increasing from a negative value to zero at critical temperature T_c. If we choose $r_3(T = 0) = -r_2(T = 0) = -0.02$, $u = 1$, $v = 0.5$, $\beta = 0.5$ and $m_0 = 1$, we find the free energy, Eq. (III.138), as a function of m_3 as shown in Fig. 3.3. for a transverse magnetic field of 10 T.

From the plot we see that there exists a $m_{3c} \neq 0$ such that f has a minimum at $m_3 = m_{3c}$ with $f(m_{3c}) = f(m_3 = 0)$. That is, there is a first order transition at m_{3c}. Thus we have shown that our free energy for the anisotropic case does indeed give a first-order ferromagnetic phase transition at zero temperature. We also have

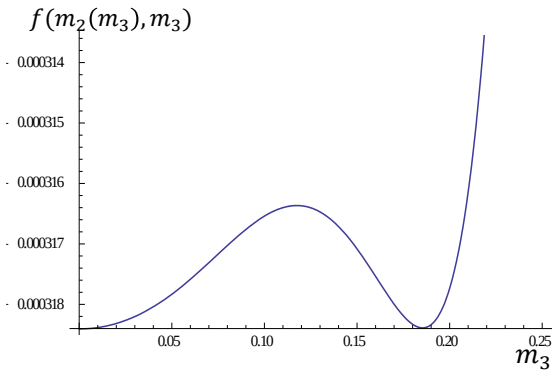

Figure 3.3. Plot of free energy density at the transition as a function of m_3. From the phase diagram we can see that there is a first order quantum ferromagnetic phase transition which happens at a non-zero m_3.

shown, below Eq. (III.107), that the critical temperature decreases with increasing transverse magnetic field h_2. In summary we now see that at zero magnetic field there is a second-order ferromagnetic phase transition, and the critical temperature decreases with increasing transverse magnetic field h_2. We also know that there is a first-order transition at zero temperature and a finite critical transverse magnetic field h_{2c}. We therefore conclude that there must be a tricritical point in between. If an external magnetic field in the b-direction is applied, the first-order transition line which connects the tricritical point and the zero-temperature transition point will bifurcate into two first-order transition wings. We thus have shown that our anisotropic theory in the clean limit yields a phase diagram that is consistent with the experimental observations on URhGe. The quenched disorder entered the free energy density in the same way as for isotropic systems, so our previous discussion on three distinct disorder regimes also apply to URhGe. Since the critical

temperature can be tuned by an external transverse magnetic field, this should be easy to test in experiments.

CHAPTER IV

SUMMARY

In this dissertation we studied the phases and phase transition properties of weak ferromagnets and related systems. We first focused on the ordered phases of the helical magnet MnSi, and discussed the form and effects of the Goldstone mode in the helical and conical phases. We then studied how the ferromagnetic phase transition evolves with increasing quenched disorder by deriving a comprehensive generalized mean-field theory which is suitable for both clean and disordered weak ferromagnetic systems. We finally generalized our originally isotropic theory to an anisotropic form which applies to the anisotropic ferromagnet URhGe.

In Chapter II we studied the properties of the Goldstone mode in the ordered phases of MnSi, both classically and quantum mechanically. MnSi has a Curie temperature of about 30K, and a magnetic moment per formula unit of about $0.4\mu_B$. Without a magnetic field, MnSi is helically ordered. If one neglects crystal-field effects, which are weak, the system is invariant under rotations of the pitch vector of the helix. In the presence of an external magnetic field, the helix becomes pinned to the direction of the magnetic field, forming the conical phase. In both phases, the ground state spontaneously breaks translational symmetry, which leads to a Goldstone mode.

We systematically calculated the Goldstone modes, following an energy hierarchy that starts with ferromagnons at the zeroth order, where one neglects the spin-orbit interaction that causes the helical order. For an isotropic Heisenberg ferromagnet, one finds two ferromagnons, which are the transverse fluctuations of the magnetization. They have a dispersion relation given by $\omega = Dk^2$. Taking into account the spin-orbit interaction, one finds a helical phase with one Goldstone mode, the helimagnon. Due to the anisotropic nature of the helical magnetization, the helimagnon has an anisotropic dispersion relation, $\omega = \sqrt{c_z k_z^2 + c_\perp k_\perp^4}$, where z and $\perp$ refer to directions parallel and perpendicular, respectively, to the pitch vector. The helimagnon is thus softer in the transverse direction than in the longitudinal one: In the pitch-vector direction, the frequency scales as the momentum, which is similar to the antiferromagnets, while in the transverse direction, the frequency scales as the momentum squared, which is similar to the ferromagnetic case. An external magnetic field breaks the rotational symmetry of the pitch vector direction, which leads to a dispersion relation for the helimagnon of the form $\omega = \sqrt{c_z k_z^2 + \tilde{c} k_\perp^2 + c_\perp k_\perp^4}$, with $\tilde{c} \propto H^2$, where H is the magnetic field. Since the frequency of the soft mode scales as the temperature, these different Goldstone modes contribute differently to the thermodynamic and transport observables, such as the specific heat and the electronic resistivity.

In Chapter III we studied the evolotion of the phase transition properties of weak ferromagnets with increasing quenched disorder strength. Previous research

has shown that the quantum ferromagnetic phase transitions in cleans systems is generically of first order, due to the coupling of the order-parameter fluctuations to soft spin-triplet particle-hole excitations. It also was concluded that in strongly disordered systems, the quantum ferromagnetic phase transition is of second order with non-mean-field critical exponents. We have developed a theory that interpolates between these two extreme cases. Our comprehensive generalized mean-field theory is capable of describing systems with different amounts of quenched disorder, from extremely clean to extremely disordered. From this comprehensive generalized mean-field theory we conclude that there exist three distinct regimes: 1) A clean regime, where the quantum ferromagnetic phase transitions is first order; 2) an intermediate regime, where the transitions appears second order and the critical phenomena are effectively characterized by mean-field exponents; and 3) a disordered regime where the transition is of second order and is characterized by non-mean-field exponents. In the clean regime there is a tricritical point at nonzero temperature in the phase diagram. As the disorder increases, the tricritical temperature is suppressed until it reaches zero and the transition becomes second order. Initially, the observable critical exponents appear to be mean-field like, but in a very small region close to the transition the critical phenomena are characterized by non-mean-field exponents. As the disorder continues to increase, the region with non-mean-field critical phenomena expands and become observable.

If the disorder continues to increase, the non-mean-field critical phenomena will expand to the entire critical region.

These predictions can be tested experimentally by introducing different amounts of disorder into a suitable the system and measuring the phase transition properties. URhGe is a promising system for this purpose.

APPENDIX

MATRIX INVERSE

Consider a matrix $M_{12,34}$, with $1, 2, 3, 4$ representing indices n_1, n_2, n_3, n_4 subject to the constraints n_1, $n_3 > 0$, n_2, $n_4 < 0$, of the form

$$M_{12,34} = \delta_{13}\delta_{24}A_{1-2} + \delta_{1-2,3-4}B_{1-2} \tag{A.1}$$

The inverse of M is given by

$$\begin{aligned}
\delta_{12}\delta_{34} &= (MM^{-1})_{12,34} \\
&= (M^{-1}M)_{12,34} \\
&= \sum_{56} M_{12,56}M^{-1}_{56,34} \\
&= A_{1-2}M^{-1}_{12,34} + B_{1-2}\sum_{56}\delta_{1-2,5-6}M^{-1}_{56,34}
\end{aligned} \tag{A.2}$$

We also have

$$\begin{aligned}
\delta_{1-2,3-4} &= \sum_{56}\delta_{53}\delta_{64}\delta_{1-2,5-6} \\
&= \sum_{56}(A_{5-6}M^{-1}_{56,34} + B_{5-6}\sum_{78}\delta_{5-6,7-8}M^{-1}_{78,34})\delta_{1-2,5-6} \\
&= (A_{1-2} + \sum_{78}\delta_{1-2,7-8}B_{1-2})\sum_{56}\delta_{1-2,5-6}M^{-1}_{56,34}
\end{aligned} \tag{A.3}$$

Combining Eq. (A.3) and Eq. (A.2) we thus get

$$M^{-1}_{12,34} = \frac{\delta_{12}\delta_{34}}{A_{1-2}} - \frac{\delta_{1-2,3-4}B_{1-2}}{A_{1-2}(A_{1-2} + (1-2)B_{1-2})} \tag{A.4}$$

where we have used

$$\sum_{n_3 n_4} \delta_{n_1-n_2,n_3-n_4} = n_1 - n_2 \tag{A.5}$$

which follows from the constraint on the signs of the indices.

REFERENCES CITED

[1] N. W. Ashcroft and N. D. Mermin, *Solid State Physics* (Holt, Rinehart and Winston, New York, 1976).

[2] G. G. Lonzarich and L. Taillefer, Journal of Physics C: Solid State Physics **18**, 4339 (1985).

[3] L. Lundgren, O. Beckman, V. Attia, S. P. Bhattacherjee, and M. Richardson, Physica Scripta **1**, 69 (1970).

[4] Y. Ishikawa, K. Tajima, D. Bloch, and M. Roth, Solid State Communications **19**, 525 (1976).

[5] I. E. Dzyaloshinskii, Sov. Phys. JETP **19**, 960 (1964).

[6] I. E. Dzyaloshinskii, J. Phys. Chem. Solids **4**, 241 (1958).

[7] T. Moriya, Physical Review **120**, 91 (1960).

[8] S. J. Thomson, F. Krüger, and A. G. Green, Physical Review B **87**, 224203 (2013).

[9] Y. A. Izyumov, Soviet Physics Uspekhi **27**, 845 (1984).

[10] D. Forster, *Hydrodynamic Fluctuations, Broken Symmetry, and Correlation Functions* (W. A. Benjamin, Inc, 1975).

[11] D.Belitz, T. Kirkpatrick, and A. Rosch, Phys. Rev. B **73**, 054431 (2006).

[12] S.-K. Ma, *Modern Theory of Critical Phenomena* (W. A. Benjamin, Inc, 1976).

[13] K. G. Wilson and J. Kogut, Physics Reports **12**, 75 (1974).

[14] C. Pfleiderer, G. J. McMullan, S. R. Julian, and G. G. Lonzarich, Phys. Rev. B **55**, 8330 (1997).

[15] R. B. Stinchcombe, J. Phys. C: Solid State Phys. **6**, 2459 (1973).

[16] E. C. Stoner, Proc. R. Soc. Lond. A **165**, 372 (1938).

[17] J. A. Hertz, Phys. Rev. B **14**, 1165 (1976).

[18] A. Millis, Phys. Rev. B **48**, 7183 (1993).

[19] D. Belitz, T. R. Kirkpatrick, and T. Vojta, Phys. Rev. Lett. **82**, 4707 (1999).

[20] D. Belitz, T. R. Kirkpatrick, M. T. Mercaldo, and S. L. Sessions, Phys. Rev. B **63**, 174427 (2001).

[21] D. Belitz, T. Kirkpatrick, and J. Rollbuhler, Phys. Rev. Lett. **94**, 247205 (2005).

[22] V. Taufour, D. Aoki, G.Knebel, and J. Flouquet, Physical Review Letter **105**, 217201 (2010).

[23] M. Uhlarz, C. Pfleiderer, and S. M. Hayden, Physical Review Letters **93**, 256404 (2004).

[24] A. Huxley, I. Sheikin, and D. Braithwaite, Physica B **284-288**, 1277 (2000).

[25] O. Nakanishi, A. Yanase, A. Hasegawa, and M. Kataoka, Solid State Communications **35**, 995 (1980).

[26] P. Bak and M. H. Jensen, Journal of Physics C: Solid State Physics **13**, L881 (1980).

[27] Y. Ishikawa, G. Shirane, J. A. Tarvin, and M. Kohgi, Phys. Rev. B **16**, 4956 (1977).

[28] S. Mühlbauer, B.Binz, F. Jonietz, C. Pfleiderer, A. Rosch, A. Neubauer, R.Georgii, and P. Boni, Science **323**, 915 (2009).

[29] K. Ho, T. Kirkpatrick, Y. Sang, and D. Belitz, Phys. Rev. B **82**, 134427 (2010).

[30] D. Belitz and T. Kirkpatrick, Phys. Rev. B **81**, 184419 (2010).

[31] J. Zinn-Justin, *Quantum Field Theory and Critical Phenomena* (Oxford Science Publications, 1989).

[32] D. Belitz, T. Kirkpatrick, A. J. Millis, and T. Vojta, Phys. Rev. B **58**, 14155 (1998).

[33] P. Chaikin and T. Lubensky, *Principles of Condensed Matter Physics* (Cambridge University Press, 1995).

[34] J. Ziman, *Principles of the Theory of Solids* (Cambridge University Press, 1972).

[35] D. Belitz, T. Kirkpatrick, and A. Rosch, Phys. Rev. B **74**, 024409 (2006).

[36] T. Kirkpatrick, D. Belitz, and R. Saha, Phys. Rev. B **78**, 094407 (2008).

[37] D. Belitz, T. Kirkpatrick, and A. Rosch, Phys. Rev. B **78**, 094408 (2008).

[38] A. Huxley, I. Sheikin, E. Ressouche, N. Kernavanios, D. Braithwaite, R. Calemczuk, and J. Flouquet, Phys. Rev. B **63**, 144519 (2001).

[39] V. Taufour, D. Aoki, G. Knebel, and J. Flouquet, Phys. Rev. Lett. **105**, 217201 (2010).

[40] H. Kotegawa, V. Taufour, D. Aoki, G. Knebel, and J. Flouquet, J. Phys. Soc. Japan **80**, 083703 (2011).

[41] A. Huxley, S. Yates, F. Levy, and I. Sheikin, Journal of the Physical Society of Japan **76**, 051011 (2007).

[42] T. R. Kirkpatrick and D. Belitz, Phys. Rev. B **85**, 134451 (2012).

[43] T. Kirkpatrick and D. Belitz, Phys. Rev. B **53**, 14364 (1996).

[44] D. Belitz, T. Kirkpatrick, M. T. Mercaldo, and S. L. Sessions, Phys. Rev. B **63**, 174428 (2001).

[45] A. Aharony, in *Phase transition and Critical Phenomena*, edited by C. Domb and M. S. Green (Academic, New York, 1976), vol. 6, p. 358.

[46] G. A. Gehring, EPL(Europhysics Letters) **82**, 60004 (2008).

[47] G. A. Gehring and M. R. Ahmed, J. Appl. Phys. **107**, 09E125 (2010).

[48] V. P. Mineev, Comptes Rendus Physique **12**, 567 (2011).

[49] D. Belitz and T. Kirkpatrick, Phys. Rev. B **85**, 125126 (2012).

[50] E. Yelland, J. Barraclough, W. Wang, K. Kamenev, and A. Huxley, Nature Physics **7**, 890 (2011).

[51] D.Belitz and T. Kirkpatrick, Phys. Rev. B **56**, 6513 (1997).

[52] D. Belitz and T. Kirkpatrick, Review of Modern Physics **66**, 261 (1994).

[53] S. Edwards and P. Anderson, J Phys. F: Metal Phys **5**, 965 (1975).

[54] G. Grinstein, in *Fundamental Problems in Statistical Mechanics*, edited by E.G.D.Cohen (Elsevier Science Ltd, Amsterdam, 1985), vol. VI, p. 147.

[55] A.M.Finkelstein, Sov. Phys. JETP **57**, 97 (1983).

[56] C. Pfleiderer, D. Reznik, L. Pintschovius, H. Lohneysen, M. Garst, and A. Rosch, Nature **427**, 227 (2004).

[57] K. Prokes, T. Tahara, Y. Echizen, T. Takabatake, T. Fujita, I. Hagmusa, J. Klaase, E. Bruck, F. de Boer, M. Davis, et al., Physica B **311**, 220 (2002).

[58] P. Boulet, A. Daoudi, M. Potel, H. Noel, G. Gross, G. Andre, and F. Bouree, J. of Alloys and Compounds **247**, 104 (1971).

[59] T. Smith, J. Mydosh, and E. Wohlfarth, Phys. Rev. Lett. **27**, 1732 (1971).

[60] C. Pfleiderer, S. Julian, and G. Lonzarich, Nature **414**, 427 (2001).

[61] Y. Sang, D. Belitz, and T. Kirkpatrick, Phys. Rev. Lett. **113**, 207201 (2014).

[62] T. Vojta, Journal of Low Temperature Physics **161**, 299 (2010).